

MINISTRY OF EDUCATION AND SCIENCE OF THE RUSSIAN FEDERATION
NATIONAL UNIVERSITY OF SCIENCE AND TECHNOLOGY 'MISIS'

I.B. Ulanovskiy

HYDROGEN DIFFUSION AND POROSITY FORMATION IN ALUMINIUM



Moscow 2015

УДК 544.72
У47

Ulanovskiy, I.B.

У47 Hydrogen Diffusion And Porosity Formation In Aluminium /
I.B. Ulanovskiy. – M. : Izdatelskiy Dom ‘MISIS’, 2015. – 122 c.
ISBN 978-5-87623-939-6

This book presents experimental data obtained by the author on hydrogen permeability, solubility and diffusion of hydrogen in aluminum and its alloys, as well as on porosity formation in aluminum and its alloys. The author offers new techniques for determining the surface tension of solid metals and the hydrogen content in aluminum alloys containing components with high vapour pressures. The book also considers the theory of porosity formation in metals. For the first time ever, the author presents a technique for metals and alloys treatment securing the removal of gases and eliminating gas unsoundness, known as the ‘hot isostatic pressing technique’. The author proposes a technology, which ensures cutting down flaws caused by gas cavities in aluminum aircraft shell plates.

The book is aimed at professionals in the field of materials science, undergraduate and graduate students of technical universities

УДК 544.72

CONTENTS

Foreword.....	5
Introduction	8
Chapter 1. Hydrogen solubility in solid aluminium and its alloys	13
1.1 Research work on determination of hydrogen content in aluminium and its alloys.....	13
1.2 A new technique for hydrogen content determination in aluminium alloys, containing components characterized by high vapor pressure.....	22
1.3 Comparison between the present results and literature	23
Chapter 2. Hydrogen diffusion in solid aluminium	28
2.1 A new technique for determination of hydrogen diffusion coefficient and activation energy.....	28
2.2 Comparison between the present results and literature	30
Chapter 3. Hydrogen diffusion in the aluminium-aluminium oxide system	35
3.1 Hydrogen diffusion through an oxide film on aluminium s urface	35
3.2 Hydrogen diffusion in aluminium specimens in the presence of aluminium oxide particles	35
Chapter 4. Hydrogen permeability of aluminium.....	41
4.1 The technique of hydrogen permeability investigation at temperatures below 350 °C.....	42
4.2 Comparison between the present results and literature	46
4.3 The effect of preliminary annealing on experimental results of hydrogen permeability of aluminium.....	50
Chapter 5. The study of the mechanism of aluminium degassing during air and vacuum annealing.....	54
5.1 Hydrogen emission from metal during vacuum annealing.....	54
5.2 The results of hydrogen extraction during air and inert atmosphere annealing	55
Chapter 6. Working out a method of metal and alloy processing to remove gases and porosity (hot isostatic pressing technique)	64

Chapter 7. Of the theory of gas porosity evolution in metals.....	66
Chapter 8. The experimental testing of the theory of gas porosity formation in metals.....	78
Chapter 9. The application of the results obtained to the development of the process technique, providing the minimization of aluminium alloy sheets rejects caused by hydrogen blisters.....	90
Chapter 10. A new method of measuring the surface tension of solid metals.....	94
Referenses.....	97
Appendices (author's certificates).....	105
Biography	121

*Dedicated to my Teacher,
an outstanding scientist, Professor
Alexander Abramovich Zhukhovitsky*

FOREWORD

This monograph is based on the author's thesis on 'Hydrogen diffusion and development of porosity in aluminum' towards the degree of PhD in technical sciences and defended in 1972, that is, more than forty years ago. I suppose that this fact makes it desirable or even necessary to explain why this monograph has not been published earlier and the motives that have impelled me to do it now.

To begin with, let me present you with a brief retrospect illustrating the circumstances under which this book was written, and besides providing an overall view of the conditions of scientific research work in high-security research and production organizations, serving the vital needs of the military industry of the USSR.

Many Soviet scientists who carried out numerous studies in the most important scientific and production technology fields worked in secretive research and production centers of the military industry of the USSR. Moreover, most of their work was classified as 'For Official Use Only' (ADI), the status that was often assigned for merely formal and bureaucratic reasons. Therefore, numerous scientific results of specific studies were not available to a sufficiently broad academic community. This practice resulted in scientific reputation losses for authors and did not provide proper recognition of their pre-eminence in methodological, theoretical and practical work.

The collapse of the USSR prompted an easing of the regime's secrecy and abolished ridiculous bureaucratic restrictions on sharing scientific information and publication of research papers, and with the increase in 'statute of limitations' earlier confidentiality constraints became obsolete. Therefore, I hope, and even believe that my decision to publish this monograph based on the results of my thesis is not going to cause any trouble, because things that were impossible yesterday are feasible today.

This thesis had been prepared in the All-Union Institute of Light Alloys (VILS), one of the major aviation research and technology centers in the USSR. The head of research work was Alexander Abramovich Zhuk-

hovitsky – the outstanding physical chemist, head of the Physical Chemistry Department of the Moscow Institute of Steel and Alloys, Doctor of Engineering Sciences, professor, and Honored Worker of science and technology, whom I regard as my Teacher.

Let me give a little example for the reader to have an idea of our working environment in those days.

This thesis took me two and a half years to complete and when it was reviewed by the administration of the institute, they came up with two significant comments.

Firstly, ‘Your volunteer work is kind of sloppy, so you must promote sport activities in the division of the institute and thus show your public profile.’ As a result, the sport activities in the division of the VILS institute, where I worked, were certainly enhanced greatly. Secondly, ‘Our institute is focused on engineering tasks, therefore, along with the solution of theoretical and methodological issues we have to apply the research outcome to industrial needs. Currently, they stopped the production of shell plate for aircraft at two Soviet aviation metallurgy plants. Go there, develop and implement the technology preventing the formation of air cavities on shell plate, and then we will let you defend your thesis.’

Thus, through the requirement of ‘implementation’ of inventions, Soviet candidates for a degree in technical sciences were used for solving problems of cooperation between science and industry.

Frankly speaking, I happened to be very lucky to be imposed with the ‘production’ component of my thesis. At the Kuibyshev Metallurgical Plant, now the city of Kuibyshev renamed back to Samara, I met true experts headed by Leonid Mordukhovich Koganov, an outstanding specialist in rolling-mill practice, Kandidat of technical sciences, and the winner of two state awards. The administration of the plant wanted me to observe the following advice: ‘Air cavities should be removed and you must use a process excluding the formation of the air cavities, but without changing any part of production equipment; if you alter just one bolt or a nut, we should wait for the regulatory approval of these changes for years’. Therefore, basing on the results of my studies, I managed to develop the technique of production of aircraft shell plate without air cavities, only by changing the heat treatment of sheets and ingots, which did not require any changes in the design of production equipment and thus any official regulatory approvals.

Now just a few words about reasons of my looking back to the past that stimulated my work.

I believe, and this is confirmed by comparison of our data with publications in the last few years, that even today our scientific and experimental data concerning the theory of the formation of gas porosity in solid metals, and the behavior of hydrogen in aluminum are of pronounced importance.

The results of our studies had confirmed the efficacy of research techniques that we had been developing or improving and therefore deserve attention.

For example, the original methodology of determining the hydrogen permeability, the technique for the determination of hydrogen percentage in aluminum alloys, containing elements with a high vapor pressure and so forth.

So far, there are no similar methods of measurement of the surface tension of solid metals.

The technique of gas removal providing the elimination of metal porosity is of great practical importance. Today it is known as HIP (hot isostatic pressing). The invention certificate confirming our pre-eminence' is enclosed in the appendix hereto. The proposed technique of preventing the formation of air cavities at the interfaces of aluminum alloys of aircraft skin sheets may be of practical importance too.

One of the crucial goals in writing this monograph was the desire to lead the way for the research scientists who, like me, for objective reasons could not present the results of their work to the scientific community though being worthy of attention and recognition, in their opinion.

Some flaws found in previous publications (typos, insignificant arithmetic errors) of course having no effect on the final results were corrected.

I would like to express my gratitude to Irina Vladimirovna Apykhtina for her invaluable help in editing this monograph and to Professor Mikhail Vasilyevich Astakhov, Head of the Department of Physical Chemistry of NITU 'MISiS', Doctor of Physics and Mathematics, as well as to Yury Rahmilevich Nemirovsky, Doctor of Physics and Mathematics for their attention to this work and useful comments.

INTRODUCTION

The studies aiming to improve quality of products and semi-finished products, made from aluminum and its alloys, are explained by their use in elements of structures of aircrafts and missiles.

The most common defects in products and semi-finished products of aluminum alloys are of a gaseous nature, including porosity, delamination and air cavities associated with hydrogen dissolved in the metal.

In order to develop effective techniques to combat gas-originated defects it is necessary to know the mechanism of their development. Therefore, the study of phenomena linked to the redistribution of hydrogen within the metal, its saturation with a gas and gaseous release from solid aluminum and its alloys, along with the study of the development of porosity is of great interest.

Graham first described the phenomenon of penetration of gases through metals in 1866. So far, the scientists have accumulated an extensive array of experimental data concerning diffusion and penetration of gases through iron, copper, nickel, palladium and other metals.

The process of penetration of gases through metals in the presence of corresponding concentration gradients includes several stages [1].

The first stage is the activated adsorption of gas molecules on the surface of the metal occurs. It is accompanied by dissociation of molecules into atoms as well as by formation of ions. Then dissolution of gas ions in the boundary layer of metal takes place.

The second stage – the diffusion of the gas along metal in the direction of gas concentration reduction.

The third stage – the liberation of the gas from the opposite surface of the specimen into inner cavities, including the association and desorption of gas molecules.

The oxide films formed on the surface of the specimen may create additional resistance to gas transfer.

Each of these stages may determine the rate of the entire process. In most cases, the limiting element of the mass transfer is the diffusion of gas ions through the metal.

According to the Gaussian distribution

$$\frac{C_{\text{H}}(\text{solid})}{C_{\text{H}}(\text{gas})} = K_1 \quad (\text{I.1})$$

From the law of Mass Action we have

$$\frac{C_{\text{H}}^2(\text{gas})}{C_{\text{H}_2}(\text{gas})} = K_2 \quad (\text{I.2})$$

According to Fick's first law the rate of penetration can be expressed as follows

$$Q = -D \frac{dC_{\text{H}}(\text{solid})}{dx} \quad (\text{I.3})$$

Taking into consideration equations I.1 and I.2 we obtain

$$C_{\text{H}}(\text{solid}) = K_1 \sqrt{K_2} \sqrt{C_{\text{H}_2}(\text{gas})} \quad (\text{I.4})$$

Equation (I.4) expresses Siverts' law, which states that in the thermodynamic equilibrium the concentration of a gas dissolved in the metal is directly-proportional to the square root of the partial pressure of the gas above the metal.

Assuming that

$$\frac{dC_{\text{H}}}{dx} = \frac{C_{\text{H}|0} - C_{\text{H}|\ell}}{\ell} \quad (\text{I.5})$$

and plugging it into (I.3), we get (I.4)

$$Q = DK_1 \sqrt{K_2} \left(\sqrt{C_{\text{H}_2|0}} - \sqrt{C_{\text{H}_2|\ell}} \right), \quad (\text{I.6})$$

and if $C_{\text{H}_2|\ell}$, is considerably less than $C_{\text{H}_2|0}$, then we get

$$Q = DK_1 \sqrt{K_2} \sqrt{C_{\text{H}_2}} = DK_s \sqrt{P}, \quad (\text{I.7})$$

where K_s – solubility coefficient.

The definition of permeability or the permeability factor (Π), given in [1], says that permeability is the coefficient of proportionality in the equation, describing the dependence of gas flow through the metal Q on the gas pressure at the entry end of the metallic membrane.

Hence, from (I.7) it follows that

$$\Pi = DK_s$$

The exponential relationship of diffusion coefficients and gas solubility with temperature explains the nature of the exponential dependence of permeability on temperature, i.e.

$$D = D_0 \exp\left(-\frac{E_{Diff}}{RT}\right), \quad (I.9)$$

$$K_S = K_{S_0} \cdot \exp\left(-\frac{E_S}{RT}\right)$$

As it follows from equation (I.8), the permeability factor as well as diffusion coefficients and solubility are strictly determined values for a given gas. This statement is correct when gas diffusion through the metal is the limiting element of the mass-transfer process.

The exponential nature of the temperature dependence of the flow corresponds with experimental data [1–4]. At the same time, the true nature of the relationship between Q and pressure is still unknown. G.Borreluis and S.Lindblom [5] first demonstrated that the straight line $Q - \sqrt{P}$ does not come to the central point of coordinates but cuts the straight-line segment $\sqrt{P_t}$ from the axis of abscissas. Herewith, equation (I7) takes on the form as follows

$$Q = K\left(\sqrt{P} - \sqrt{P_t}\right) \quad (I.10)$$

More studies, carried out by Smithells C.J. and Ransley C.E. [6], show that at a low gas pressure the isotherm of permeability bends and passes through the central point of coordinates. This fact says in favor of adsorption influence on gas permeability at low pressures. Assuming that the rate of gas penetration is proportional to the degree of covering the authors [6] obtained the expression

$$Q = K\Theta\sqrt{P} \quad (I.11)$$

where Θ is the degree of covering.

If monomolecular adsorption with dissociation is governed by the Langmuir equation, then

$$\Theta = \frac{\alpha\sqrt{P}}{1 + \alpha\sqrt{P}}, \quad (I.12)$$

$$\text{where } Q = K_2 \frac{P}{1 + \alpha\sqrt{P}}. \quad (\text{I.13})$$

At low pressures

$$Q = KP, \quad (\text{I.14})$$

while at high pressures

$$Q = K\sqrt{P}. \quad (\text{I.15})$$

Equation (I.11) corresponds to the experimental data and besides it has been found that α grows with temperature. R.Barrer in [1] indicates that α reduces with temperature since the process of adsorption is an isothermal reaction.

The data of Stross and Tomkins in [7] say against the explanation given by Smihtells and Ransly. They determined that the coating of iron wire with nitrogen or oxygen does not change the rate of hydrogen desorption from the specimen surface.

To explain the phenomenon of deviations of $Q - \sqrt{P}$ dependence from the linear nature (at low pressures) the authors [8–12] assumed that concentration of the gas dissolved near the specimen surface is not at the equilibrium relatively to the gas phase.

If diffusion processes are able to remove more gas than is transferred due to surface reactions, the concentration of the adsorbed gas on the surface should not be less than the equilibrium concentration. Similarly, the concentration of the dissolved gas on the outflow surface will be in equilibrium, if the rate of surface processes exceeds the rate of diffusion processes, and on the contrary, it will be higher than the equilibrium value at slow surface processes.

R.Barrer in [1] gives six equations, describing the phenomenon of gas penetration in metals (i.e. gas permeability) for the case when the gas concentration near the specimen surface is not equilibrium relatively to its concentration in the gas phase. However, these equations are hardly to be used for clear presentation of the relationship between the gas flow through the metal and the gas pressure. Chang and Bennett [12] had simplified the gas transfer model accounting only the direct solution from the gaseous phase.

Two equations expressing the ratio between process rate and pressure have been derived: for near-equilibrium concentrations on the surface and

for the case when the surface reactions determine the mass-transfer rate. The ratio between gas permeability and pressure is difficult to establish for the rates of surface and diffusion processes.

At high pressures, the rate of diffusion mainly depends upon collisions of gas molecules with adsorbed atoms [3]. Only collisions providing simultaneous adsorption of gas molecules support the diffusion. Under these conditions, the dependence of gas permeability on pressure is the following [3].

$$Q = A\sqrt{1 + Kf(P)} - 1, \quad (\text{I.16})$$

where A and K are the terms comprising Θ

In a simplified form equation (I.16) can be presented in this way

$$Q = A(\sqrt{1 + K\Theta P} - 1). \quad (\text{I.17})$$

At high pressures

$$Q \sim \sqrt{P}. \quad (\text{I.18})$$

At low pressures

$$Q \sim P. \quad (\text{I.19})$$

Until present, there is no any unified theory, providing a quantitative presentation of the perfect relationship between rate of permeability and gas pressure. The influence of surface processes on gas penetration into metals is still not known in detail. Surface oxide layers on aluminium impede hydrogen penetration through aluminium.

Therefore, the study of the isotherm of gas penetration through aluminium is of significant academic interest

CHAPTER 1. HYDROGEN SOLUBILITY IN SOLID ALUMINIUM AND ITS ALLOYS

1.1 Research work on determination of hydrogen content in aluminium and its alloys

Low concentrations of the analyte in aluminium ($10^{-4} - 10^{-5} \%$) as well as the presence of `surface` hydrogen result in consistent analytic problems.

Most gas analyzers show the total gas mixture pressure, but not the partial pressure of hydrogen, and thus having a comparatively low sensitivity cannot provide a continuous measurement of gas liberation kinetics – all this complicates research of hydrogen diffusion in aluminium.

There are several methods of measurement of hydrogen content in aluminium:

- isotonic equation [13–15];
- vacuum melting [16–23]
- vacuum degassing [16, 24–27].

Aggregated characteristics of the vacuum degassing method make it the most propagated technique for the analysis of hydrogen content in aluminium and its alloys. Within this method, we have developed a technique for defining hydrogen content in aluminium using a mass-spectrometric analyzer (ИПДО-1) and a mass-spectrometric sensor connected in parallel to the vacuum degassing system.

The idea and technical details of the proposed technique are as follows. A standard specimen is heated up to 600°C under a high vacuum while the mercury vapor diffusion pump ДРН-10 continuously removes gases released from the specimen. The mass-spectrometric analyzer (ИПДО-1) registers the partial pressure of hydrogen in the mixture of gases [28–30]. The area under the curve demonstrating the variation of hydrogen partial pressure with time shows the total volume of hydrogen extracted from the specimen.

Measurements of the ion current of the ion target capturing the resonance ions formed due to the interaction between constant magnetic and high frequency electromagnetic fields allow quantifying the partial pressure of gases with the use of the mass-spectrometric analyzer (ИПДО-1) (Fig. 1.1).

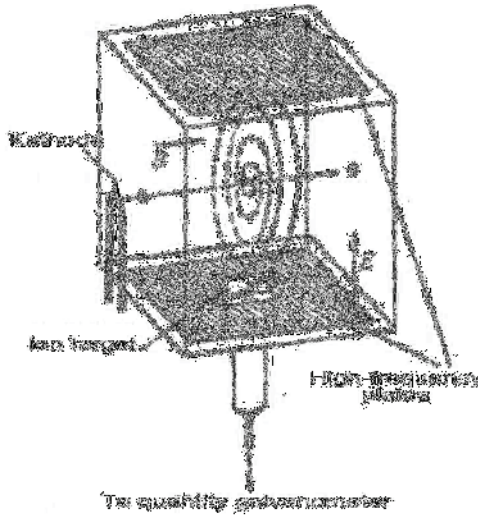


Fig. 1.1 Diagram of mass-spectrometric analyzer sensor

Ions of definite mass reach the surface of the ion target only at a corresponding electric field frequency. The electric field frequency required for the measurement of hydrogen partial pressure makes around 1.8 MHz. The ionic current value of the ion target circuit is proportional to partial pressures of corresponding gases in the mixture at definite values of the electron beam current, depending on high-frequency voltage of the omegatron and its orientation in the magnetic field. The background ionic current caused by small amounts of ions of other masses, which attain the surface of the collector, should be taken into consideration while working with the mass-spectrometric analyzer (ИПДО-1). Therefore, to determine the ionic current value corresponding to the partial pressure of the analyzed gas it is necessary from time to time to shift the electric field frequency relatively to the resonant frequency and to measure the background ionic current.

The diagram of the original installation is presented in Fig. 1.2.

The installation consists of a glass extraction-analytic system, a calibration system and a mass-spectrometer.

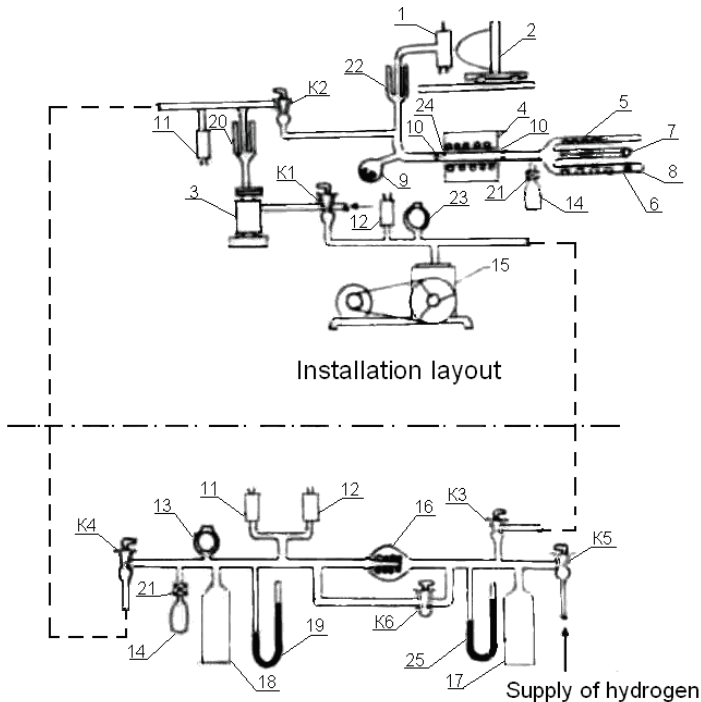


Fig. 1.2 Installation layout and calibration system for mass-spectrometric hydrogen-in-aluminium test:
 1 – the glass omegatron sensor PMO-4c of the mass-spectrometric analyzer (ИП/ДО-1); 2 – permanent magnet, 3 – the mercury vapor diffusion pump ДРН-10 with a nitrogen trap; 4 – resistance furnace; 5, 6 – glass tube containers for specimens keeping; 7, 8 – pushers; 9 – glass receiver for analyzed specimens; 10 – quartz-glass junctions; 11, 12 – pressure gauge sensors ЛМ2 and ЛТ2; 13, 20, 22, 23 – glass traps cooled with liquid nitrogen; 14 – standardized glass bottle; 15 – fore pump BH-461-M; 16 – palladium filter; 17, 18 – glass bottles; 19, 25 – U-type mercury pressure gauges; 21 – valve ДУ-2 with fine adjustment of flow rate; 24 – degassing quartz tube; K1-K6 – vacuum glass traps

The gas extraction analytical system provides high vacuum conditions in the installation, extraction of gases from the specimen and determination of hydrogen partial pressure in the mixture of gases by means of the glass sensor PMO-4C of the mass-spectrometric analyzer.

Fore pump BH-461-M (15), mercury vapor diffusion pump ДРН-10 (3) and vacuum glass traps (13, 20) cooled with liquid nitrogen provide a rarefaction of approx $5 \cdot 10^{-7}$ mm Hg (i.e. $7 \cdot 10^{-5}$ Pa).

The elimination of gases from degassing quartz tube (24) proceeds within an hour at 900 °C. This operation should be required if the vacuum system was connected to the atmosphere.

The glass sensor (1) of the mass-spectrometric analyzer is connected to the gas-evacuating pipeline through glass sealing, in so doing the connecting coupling, glass piece must not have a necking and the sensor should be as near as possible to the pipe.

In the case of a parallel connection of the mass-spectrometric analyzer sensor to the system of gas evacuating these conditions are obligatory. They ensure almost similar values of hydrogen pressure both in the sensor and in the pipeline of the gas evacuating system.

The liquid nitrogen glass trap (22) mounted before the sensor prevents penetration of water, mercury and oil vapors to the surface of the ion target and electrodes of the sensor PMO-4C.

To minimize the negative background effect of hydrogen there are only few taps in the installation. The specimens are loaded through the open rears of glass tubes (5, 6) unsealed with a blowpipe burner. Glass tubes are to be sealed again after loading the specimens. There can be loaded forty specimens at a time.

A cylindrical specimen loaded into the extraction pipe is heated in external resistance furnace (4) providing permanent temperature within the range of 400 – 900 °C. The chromel-alumel thermocouple and the electronic potentiometer ЭПП-09 provide temperature control and registration. The operation temperature of the analysis procedure makes 600 °C. Degassing quartz tube (24) is connected to the system with ‘quartz-molybdenum glass’ coupling piece (10). Pushers (7, 8) unload the specimens from glass pipes (5, 6) into the degassing tube. On completion of the analysis, the specimens slip into receiver (9).

The amount of hydrogen dQ , cm^3 (in normal conditions), passing through the mass-spectrometer within dt sec. can be expressed as follows:

$$dQ = pSdt = KSJdt \quad (1.1)$$

where p – partial pressure of hydrogen; S – pump suction effect within the mass-spectrometer cross-section, cm^3 (at normal conditions); K – coefficient of mass-spectrometer sensitivity to hydrogen; J – ionic current of the mass spectrometer, V.

The total volume of hydrogen extracted from the specimen during the analysis can be obtained through integration of equation 1.1

$$Q = K \int_0^t JS dt \quad (1.2)$$

It is possible to remove S from the integral if the pump suction effect in the sensor cross-section remains constant during whole time of the analysis.

$$Q = KS \int_0^t J dt = K_n \int_0^t J dt \quad (1.3)$$

The area under the curve of time dependence of the current in the circuit of the ion target of the mass-spectrometric analyzer corresponds to the integral in equation (1.3).

The mercury vapor diffusion pump ДРPH-10 having the constant evacuation rate within a wide range of pressures $10^{-5} - 10^{-8}$ mm Hg (i.e. $10^{-3} - 10^{-6}$ Pa) provides the permanent suction effect within the cross-section of the mass-spectrometric analyzer. Besides, it must be noted that the pipeline capacity is far less than the rate of pumping in the upper flange of the pump (that is 1 l/sec. against 10 l/sec. respectively).

The speed fluctuations do not affect much the effective rate of pumping, since

$$S_{\text{eff}} = \frac{1 \times 10}{1 + 10} \approx 1 \text{ l/sec} \quad (1.4)$$

Therefore, the use of pipelines having a significantly lower capacity than the capacity within the upper flange of the mercury vapor diffusion pump helps to stabilize additionally the pump evacuation effect in the cross-section of the mass-spectrometric analyzer.

For quantitative measurements, it is necessary to know the values K and S or K_n .

The calibration system was used to determine K_n . The strip heaters heated the high-vacuum part of the system up to 350 °C during 1.5 hour to minimize gas emission from walls of the installation while a special furnace heated the glass sensor PMO-4C of the mass spectrometric analyzer.

The calibration system comprises (see Fig. 1.2) palladium filter for hydrogen cleaning (16), standardized glass bottle (14) with a fine tuning gas valve ДУ-2, U-type mercury gauge (19) for measuring hydrogen in the standardized bottle, liquid nitrogen trap (13), vacuum gages ЛМ-2 and ЛТ-2 (11, 12) and glass vacuum valves K3-K6.

The fore pump main pipe and the high-vacuum main pipe connect the calibration system with the installation via taps K3 and K4, respectively (see dotted lines in Fig. 1.2). U-type pressure gauge (19) measures the pressure of hydrogen passing through palladium filter (16) and high-vacuum processed standardized bottle (14). Then the valve ДУ-2 (21) is shut and the standardized glass bottle together with the valve ДУ-2 are sealed off of the calibration system and connected to the installation where a high vacuum should be then developed. The valve ДУ-2 is opened and hydrogen can pass from the standardized bottle into the installation. The valve ДУ-2 is to be open in such a way as to ensure the pressure in the installation not higher than $1 \cdot 10^{-5}$ mm Hg (i.e. $1.3 \cdot 10^{-3}$ Pa). The mass-spectrometer analyzer controls the hydrogen partial pressure.

The value K_n , $\text{cm}^3(\text{NTP})/(\text{V} \cdot \text{sec.})$ is determined by equation (1.3) as

$$K_n = \frac{Q}{A}, \quad (1.5)$$

where A – the area under the characteristic curve ‘ionic current – time’ of the mass-spectrometer analyzer potentiometer, expressed in $\text{V} \cdot \text{sec.}$;
 Q – the volume of hydrogen in the standardized bottle, cm^3 .

The calibration was repeated several times with different volumes of hydrogen in the standardized bottle to check the correctness of equation (1.5) for quantitative estimation of the results (Fig. 3).

This figure clearly demonstrates the linear dependence between the hydrogen volume and the area under the curve, what shows in turn at the use of equation (1.5) in estimation of the results.

The value of K_n for this apparatus was $4.6 \cdot 10^{-7} \text{ cm}^3/\text{V} \cdot \text{sec}$ at normal conditions.

Standard cylinder specimens, 20 mm long and 8 mm in diameter, are lathed to the surface roughness of $\nabla 7$, and charged into glass pipes (5, 6), see Fig. 1.2.

The flat ends of the glass pipes are sealed with a gas burner. The fore pump provides preliminary degassing down to pressure of $2 \cdot 10^{-3}$ mm Hg (i.e. $2.7 \cdot 10^{-1}$ Pa), approximately. Then within 1.5 hour, the mercury vapor diffusion pump and the nitrogen traps bring the pressure down to $2 \cdot 10^{-7}$ mm Hg (i.e. $2.7 \cdot 10^{-5}$ Pa). Then the mass-spectrometric analyzer is switched on.

The high-vacuum system and the sensor of the mass-spectrometric analyzer must be heated up to the temperature of 900°C for an hour, while the quartz tube must be degassed, if the installation was previously in contact with the atmosphere.

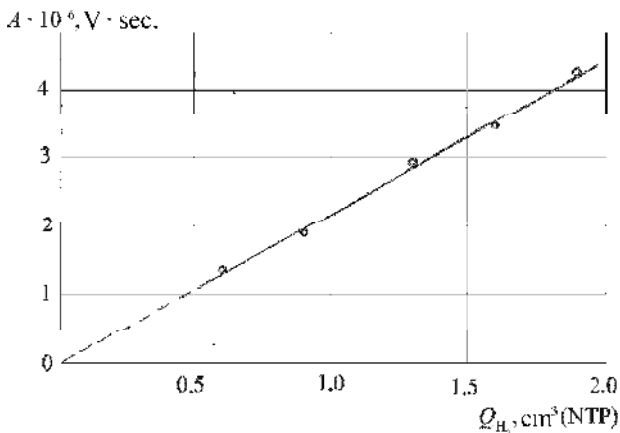


Fig. 1.3 The dependence of the area under the calibration curve of the mass-spectrometer recorder strip on the initial volume of hydrogen in the standardized bottle

Then the required temperature is set to determine the blank test correction. To this purpose, the hydrogen resonant frequency of ~ 1.8 MHz is set and the ionic current is measured, while the background ionic current is checked by shifting the frequency from the resonant values.

Hereupon the analysis of hydrogen is carried out. The procedure is as follows. The pusher moves the specimen into the degassing quartz tube. During the process, the blank test correction value is measured by shifting the frequency from the resonant values.

The extraction is considered complete when the ionic current of hydrogen exceeds the initial background level not more than by 0.3V. On completion of the analysis the specimen, pushed by the pusher, drops into the glass receiver, the blank test correction is measured and the next specimen is placed into the quartz degassing tube. The total amount of hydrogen eliminated from the specimen, $\text{cm}^3(\text{NTP})/100\text{g}$ is

$$Q_{H_2}^{Total} = \frac{K_n A}{q} \cdot 100 \quad (1.6)$$

where q – mass of a specimen, g; A – area under the curve ‘Current–time’ from the mass-spectrometer recorder strip, V·sec.

In the first place, to determine the area we have to draw the line, showing the variation of the background ionic current with time, through cor-

responding points on the mass-spectrometer recorder strip (Fig. 1.4, curve 1). Then above the first line it is necessary to draw the second line demonstrating hydrogen background ionic current variation (curve 2), which is spaced from the first line at a distance, equal to the value of the initial the ionic current, corresponding to partial pressure of hydrogen. Finally, using an integrating instrument, we can determine the area between curves 1 and 3, where curve 3 shows the variation of the ionic current, corresponding to the partial pressure of hydrogen, with time.

For calibration of the system it is necessary to provide the rarefaction about $2 \cdot 10^{-7}$ mm Hg ($2.7 \cdot 10^{-5}$ Pa) both in the system and the calibration system. Thereafter the calibration system shall be disconnected from the installation and the hydrogen passing the heated palladium enters the standardized bottle. Then the valve ДУ-2 is closed.

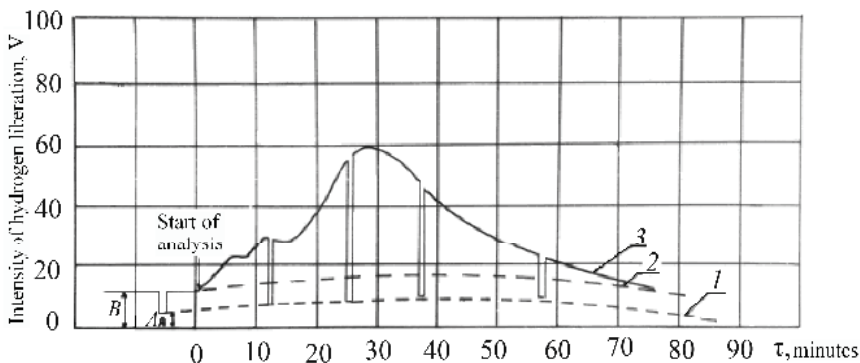


Fig. 1.4 Kinetics of hydrogen liberation from the specimen in vacuum:
A – initial background of gases; *B* – initial background of hydrogen; *1* – variation of gases background during the time of the analysis; *2* – total variation of gases background and the initial background of hydrogen; *3* – variation of hydrogen partial pressure in the system with time

We seal off the standardized bottle together with the valve from the calibration system and then seal it to the analytical part of the installation. The gas pressure in the installation must be preliminary equalized with the atmospheric pressure. Thereafter we create high vacuum in the installation $2 \cdot 10^{-7}$ mm Hg ($2.7 \cdot 10^{-5}$ Pa) and switch on the mass-spectrometric analyzer to measure the value of blank inleakage and then open the valve ДУ-2.

The calibration is considered to be completed if the value of hydrogen ionic current does not exceed the initial hydrogen ionic current more than by 0.3V when the valve ДУ-2 is full open.

The arresting and high voltages as well as the speed of the strip of the mass-spectrometric analyzer recorder and the beam voltage scale during calibration of the electron beam current should be similar to the respective parameters during the specimen analysis.

The relative error of area determination on the recorder strip makes 1 %, approximately.

The error of quantitative determination of hydrogen in the standardized volume is

$$\frac{\Delta(PV)}{PV} = \frac{\Delta P}{P} + \frac{\Delta V}{V} = \frac{0.4}{20} + \frac{0.15}{15} = 0.03,$$

where V – standardized volume value, cm^3 , P – hydrogen pressure in the standardized volume, mm Hg (Pa).

Hence, the total error of calibration and measurement of area is less than 5 %. The relative sensitivity of hydrogen determination makes $0.02 \text{ cm}^3/100\text{g}$ by 2 σ -test.

This technique providing one evaluation per hour is considerably more efficient as compared to the method of vacuum heating. Decreasing evaluation time is achieved due to the exclusion of the gas mixture passing through the palladium filter, the possibility of quantitative accounting for the blank test correction and a lower time of vacuum degassing of the installation before each analysis [31].

Besides, the proposed method has higher reliability than the vacuum heating method since it makes possible continuous recording of the kinetics of hydrogen release from the specimen thus identifying any anomalous effects.

One of peculiar details of the vacuum heating technique is formation of ‘surface’ hydrogen in addition to dissolved hydrogen. The concept of ‘surface’ hydrogen was first offered by U.A.Klyachko [32–35] who arrived at the decision that ‘surface’ hydrogen was formed due to the reaction of aluminium with the moisture, adsorbed on the specimen surface.

The kinetic curve given in Fig. 1.4 demonstrates several maximums the 3^d the fifth, the 8th – 12th, the 20th – 30th minutes.

The presence of several maximums on curve is caused by liberation of hydrogen dissolved in the specimen and surface hydrogen formed as the result of reactions on the specimen surface.

The pollution of surfaces results in growth of the ‘surface’ hydrogen volume, simultaneously grow the values of corresponding maximums at

the third the fifth, the eighth and the twelfth minute. It is possible to use this phenomenon for estimation of the degree of pollution.

Too strong difference between maximums corresponding to 'surface' hydrogen and the respective values for the standard specimens says in favor of necessity to repeat the test with specimens having well prepared surface.

The mass-spectrometer analyzer allows to study in the course of vacuum (Fig. 1.5) degassing the liberation of various gases along with hydrogen.

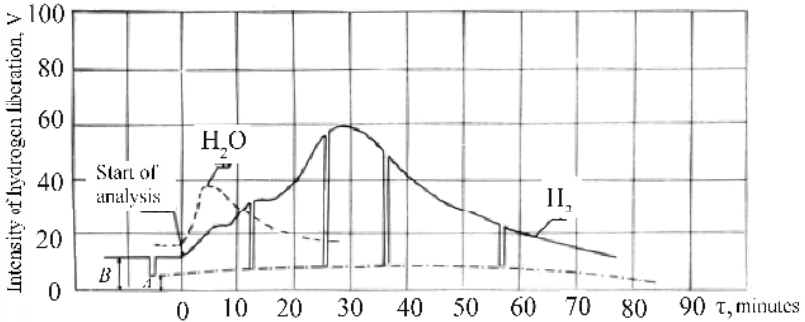


Fig. 1.5 Kinetics of hydrogen and moisture release during vacuum annealing of aluminium

1.2 A new technique for hydrogen content determination in aluminium alloys, containing components characterized by high vapor pressure

All known evaluation methods of hydrogen in alloys containing components with a high vapor pressure do not allow a complete extraction of hydrogen from specimens, and besides, their efficiency is comparatively low. To improve the extraction of hydrogen and to enhance the performance of the method the test specimens are coated with a thin film of pure aluminium before placing them into the vacuum degassing system. This procedure may proceed as follows, for example.

Aluminium alloy specimens are coated with pure aluminium by hot-dipping, i.e. by quickly immersing them into molten high purity aluminium. Then the specimens are loaded into the vacuum-degassing apparatus.

tus, heated under vacuum and the amount of released hydrogen is measured with the mass-spectrometric analyzer.

The pure aluminium layer covering the surface of a specimen impedes the fumes of volatile components but lets out hydrogen freely.

Thereby we propose a method to evaluate the hydrogen concentration in alloys, containing components with a high vapor pressure. The method consists of heating a specimen in vacuum and measuring the amount of hydrogen released from the specimen. The proposed method differs from others by coating test specimens with a layer of high-purity aluminium [36], thus increasing the efficiency of the analyses and ensuring the completeness of hydrogen extraction.

1.3 Comparison between the present results and literature

Fig. 1.6 and Table 1.1 demonstrate the results of our studies.

We have studied possibilities of increasing the efficiency of the vacuum heating technique by reducing the analysis time due to a smaller specimen size.

The ‘surface’ hydrogen was determined on 99.996 % Al specimens. The specimens were lathed from hot-pressed 12 mm rods annealed at approximately $1 \cdot 10^{-7}$ mm Hg (i.e. $1.3 \cdot 10^{-5}$ Pa) during 10 – 15 hours. Owing to this almost all the hydrogen dissolved in aluminium was eliminated.

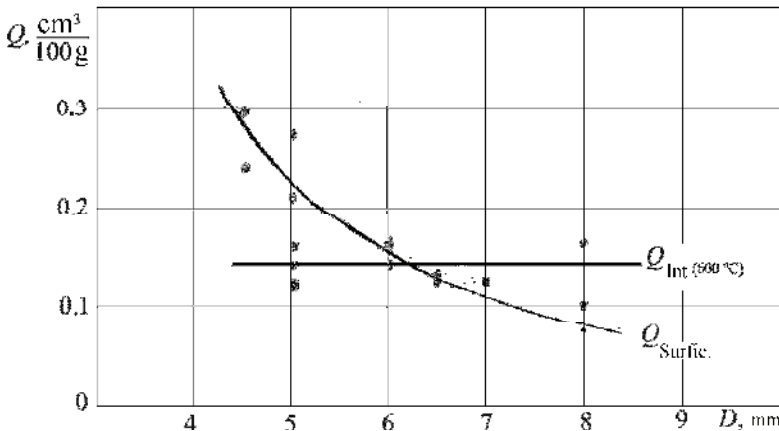


Fig. 1.6 The dependence of ‘surface’ hydrogen Q_{Surfic} for aluminium on specimen size (Q_{Int} , amount of dissolved hydrogen)

Table 1.1

Experimental results

Specimen No	'Surface' hydrogen, cm ³ /100 g	Specimen No	'Internal' hydrogen, cm ³ /100 g
1	0.05	1	0.11
2	0.06	2	0.09
3	0.04	3	0.09
4	0.05	4	0.09
5	0.06	5	0.11
6	0.07	6	0.11
7	0.09	7	0.08
8	0.06	8	0.09
9	0.04	9	0.10
10	0.06	10	0.11
Mean	0.06	Mean	0.10
Root mean square	0.01	Root mean square	0.01

According to equation 1.6, the fraction of 'surface' hydrogen abruptly grows and determination of the hydrogen dissolved in aluminium becomes more and more difficult for specimens whose diameter is smaller as compared to standard dimensions (diameter 8 mm, and length – 20 mm). At the same time the amounts of 'surface' and 'internal' hydrogen are comparable even for 8 mm specimens within the range of the research. Hence for reliable determination of the amount of hydrogen dissolved in aluminium (Q_{H_2}) one must subtract the amount of surface hydrogen ($Q_{H_2}^{Surf.}$) from ($Q_{H_2}^{Total}$)

$$Q_{H_2} = Q_{H_2}^{Total} - Q_{H_2}^{Surf.} \quad (1.7)$$

The data in Table 1.1 illustrate the range of experimental estimates of the amounts of 'surface' and 'internal' hydrogen received on standard size specimens, as well as their mean values.

The amount of 'surface' hydrogen in the studied series of specimens, comprised 10 aluminium specimens, having a purity of 99.996 %, was estimated as (0.06 ± 0.01) cm³/100 g.

The content of hydrogen in the series of ten pure aluminium specimens, lathed from 12 mm rod of not-degassed hot-pressed 99.996 % aluminium was (0.1 ± 0.01) cm³/100 g (we subtracted the amount of 'surface' hydrogen 0.06 cm³/100 g).

The instrumental error estimated in p.1.1 is substantially lower than the total error of the hydrogen–in aluminium test (< 5 % or 0.005 cm³/100 g against 10 % or 0.01 cm³/100 g, respectively), see table 1.1. The latter value corresponds with the error of hydrogen amount determination in pure degassed aluminium. This implies that fluctuations of the ‘surface’ hydrogen amount limit the accuracy of our technique; nevertheless, it can be used for quantitative hydrogen–in aluminium testing because of its more than sufficient accuracy.

The accuracy of the proposed technique is approximately two times higher than the accuracy of the standard vacuum heating method. Its relative sensitivity in hydrogen content evaluation by the 2σ criterion makes 0.02 cm³/100 g.

Table 1.2 gives the results of hydrogen solubility obtained by other authors.

Table 1.2

Solubility of hydrogen in aluminium

Material	Temperature, K	Solubility L , cm ³ /100 g	Source
Al	273	10 ⁻⁷	[37]
	573	0.001	
	673	0.005	
	773	0.0125	
	873	0.026	
	933(solid)	0.036	
		$\lg L = -\frac{2080}{T} + 0.788 + \frac{1}{2} \lg P, (P, \text{ atm})$ $\lg L = -\frac{2080}{T} - 0.652 + \frac{1}{2} \lg P,$ <p style="text-align: center;">(P, mm mercury)</p>	
99.994 % Al	673	0.0028	[38]
	773	0.011	
	873	0.030	
	933(solid)	0.050	
		$\lg L = -\frac{3042}{T} - 0.521 + \frac{1}{2} \lg P,$ <p style="text-align: center;">(P, mm mercury)</p>	
99.999 % Al	723	0.004	[39]
	773	0.007	
	823	0.012	
	873	0.021	
	913	0.033	
Al–7 % Mg	773	0.05	[40]
	$P_{\text{H}_2} = 700 \text{ mm Hg}$		

Material	Temperature, K	Solubility L , cm ³ /100 g	Source												
99.999 % Al	873 $P_{H_2} = 700$ mm Hg	0.1	[40]												
Al	673 – 903	$\lg C_H [\% (atm.)] = 0.51 \lg P_H - 3.01 - \frac{3300}{T}$	[41]												
Al-AB000 Wire specimens $S_1 = 5$ cm ² ; $d = 0,8$ mm $S_2 = 20$ cm ² ; $d = 0,2$ mm	873	0.143±0.06 0.174±0.008	[42]												
99.99 % Al Wire specimens $d = 0,8$ mm $m = 0,25$ g	878 783 683	0.026 0.015 0.007 $\lg L = 0.36 - \frac{1700}{T}$	[43]												
99.99 % Al Cylindric specimens $d = 4$ mm $\ell = 20$ mm $m = 0,5 - 0,6$ g	823	0,026	[44]												
Solid alloy Al+7% Mg Cylindric specimens $d = 4$ mm $\ell = 20$ mm	723	$L = 0.14 \pm 0.04$	[44]												
Solid alloy Al–Mg 0.48 % Mg 5.25 % Mg 5.25 % Mg	773 773 698	0.04±0.01 0.06±0.01 0.05±0.01	[45]												
99.99 % Al Cylindric specimens $d = 4$ mm, $\ell = 20$ mm Preliminary boiling in distilled water at 373K	823	<table border="1"> <thead> <tr> <th>$M_{\text{specimen, g}}$</th> <th>0.250</th> <th>0.420</th> <th>0.479</th> <th>0.800</th> <th>1.478</th> </tr> </thead> <tbody> <tr> <td>L</td> <td>0.062</td> <td>0.061</td> <td>0.063</td> <td>0.062</td> <td>0.057</td> </tr> </tbody> </table>	$M_{\text{specimen, g}}$	0.250	0.420	0.479	0.800	1.478	L	0.062	0.061	0.063	0.062	0.057	[46]
$M_{\text{specimen, g}}$	0.250	0.420	0.479	0.800	1.478										
L	0.062	0.061	0.063	0.062	0.057										
Al A99	773–923	$\lg L = -\frac{1900}{T} + 0.78 + \frac{1}{2} \lg P$	[47]												

It is obvious that the amount of hydrogen dissolved in aluminium differs significantly in various works. This fact makes our high precision and efficient technique greatly useful both for technological and academic research, requiring reliable knowledge of the amount of hydrogen dissolved in a given alloy and/or semi-finished products of aluminium and its alloys with their technological prehistory.

CHAPTER 2. HYDROGEN DIFFUSION IN SOLID ALUMINIUM

The quantitative description of the formation of gas porosity requires knowledge of kinetic parameters of the interaction between hydrogen and the metal.

The method described in Ch.1 was used to determine hydrogen diffusion coefficients in the “aluminium-aluminium oxide” system, as well as to study the kinetics of hydrogen release from aluminium during annealing.

2.1 A new technique for determination of hydrogen diffusion coefficient and activation energy

Numerous literature sources contain contradictory data concerning the values of activation energy and pre-exponential factor of hydrogen diffusion in aluminium.

In our opinion, the insufficient sensitivity of analytical methods is the main reason of these contradictions, besides these methods measure only the total pressure of gas mixtures but do not provide a continuous measurement of hydrogen release kinetics and a direct measurement of hydrogen partial pressure.

The mass-spectrometric analyzer allows eliminating these disadvantages to a considerable extent. We determined the coefficients of hydrogen diffusion in aluminium from kinetic curves of hydrogen release in the course of vacuum heating.

There are several methods to determine hydrogen diffusion coefficients in metals such as processing hydrogen distribution curves along the sample cross-section [48], measuring the resistance of the metal wire saturated with hydrogen [49], evaluating the displacement of the blackened zone of the photographic plate placed on the wire surface [50].

However, the determination of hydrogen diffusion coefficients from kinetic curves of hydrogen release from specimens seems to be the most propagated method [40, 51–53, 55].

According to this method, a test specimen is subjected to vacuum heating with further continuous recording of pressure variations in the system with time. Thereby, it is possible to determine the fraction of the gas remained in the specimen at any time.

The phenomenological diffusion theory, using Fick’s laws presents the dependence of the gas amount remained in the specimen as a time function.

Fick's second law for cylindrical bodies says

$$\frac{\partial C}{\partial t} = \frac{D}{r} \left[\frac{\partial}{\partial r} \left(r \frac{\partial C}{\partial r} \right) + \frac{\partial}{\partial \Theta} \left(\frac{1}{2} \frac{\partial C}{\partial \Theta} \right) + \frac{\partial}{\partial z} \left(r \frac{\partial C}{\partial z} \right) \right]. \quad (2.1)$$

Corresponding initial and boundary conditions for vacuum degassing of specimens having radius K and height l with initial concentration of hydrogen C_0 are the following

$$C_{|z=-\frac{\ell}{2}} = C_{|z=\frac{\ell}{2}} = 0; \quad C_{|r=R} = 0; \quad C_{|t=0} = C_0.$$

On the assumption that

- the gas is uniformly distributed in the solution
- the extraction rate is limited by the diffusion within the specimen rather than by the surface reactions;
- the diffusion coefficient does not depend on concentration.

Equation (2.1) takes the following form

$$\frac{Q_t}{Q_0} = 1 - \left\{ 4 \sum_1^{\infty} \frac{1}{\beta_n^2} \exp \left(-\frac{D\beta_n^2 t}{r^2} \right) \right\} \left\{ \frac{8}{\pi^2} \sum_1^{\infty} \frac{1}{(2n-1)^2} \exp \left[-\frac{D(2n+1)^2 \pi t}{\ell^2} \right] \right\}, \quad (2.2)$$

where $-Q_t$ is the amount of the gas released from the specimen within time t , cm^3 (NTP)/ cm^3 ; Q_0 – the initial content of gas, cm^3 (NTP)/ cm^3 ; ℓ and r – length and radius of the specimen, respectively, cm; D – diffusion coefficient, cm^2/sec ; β_n is the n -th root of the Bessel function of the first kind order zero.

For low values of time t and for all time values when the ratio ℓ/r is not too small the series in the right part of equation (2.2) can be replaced with its first summand

$$1 - \frac{Q_t}{Q_0} = \frac{32}{\pi^2 \beta_1^2} \exp \left[-\left(\frac{\pi^2}{\ell^2} + \frac{\beta_1^2}{r^2} \right) Dt \right], \quad (2.3)$$

where $\beta_1 = 2.405$.

Giving experimental data as the dependence of $\lg \left(1 - \frac{Q_t}{Q_0} \right)$ on time the coefficient of hydrogen diffusion may be defined by slope ratio (tg α) of the linear part of the curve,

$$D = -2,3\text{tg}\alpha \frac{1}{\left(\frac{\pi^2}{\ell^2} + \frac{\beta_1^2}{r_0^2}\right)}. \quad (2.4)$$

In particular, authors [40, 52] used this method to determine hydrogen diffusion coefficients in aluminium

For precise determination of diffusion coefficients the gas must be in solid solution, i.e. the specimen must not contain pores and hydrides. Aluminium hydride –AlH forms only under special conditions (in sparks or an electric arc) [56, 57].

Therefore it is necessary to prevent any evolution of metal porosity during the extraction. To this effect, pore-free aluminium specimens with a low gas content were prepared.

First, 90-mm cylindrical bars 250 mm long were lathed from from a 100 mm round ingot of 99.996 % Al, continuously cast at the speed of 20 cm/min, and then pressed at 600 °C to obtain 12 mm rods. The metallographic analysis as well as the X-ray microradiography did not show any discontinuity flaws in the metal. The content of gases in the rod was 0.10 cm³/100 g. Then 8 mm round specimens, 20 mm high, were lathed from these rods as described in [58].

2.2 Comparison between the present results and literature

Table 2.1 and Fig. 2.1 give the results of the determination of hydrogen diffusion coefficients in aluminium within the temperature range of 500–640 °C. Later, using the same technique we determined the value of the diffusion coefficient at 400 °C that made around 8.3·10⁻⁶ cm²/sec.

Table 2.1

Coefficients of hydrogen diffusion in aluminium in the range of 500 – 600 °C

Temperature, °C	Coefficient of diffusion, $D \cdot 10^5$ cm ² /sec
500	3.15
550	6.30
600	10.50
640	14.80

The temperature dependence of the hydrogen diffusion coefficient in aluminium D_4 , cm^2/sec , obtained by four points (see table 2.1) is as follows:

$$D_4 = 0.776 \cdot \exp\left(-\frac{64780 \pm 2675}{RT}\right). \quad (2.5a)$$

where $R \sim 8,314$ (J/mol·K)

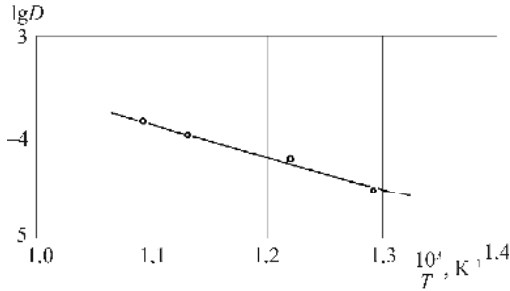


Fig. 2.1 The temperature dependence of hydrogen diffusion coefficient in aluminum

For the straight line $y = ax + b$ (Fig. 2.1), calculated by the least square method, the correlation coefficient $k_4 = 0.9983$, variances $d_a = 0.13970$ and $d_b = 0.16620$.

The calculation carried out through five points, i.e. accounting for the point corresponded to the hydrogen diffusion coefficient at 400°C (D , cm^2/sec) gave

$$D_5 = 0.525 \cdot \exp\left(-\frac{62002 \pm 1393}{RT}\right). \quad (2.5b)$$

In this case for the calculated straight line $k_5 = 0.9992$ and variances $d_a = 0.07277$ and $d_b = 0.09129$.

Expressions (2.5a) and (2.5b) are very much alike, but parameters k and d make expression (2.5b) preferable.

The comparison of theoretical [59] and experimental [60] results for the hydrogen diffusion coefficient at 300 K ($D = 1.4 \cdot 10^{-11} \text{ cm}^2/\text{sec}$ and $D = 1.1 \cdot 10^{-11} \text{ cm}^2/\text{sec}$, respectively) leads to the same conclusion. The extrapolation of equations 2.5a and 2.5b to this temperature gives $D = 0.41 \cdot 10^{-11} \text{ cm}^2/\text{sec}$ and $D = 0.84 \cdot 10^{-11} \text{ cm}^2/\text{sec}$, respectively.

At the same time, the facts above prove the truthfulness of the temperature dependence of the coefficient of hydrogen diffusion in aluminium (2.5b) within a wide range of temperatures (300 – 913 K).

We studied hydrogen release from 5 mm aluminium specimens, 15 mm high, to estimate the possibility of the influence of surface reactions as well as the influence of the oxide film itself.

The values of the hydrogen diffusion coefficient in aluminium in the temperature range of 500 – 640 °C happened to be identical both for the 5 mm specimens, 15 mm high, and the 8 mm specimens, 20 mm high. In our method this fact speaks in favor of the limiting role of hydrogen diffusion in aluminium in the process of hydrogen release from the metal rather than that of surface reactions or the oxide film effect.

Table 2.2 and Fig. 2.2 give other authors' data. Our data are close to the results from [61–63] but they differ significantly from those by the others. It is possible to explain some of these discrepancies.

Table 2.2

Data of hydrogen diffusion in aluminium

Material	Method	D_0 , cm ² /sec	E, kJ/mol	Source
99.999 % Al	Desorption 633 – 875 K	0.11	41	[38]
99.999 % Al	Desorption 673 – 773 K Cylindrical specimens $d = 100$ mm; $\ell = 40$ mm	$1.5 \cdot 10^5$	140	[51]
Al-7 % Mg	Calculation by vacuum- degassing curves 613 – 772 K	340	102.8	[40]
Al	Calculation by degassing curves Cylindrical specimens $d = 16 - 20$ mm; $\ell = 150$ mm	0.21	45.6	[52]
Al	Desorption 843 – 903 K	$2 \cdot 10^{-2}$	50.28	[64]
99.8 % Al	Desorption 723 – 863 K	$2.5 \cdot 10^{-2}$	90±6	[65]
99.999 % Al	Desorption 723 – 863 K	$1.9 \cdot 10^{-1}$	40±4	[66]

Material	Method	D_0 , cm ² /sec	E, kJ/mol	Source
99.999 % Al water treated	Desorption 723 – 863 K	$1.27 \cdot 10^{-3}$	71±9	[66]
99.995 % Al	Desorption 723 – 898 K	$1.01 \cdot 10^{-1}$	47.7	[67]
Al	573 – 923 K	$4.6 \cdot 10^{-3}$	37.03	[68]
99.9999 % Al	Quadruple mass analyzer 573 – 673 K	$2.6 \cdot 10^{-1}$	58.6	[61]
Al	Electrolytic 283 – 681 K	$9.2 \cdot 10^{-4}$	55.25	[62]
99.999 % Al	Penetrating glow-discharge 446 – 681 K	$(6.1 \pm 0.5) \cdot 10^{-5}$	54.8	[69]
99.99 % Al	Gross specimen averaged data from various methods 673 – 933 K	$2.1 \cdot 10^{-1}$	45.4	[70]
99.99 % Al	Desorption 293 – 893 K	$6.0 \cdot 10^{-3}$	83.6	[71]
99.99 % Al Cylindrical specimens: $d = 4$ mm; $\ell = 20$ mm; $m = 0.5 - 0.6$ g	Mass-spectrometry 673 – 878 K	10^{-2}	40.96±2	[44]
99.5 % Al Membrane Thickness – $0.5 \cdot 10^{-3}$ m; $d = 3.5 \cdot 10^{-2}$	Hydrogen concentration impulse 573 – 698 K	4±2	50±4	[72]
99.999 % Al	Desorption 303 – 873 K	$(1.75 \pm 0.15) \cdot 10^{-4}$	16.2±0.15	[73]
Al A99 Cylindrical specimens: $d = 1.2$ cm; $\ell = 0.29$ cm	Mass-spectrometry 773 – 873 K	0.12	60.6	[63]

E.g., the initial content of hydrogen in the aluminium specimens studied was around $0.1 \text{ cm}^3/100 \text{ g}$ while in work [51] it was approximately $0.2 \text{ cm}^3/100 \text{ g}$. Therefore, this may evidence in favor of a considerably lower metal unsoundness developed in our aluminium specimens than in the specimens used in [51].

Hence, it is possible to suppose that the formation of a greater porosity, in absolute value, in specimens during the analysis in [51] led to changes of the nature of hydrogen diffusion in aluminium. The process of hydrogen transfer from pores into the metal could contribute significantly into the gas release kinetics. Herewith the kinetics of the whole process of hydrogen liberation from aluminium changed too. Therefore, we might suppose that the authors of [51] had studied not the diffusion of hydrogen in

aluminium, but the overall process of hydrogen transfer from pores into the metal as well as hydrogen diffusion in the metal.

The discrepancies in the hydrogen diffusion coefficients and the activation energy values might be caused by differences of the materials used, as well as by not accounting for 'surface' and captured-by-traps hydrogen.

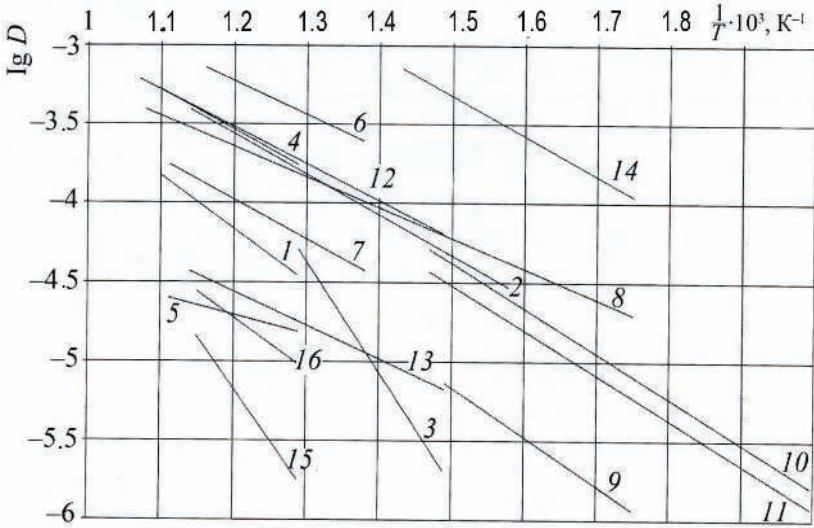


Fig. 2.2 Comparison of author's data with data from other sources:
 1 – Results of this work; 2 – [38]; 3 – [51]; 4 – [52]; 5 – [64]; 6 – [66];
 7 – [67]; 8 – [68]; 9 – [61]; 10 – [62]; 11 – [69]; 12 – [70]; 13 – [44];
 14 – [72]; 15 – [73]; 16 – [63]

CHAPTER 3. HYDROGEN DIFFUSION IN THE ALUMINIUM-ALUMINIUM OXIDE SYSTEM

3.1 Hydrogen diffusion through an oxide film on aluminium surface

The information concerning the dependence of hydrogen permeability on annealing time suggests that the reconstruction of the metal-oxide boundary resulting in the formation of crystalline $\gamma\text{Al}_2\text{O}_3$ particles [74] changes the limiting stage of the process.

The effective cross-section for hydrogen diffusion through the metal dwindles with a growing fraction of $\gamma\text{Al}_2\text{O}_3$ particles at the metal-oxide boundary. This explains the reduction of the hydrogen flow through aluminium during high-temperature annealing.

The mechanism of the process of hydrogen transfer through aluminium changes when the most part of the 'aluminium-aluminium oxide' interface gets covered with crystalline $\gamma\text{Al}_2\text{O}_3$ particles. Hereafter, the rate of hydrogen adsorption on the metal-oxide interface starts to determine the rate of hydrogen penetration through the metal.

This explains the zero order of the reaction at high pressures, as well as the growth of the activation energy of aluminium permeability to hydrogen after a long-term high-temperature annealing. These changes might not affect the mode of the dependence of aluminium permeability to hydrogen on hydrogen pressure, if the changes would occur in the oxide film but not at the metal-oxide interface.

3.2 Hydrogen diffusion in aluminium specimens in the presence of aluminium oxide particles

Many authors [32–35, 43, 75–80] say about the prominent role of aluminium oxide particles, contained in aluminium, in the development of gas flaws in the metal.

They suppose that the presence of oxide particles causes gas defects in the metal. The main role in these hypotheses is allotted to the surface of oxide particles where these defects develop easier.

At the same time, the kinetics of gas porosity depends on the rate of hydrogen redistribution within the metal structure in the course of heat

treatment. Therefore, the influence of aluminium oxide on hydrogen diffusion in aluminium also requires a thorough study. Unfortunately, there is no literature data concerning the influence of aluminium oxide on hydrogen diffusion in aluminium. The problem is complicated by difficulties both in getting aluminium with a given amount of aluminium oxide and in accurate evaluation of hydrogen diffusion coefficients.

Within our framework, aluminium specimens with various contents of aluminium oxide were prepared by adding powdered aluminium oxide (up to 0.7 %) into a 99.996 % aluminium melt with simultaneous ultrasonic stirring [81]. The melt was treated in a crucible of a 1 kg capacity.

Metallographic examinations showed that the aluminium oxide was uniformly dispersed in the metal structure (Fig. 3.1–3.3). The size of aluminium oxide particles was around $5\mu\text{m}$. The content of aluminium oxide in the alloy was determined using the bromine-methanol technique [43].

Upon adding aluminium oxide the aluminium alloy was crystalized in the crucible.

8 mm-round bars, 20 mm high, were lathed from the ingot obtained. For vacuum degassing of the specimens, the installation described in Chapter1 was used.

The efficient diffusion coefficient of hydrogen was calculated from the kinetic curves of hydrogen release.



Fig. 3.1 Microstructure of aluminium-aluminium oxide composition at 0.05 % of aluminium
(The photograph was made in polarized light)

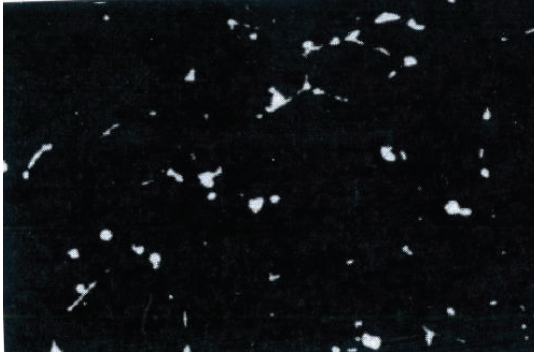


Fig. 3.2 Microstructure of aluminium-aluminium oxide composition at 0.44 % of aluminium oxide



Fig. 3.3 Microstructure of aluminium-aluminium oxide composition at 0.076 % of aluminium oxide

Fig. 3.4 presents the results for hydrogen diffusion in the aluminium-aluminium oxide system in the temperature range of 500 – 600 °C.

The values of the hydrogen diffusion coefficient in pure aluminium had been obtained earlier as described in Chapter 2. To enhance the reliability of the method we determined the coefficients of hydrogen diffusion in pure aluminium pre-treated with ultrasound.

The efficient coefficient of hydrogen in the aluminium alloy pronouncedly decreases with the addition of about 0.05 % of aluminium oxide within the total temperature range under study (Fig. 3.4). The further addition of aluminium oxide leads to slower decreasing of efficient coefficients of hydrogen diffusion in aluminium alloys.

For example, the addition of 0.05 % of aluminium oxide into the aluminium melt at 540 °C results in reduction of the efficient coefficient of hydrogen diffusion in the alloy from $5.9 \cdot 10^{-5}$ down to $4 \cdot 10^{-5}$ cm²/sec.

Increasing temperature makes the drop of the curve of the efficient coefficient of hydrogen diffusion variation with introduction of the aluminium oxide (Fig. 3.5) less expressed.

It is possible that either the Al oxide is impenetrable for hydrogen or the coefficient of hydrogen diffusion in aluminium oxide is significantly lower than in aluminium.

The authors [82, 83] present the data concerning a drastic fall of the efficient diffusion coefficient with moderate additions of the ‘slow’ phase, i.e. the phase having the coefficient of the third component diffusion lower than in the matrix.

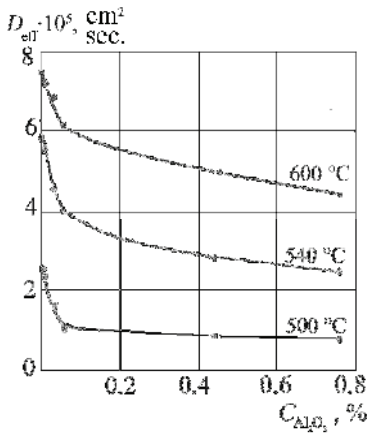


Fig. 3.4 The dependence of the efficient coefficient of hydrogen diffusion in aluminium – aluminium oxide system on oxide aluminium percentage and temperature

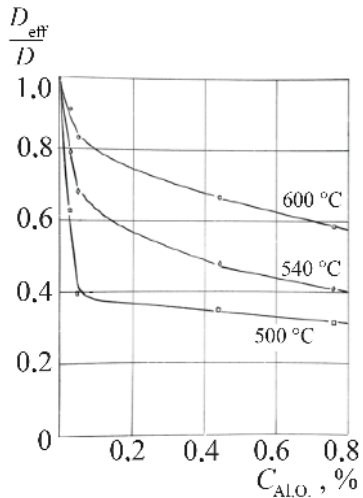


Fig. 3.5 The dependence of the ratio of the coefficients of hydrogen diffusion in the ‘aluminium – aluminium oxide’ system and in pure aluminium on oxide aluminium percentage and temperature

However, the phenomenological theory of diffusion is not able to explain our experimental results. If we assume that aluminium oxide particles are impenetrable for hydrogen and hence reduce the effective cross-section for diffusion, the efficient coefficient of hydrogen diffusion in the alloy should dwindle almost linearly with growing oxide content.

Our additions of Al_2O_3 should have reduced the efficient diffusion coefficient by only few percent, but not by 20 – 60 % as observed in the experiment (Fig. 3.5). Moreover, it is impossible to explain the drastic drop of the effective hydrogen diffusion coefficient at adding very small amounts of the “slow phase” (below 0.1 % Al_2O_3 , Fig. 3.4).

To understand this phenomenon we can suppose the following.

The time of propagation of the ‘cloud’ of atoms diffusing beyond the volume of the metal, selected so that each volume contains one particle of aluminium oxide, determines the effective rate of hydrogen travel within the metal. If the coefficient of hydrogen diffusion in the oxide phase is significantly lower than that in the aluminium matrix then the residence time for diffusing atoms within the matrix and in an oxide particle could be comparable even at a rather low ratio of oxide- to- metal volumes.

Therefore, the addition of small amounts of the ‘slow’ phase should noticeably affect the efficient coefficient of diffusion of the alloy.

The plain reduction of the efficient coefficient of hydrogen diffusion in the alloy and the subsequent growth of the ‘slow’ phase right after the dramatic drop, could be explained by the diffusion of hydrogen in the slower phase, starting from a definite concentration of aluminium oxide.

It seems likely that the activation energy of hydrogen diffusion being higher in the aluminium oxide as compared to the activation energy of hydrogen diffusion in aluminium causes a less expressed reduction of the efficient diffusion coefficient with temperature [84].

The possibility of the effect of the specific structural features of the specimens obtained by the melt crystallization in the ultrasonic field calls for special attention.

It is known that over than the threshold values of the power of ultrasonic vibrations lead to a smaller grain size in the alloy. It has been shown also that even very small additions of insoluble fine inclusions can cause a manifold increase of the ultrasonic effect. The impact of grain refinement rises with growing ultrasonic power and/or increasing volume fraction of inclusions.

Both the Al refined grain structure formed through ultrasonic processing and the Al_2O_3 particles located on its elements (e.g. grains, subgrains) create a system of ‘traps’ and, therefore, must affect the effective hydrogen diffusion coefficient by reducing it.

Following this reasoning the concentration dependence of the effective hydrogen diffusion coefficient on the Al_2O_3 content (Fig. 3.4) is caused by

the effective refinement already by small additions of Al_2O_3 (up to ~ 0.05 mass %) whereas an additional grain refinement with the further increase in the specific density of Al_2O_3 particles will have a much lower influence on the diffusion of the hydrogen present in the alloy.

It can be expected that increasing Al_2O_3 content in the alloy from 0.1 % to 0.76 % must produce the observed lower decrease of the diffusion coefficient also due to the impact of such factors as the already mentioned ‘classical’ reduction of the effective diffusion cross-section with growing amounts of Al_2O_3 both on the grain boundaries and inside grains (e.g. as suggested in [84]) owing to the influence of intragranular particles on the substructure formed during cooling of the crystallized ingot part under ultrasonic processing and the like.

Irrespective of the treatment of the experimental results we may conclude that the aluminium oxide present in aluminium ambiguously affects the process of gas porosity in aluminum alloys. The surface of oxide particles may serve as a gas flaw nucleus and, hence, favour the formation of gas cavities. On the other hand, the introduction of oxide particles into molten aluminium decreases the rate of hydrogen transfer in the metal, thus slowing down the growth of metal flaws caused by gases in the metal.

Further studies would be required to provide qualitative estimation of the contribution of each of the indicated factors to the formation of metal flaws induced by gases.

CHAPTER 4. HYDROGEN PERMEABILITY OF ALUMINIUM

Hydrogen permeability is one of the most important characteristics of hydrogen and metal.

The relationship between hydrogen permeability, solubility and diffusion of hydrogen is as follows:

$$\Pi = DK_s \quad (4.1)$$

where Π – permeability constant (the coefficient of proportionality between gas flow Q and external pressure of this gas P), D and K_s – coefficients of diffusion and gas solubility in the metal, respectively (see Introduction).

This expression often serves as a basis for calculation of hydrogen diffusion coefficients at definite values of hydrogen solubility in the metal.

Exact values of hydrogen permeability may be useful for qualitative description of processes of hydrogen penetration through the metal, hydrogen release from pores, hydrogen penetration through oxide films, what may be consistently valuable for practical purposes.

Smithells and Ransley [85] first carried out the systematic study of the hydrogen permeability of aluminium in 1935. They studied hydrogen permeability in the temperature range of 500 – 600 °C under pressure 32 – 290 mm Hg (i.e. $4.3 \cdot 10^3$ – $3.9 \cdot 10^4$ Pa).

Nevertheless up today the determination of reliable values of the hydrogen permeability of aluminium as well as the estimation of factors affecting the results of corresponding studies remained quite a difficult problem.

The matter is that during experiments at high temperatures there may occur transformations of the metal structure (e.g. the recrystallization of metal), as well as formation, growth and structural transformation of oxide films on the surface of specimens, resulting in the reduction of hydrogen flow through the specimen, thus invalidating the test.

To minimize the role of these factors we have to determine hydrogen permeability at lower temperatures.

However, the values of hydrogen permeability rapidly drop with decreasing temperature, making its measurement rather difficult according to procedures given in [85–87].

Therefore, for studies of the hydrogen permeability of aluminium and reliable data acquisition we had to develop a new technique using high-sensitive instrumentation providing the measurements at 200 – 350 °C.

4.1 The technique of hydrogen permeability investigation at temperatures below 350 °C

We have developed a method which helps to study hydrogen permeability of aluminium at temperatures below 350 °C.

The proposed method differs from the methods described in [85 – 87] by the use of a mass-spectrometric analyzer as well as by the use of a specially prepared specimen and a method of its connection to the vacuum system.

Fig. 4.1 gives the layout of the installation.

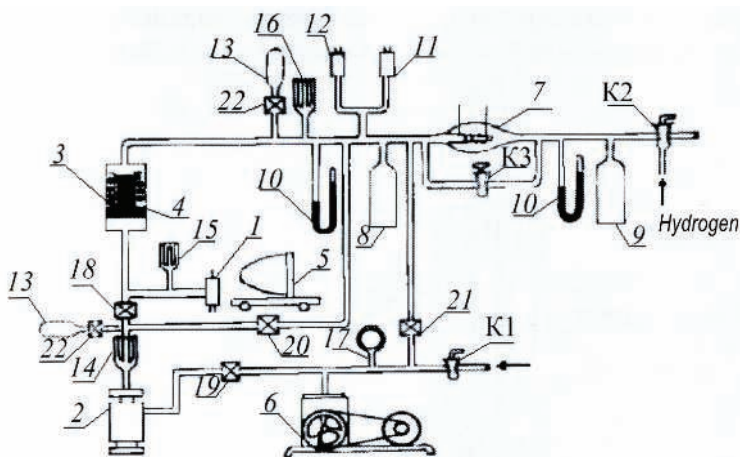


Fig. 4.1 Installation layout:

- 1 – sensor PMO-4C of mass-spectrometric analyzer ИПДО-1; 2 – mercury vapor diffusion pump ДРН-10; 3 – resistance furnace; 4 – aluminium specimen; 5 – permanent magnet; 6 – fore pump БН-461-в; 7 – palladium filter; 8 and 9 – glass bottles; 10 – U-type mercury pressure gauge; 11 and 12 – pressure gauge sensors ЛТ2 and ЛМ2; 13 – standard glass bottle; 14 – 17 – glass traps with liquid nitrogen; 18 – 21 – vacuume valves ДУ-8; 22 – valve ДУ-2 for fine flow adjustment; K₁ – K₃ – vacuum glass valves

The idea of the proposed method is as follows. Tubular aluminium specimen (4), closed from one end, is sealed to the system hermetically.

The system provides a high vacuum at both sides of the specimen. Then the specimen is heated up to a specified temperature while hydrogen supplied from the outside and then diffusing through the walls of the tube is continuously pumped. Mass-spectrometric analyzer sensor ИПДО-1 (1) measures the partial pressure of hydrogen at the high-vacuum side.

The hydrogen flow passing through the specimen (at the constant rate of pumping) is proportional to the partial pressure of hydrogen. The hydrogen permeability is calculated from the stabilized value of the hydrogen flow. Mercury vapor diffusion pump ДPH-10 (2) characterized by a steady rate of pumping within a wide range of pressures provides rarefaction about $1 \cdot 10^{-7}$ mm Hg (i.e. $1.3 \cdot 10^{-5}$ Pa). The palladium filter (7) cleans hydrogen passing through. U-type pressure gage (10) measures pressure at the inlet side. Glass trap (16) entraps mercury vapor. The background pressure of hydrogen in the system determines the accuracy of the method as well as its sensitivity. The background concentration of hydrogen particularly depends on the degree of sealing between the specimen to the vacuum system.

The authors of [85–87] say that during the heating of the specimen the joint of the specimen with the system was prone to overheating which resulted in vacuum deterioration.

In our experiments, we used intricately-shaped cylindrical specimens closed from one end (Fig. 4.2). The thin walled cylindrical part of the specimen, 100 mm long, having outer diameter of 10 mm and wall thickness of 0.5 mm, serves to determine hydrogen permeability of aluminium. The flow of hydrogen passing through the operational part of the cylinder with walls 0.5 mm thick, is much higher than that through the bottom of the 10 mm cylinder, 10 mm high, and the base of the cylinder having diameter 60 mm and height 140 mm.

The resistance furnace is mounted on the surface *A–A* at some distance from the seal joint between the specimen and the system (surface *B–B* and *C–C*), see Fig. 4.2.

The flanged ring seal provides airtight connection of this specimen to the system (Fig. 4.3).

Two flanges with stainless steel ring teeth (6), see Fig. 4.2, connected with bolts, were drawn together so that the teeth got indented into the surface *B–B* and *C–C* of the specimen, thus providing a good gas tightness of the joint.

However, flanges with wedged ring teeth did not allow the required gas tightness of the joint to be reached. The wedged teeth cut aluminium but do not provide the specified gas tightness.

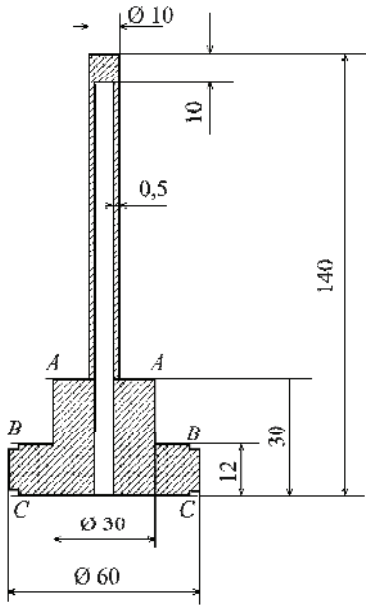


Fig. 4.2 The specimen for the installation for determination of the hydrogen permeability of aluminium

In our work we used flanges with teeth having an internal groove designed by A.V.Balitzky, N.B.Bublik, L.A.Filatovsky, A.S.Shuvalov (see Fig. 4.3). In so doing, additional stress concentration was artificially formed in the aluminium, which gave the required tightness of the coupling.

To ensure a regular temperature redistribution in the specimen and reduce the temperature near the coupling of the specimen with the system we placed the resistance furnace inside the vacuum system at the hydrogen input side.

The resistance furnace with a variable number of coils kept the temperature drop along the specimen length within $\pm 5^\circ\text{C}$.

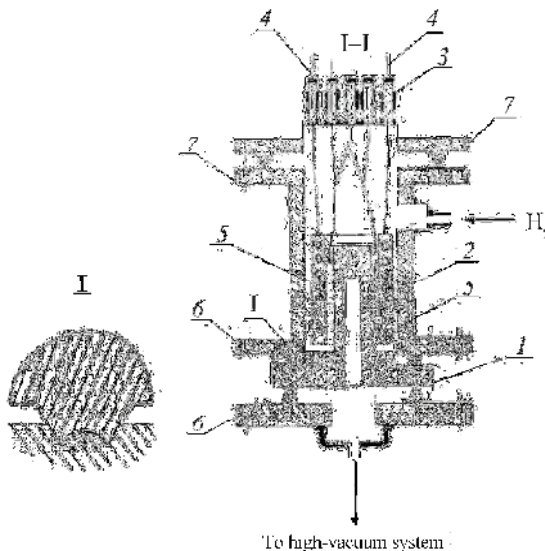


Fig. 4.3 Layout of specimen mounting in the apparatus for determination of hydrogen permeability:

- 1 – Aluminium specimen;
- 2 – resistance furnace;
- 3 – metal-ceramic inlets;
- 4 – electric cable entries;
- 5 – quartz shell;
- 6 and 7 – metallic flanges

Two chromel-alumel thermocouples ensured the temperature control. The input leads for electric supply of the resistance furnace and thermocouple wires entered the vacuum system through gas sealed metal-ceramic inlets (3). Besides, the thermocouples entered the vacuum system through rods weld into the metal – ceramic inlets. The calibration procedure was as follows.

Hydrogen was supplied into standardized bottle (13) soldered to the system from the hydrogen inlet side (see Fig. 4.1) Then the standard bottle and fine adjustment valve ДУ-2 (22) were soldered off from the system and soldered to the system from the high-vacuum side.

On obtaining the high vacuum, the valve ДУ-2 got opened so that the pressure in the system did not exceed $1 \cdot 10^{-5}$ mm Hg ($1.3 \cdot 10^{-3}$ Pa) and passed the hydrogen from the standardized bottle into the system.

K_n was calculated similarly to the case of determination of hydrogen percentage in aluminium (see chapter 1). The sensor of mass-spectrometric analyzer BGLJ-1 was connected to the system in parallel.

The flow of hydrogen through the specimen dQ , cm^3 (NTP) at each moment of time makes

$$dQ = K_1 S J dt, \quad (4.2)$$

where K_1 – sensitivity to hydrogen of the mass-spectrometric analyzer, $1/V$, S – rate of hydrogen pumping in the cross-section of the sensor of the mass-spectrometric analyzer, cm^3/sec .; J – signal value, V

At the steady values of the flow of hydrogen passing through the specimen the flow rate (i.e. the hydrogen permeability of the total specimen) will be as follows

$$\frac{dQ}{dt} = K_1 S J_{st} = K_n J_{st} = Q_{st} \quad (4.3a)$$

Then excluding the direct influence of specimen geometry on quantitative results for case specific parameters (temperature and hydrogen pressure), we obtain the specific hydrogen permeability Π' , $\frac{\text{cm}^3(\text{NTP}) \cdot \text{cm}}{\text{cm}^2 \cdot \text{sec}}$

$$\Pi' = Q_{st} \cdot \frac{\delta}{A} = \frac{K_n J_{st} \delta}{A} \quad (4.3b)$$

where δ – specimen wall thickness, cm ; A – specimen surface area, cm^2 .

4.2 Comparison between the present results and literature

We studied the hydrogen permeability of aluminium within the temperature range of 200–300 °C at hydrogen pressure 1–200 mm Hg (133.2–2.7·10⁴ Pa).

The control experiments showed that the steady flow of hydrogen through aluminium specimens did not change during the ten-hour experiment within the specified range of hydrogen pressures and temperatures; it means that one of the main goals of our method was achieved.

Fig. 4.4 presents the dependence of the hydrogen permeability of aluminium specimens on the pressure of hydrogen at 290 °C, approximately. There is a linear relationship between hydrogen permeability and square root of hydrogen pressure. This fact perfectly corresponds with literature data concerning the hydrogen permeability of metals [1–4].

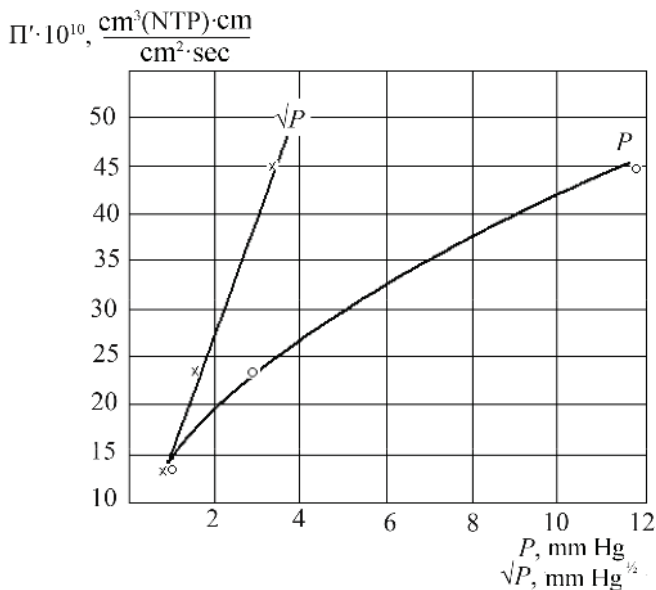


Fig. 4.4 The dependence of the hydrogen permeability of aluminium on hydrogen pressure at temperature of ~290 °C

We determined the reproducibility of the proposed technique in the series of hydrogen permeability tests, carried out on eight specimens of 99.996 % aluminium at about 230 °C and hydrogen pressure 57 mm Hg ($7.6 \cdot 10^3$ Pa).

The value of hydrogen permeability Π , $\frac{\text{cm}^3(\text{NTP}) \cdot \text{cm}}{\text{cm}^2 \cdot \text{sec} \cdot (\text{mm Hg})^{1/2}}$

$$\Pi = \frac{\Pi'}{\sqrt{P}} \quad (4.4)$$

where P – the partial pressure of hydrogen from the side of hydrogen inlet.

The obtained value of $\Pi = 1.3 \cdot 10^{-10} \pm 8.0 \cdot 10^{-12} \frac{\text{cm}^3(\text{NTP}) \cdot \text{cm}}{\text{cm}^2 \cdot \text{sec} \cdot (\text{mm Hg})^{1/2}}$ at

maximum deviations from the average value $\pm 0.1 \cdot 10^{-10}$ says in favor of high reproducibility of the obtained results.

In this way our technique of decreasing the test temperature from approximately 500 °C down to 200 – 350 °C makes it possible to remove surface defects and obtain the information concerning the hydrogen permeability of aluminium.

Fig. 4.5 presents the temperature dependence of hydrogen permeability of aluminium at hydrogen pressure about 30 mm Hg ($4 \cdot 10^3$ Pa).

We had found out that it is possible to express the dependence of hydrogen permeability of aluminium on temperature like follows.

$$\Pi = 0.35 \exp\left(-\frac{91100}{RT}\right), \quad (4.5)$$

i.e. the activation energy of the hydrogen permeability process is about 91.1 kJ/mol. This value perfectly corresponds with the data of Eichenauer [38, 52] but does not correspond with the data presented by Ranslay in [51] related to separate determination of hydrogen diffusion coefficients in aluminium.

A few words about more recent data presented in [88], where the omegatron sensor PMO-4c was used as the analyzer. The experiments were carried out in the temperature range of 723 – 863K at hydrogen pressure of 16 – 650 mm Hg ($2 \cdot 10^3$ – $8.7 \cdot 10^4$ Pa).

The experimental data (isotherms for 450, 500, 550 and 590 K) given in Fig. 4.6 [88] correspond to the activation energy of the hydrogen per-

meability process, i.e. ~ 110 kJ/mol for the diapason of hydrogen pressure $\sim 100 - 650$ mm Hg ($\sim 1.3 \cdot 10^4 - 8.7 \cdot 10^4$ Pa), where a near-linear dependence of Π' on \sqrt{P} was observed.

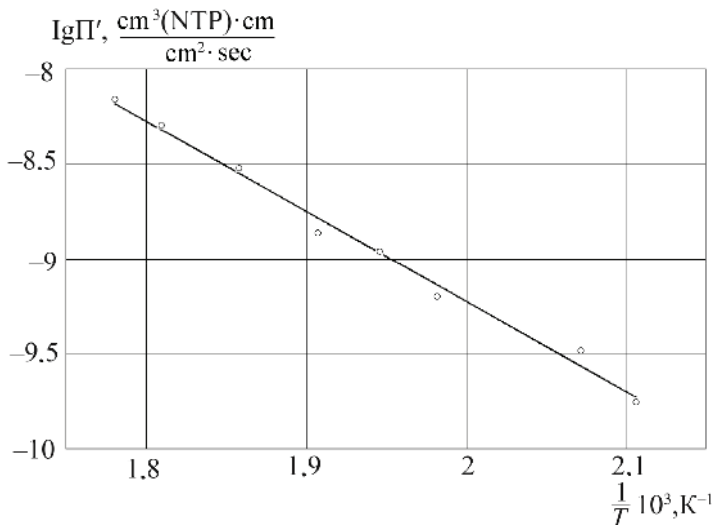


Fig. 4.5 Temperature dependence of the hydrogen permeability of aluminium

The authors gave the equation of temperature dependence of hydrogen permeability corresponding to a bit lower activation energy, ~ 104.6 kJ/mol (we use here the units of measurement accepted in this book)

$$\Pi = 3,58 \exp\left(-\frac{104600}{RT}\right). \quad (4.7)$$

The activation energy value obtained is considerably higher than that resulted from our experiments.

Fig. 4.6 gives the comparison of data obtained by several authors.

As for the given temperature range, hydrogen impermeability is connected to the square root of hydrogen pressure, while the hydrogen flow is constant during the experimental process, it can be stated that we have got reliable values of hydrogen impermeability in aluminium [89].

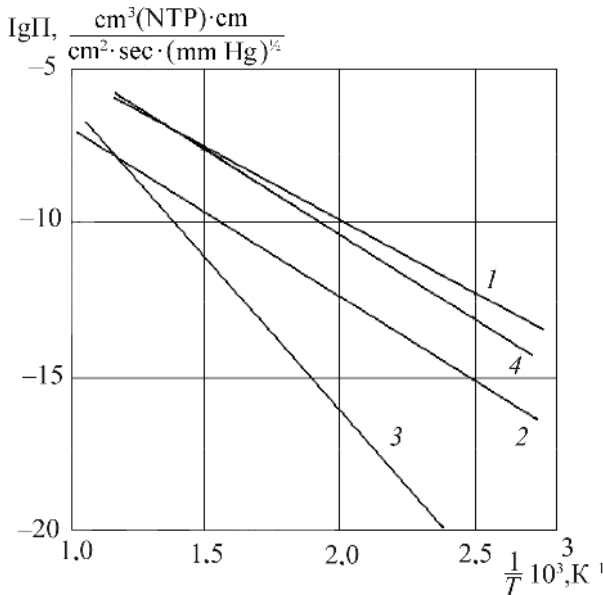


Fig. 4.6 The comparison of data concerning hydrogen permeability of aluminium (1) with other authors' data (2, 3 and 4) ((2) – [38]; (3) – [51], [37]; (4) – [88]))

The values of activation energy of hydrogen solubility in aluminium given in literature are very close.

It seems likely that the value of the activation energy of hydrogen solubility in aluminium ~ 32.6 kJ/mol given in [90] is the most accurate since the mass-spectrometric analyzer was used there.

Assuming that the activation energy of hydrogen permeability of aluminium makes 91.1 kJ/mol, and the activation energy of hydrogen solubility in aluminium 32.6 kJ/mol [90] we calculated the activation energy of hydrogen diffusion in aluminium that happened to be equal to 58.5 kJ/mol.

This value perfectly corresponds with the experimentally determined value of the activation energy of hydrogen diffusion in aluminium (62 kJ/mol) given in Chapter 2. Therefore we can state that the value of the activation energy of hydrogen in aluminium given by Ransley et al. in [51], i.e. from ~ 140 to ~ 180 kJ/mol is too high.

4.3 The effect of preliminary annealing on experimental results of hydrogen permeability of aluminium

To clarify the reasons of the hydrogen flow decrease observed in a number of studies of hydrogen permeability of aluminium at enhanced temperatures we pre-annealed aluminium specimens in vacuum at 500 °C and then reduced the temperature below 350 °C and measured its hydrogen permeability.

The data presented in Fig. 4.7 demonstrate the hydrogen permeability of pre-annealed aluminium specimens at temperatures 200 – 350 °C. The specimens were pre-annealed at 500 °C.

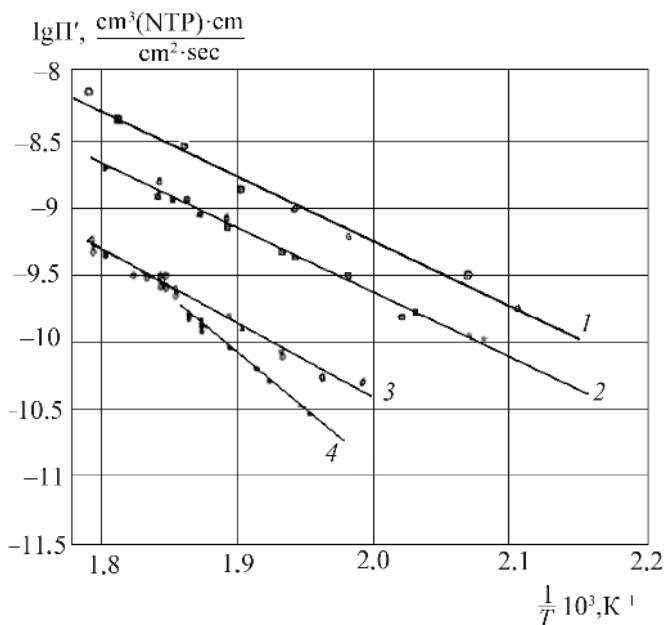


Fig. 4.7 The influence of pre-annealing of aluminium specimens at 500°C on results of determination of hydrogen permeability dependence on temperature (hydrogen pressure ~30 mm Hg (~4·10⁴ Pa)).
The annealing time: 1 – 0 hours; 2 – 12 hours; 3 – 24 hours; 4 – 30 hours

The data given in Fig. 4.7 say that pre-annealing during 12 hours, in fact, does not influence the straight line slopes $\lg\Pi' - 10^3/T$, i.e. the ob-

tained value of the activation energy (~ 91 kJ/mol). On the other hand, this annealing obviously complicates the process of hydrogen passing through the specimen, because of reducing of $\lg \Pi'$ by practically similar value at each of the temperatures within the specified range (see the comparison of straight lines 1 and 2). Increasing annealing time up to 24 – 30 hours leads to a significant growth of the slope of straight lines (3 and 4, respectively), i.e. to an obvious growth of the activation energy calculated from these straight lines. Therefore, the obtained results obviously do not correspond to the hydrogen permeability of aluminium itself.

Fig. 4.8 demonstrates the dependence of hydrogen permeability on hydrogen pressure at approximately 290 °C for specimens pre-annealed at high temperatures. We can see that the nature of hydrogen permeability isotherms changes after annealing at 500 °C. In particular, the linear relation between hydrogen permeability and the square root of hydrogen pressure is broken here. Hereby the transition from unannealed specimens (1) to specimens passed a 12-h annealing at 500 °C (2) results in a change of straight lines slope from approximately 0.5 (i.e. from the proportionality of hydrogen permeability to the square root of hydrogen pressure) to approximately 0.3. It is possible that right after the 12-h annealing, the hydrogen mass-transfer is controlled not only by hydrogen diffusion through aluminium but by surface oxide films as well.

Further increasing of the pre-annealing duration makes the dependence of hydrogen permeability on hydrogen pressure less and less expressed for the specimens under study. Finally after a longtime annealing, the dependence of their hydrogen permeability on hydrogen pressure stops in the high-pressure zone completely.

On the strength of the data in Fig. 4.7 and 4.8 it is possible to expect that the transformation of the metal-oxide interface at high-temperature annealing, bringing to the formation of the crystalline phase $\gamma\text{-Al}_2\text{O}_3$ [23] changes the limiting step of the hydrogen permeability process.

Increasing amounts of $\gamma\text{-Al}_2\text{O}_3$ crystalline particles at the interface metal-oxide result in the reduction of the effective cross-section for hydrogen diffusion through a specimen. After high-temperature, pre-annealing this can result in decreasing hydrogen flow through aluminium at preserved values of the activation energy, being specific for hydrogen diffusion in aluminium.

Therefore we can expect a successive reduction of the hydrogen flow through the specimen in course of studies of hydrogen permeability of

aluminium at higher temperatures (e.g. at temperature $\geq 500^\circ\text{C}$). Some of the authors indeed indicated this fact. It is possible to suppose that the values of the activation energy of the hydrogen permeability presented in [88] for the temperature range of $450 - 590^\circ\text{C}$, overrated as compared to our results, are also caused by oxidation processes on specimen surfaces.

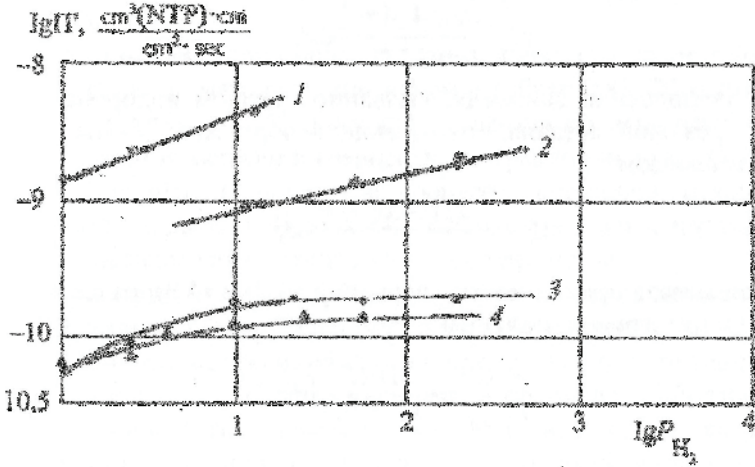


Fig. 4.8 The influence of the pre-annealing of aluminium specimens at 500°C on dependence of hydrogen permeability of specimens on hydrogen pressure
The duration of annealing: 1 - 0 hours, 2 - 12 hours, 3 - 24 hours, 4 - 30 hours

The process mechanism of hydrogen transfer through aluminium changes when the crystalline $\gamma\text{-Al}_2\text{O}_3$ blocks the largest part of the aluminium-aluminium oxide interface. The rate of hydrogen adsorption on the metal oxide (crystals of $\gamma\text{-Al}_2\text{O}_3$) starts to control the rate of hydrogen penetration through the metal. This explains the zero order of the reaction at high pressures of hydrogen, as well as the growth of the activation energy of hydrogen permeability after a long-term, high-temperature annealing. If the oxide film had been directly subjected to changes, but not the metal-oxide interface, then these changes would not have affected the nature of the dependence of hydrogen permeability on hydrogen pressure.

Therefore, the surface oxide films that can form even under vacuum conditions on aluminium specimens affect considerably the results of determination of the dependence of hydrogen permeability on both temperature and hydrogen pressure.

Using our reliable data of hydrogen permeability as the basis it is possible to estimate the possibility of hydrogen removal from pores during vacuum degassing of solid aluminium.

We can express the time t sec., required for the elimination of 99 % of hydrogen from a pore in aluminium as

$$t = \frac{22.4\delta P_0^{1/2} 0.9}{3\Pi RT}, \quad (4.6)$$

where δ – thickness of the metal above the pore, cm; r – radius of the pore; P_0 – initial pressure of hydrogen in the pore, atm.; Π – hydrogen permeability, $\frac{\text{cm}^3(\text{NTP}) \cdot \text{cm}}{\text{cm}^2 \cdot \text{sec}}$; T – temperature, K; R – characteristic gas constant ($R = 0.083 \frac{1 \cdot \text{atm}}{\text{mol} \cdot \text{K}}$).

Indeed, the reduction of pressure in the pore by dP results in decrease of hydrogen inside it (Q) by dQ , $\text{cm}^3(\text{NTP})$,

$$dQ = \frac{22.4 \cdot 4\pi r^3}{3RT} dP \quad (4.7)$$

This reduction of pressure caused by hydrogen emission through the layer of the metal coating the pore to the atmosphere can be expressed as follows:

$$dQ = -\frac{2\Pi \cdot 4\pi r^2 \sqrt{P}}{\delta} dt \quad (4.8)$$

By making equal the right parts of equations (4.7) and (4.8), then separating the variables and integrating we obtain

$$-\int_{P_0}^P \frac{dP}{\sqrt{P}} = \frac{3\Pi RT}{\delta \cdot 11.2r} \int_0^t dt \quad (4.9)$$

$$t = \frac{22.4\delta r}{3\Pi RT} \cdot P_0^{1/2} \left[1 - \left(\frac{P}{P_0} \right)^{1/2} \right] \quad (4.10)$$

Equation (4.10) transforms into (4.6) when 99 % of the gas is removed from the pore. Assuming $\delta = 4$ mm, $r = 10$ mkm, $P_0 = 100$ atm., $T = 540$ °C we obtain $t \approx 0.25$ hour.

CHAPTER 5. THE STUDY OF THE MECHANISM OF ALUMINIUM DEGASSING DURING AIR AND VACUUM ANNEALING

The evolution of gas porosity largely depends on the content of hydrogen in the metal. The degassing of metal can occur during metal heat treatment in air, in an inert atmosphere or under vacuum. This process directly influences metal porosity, and, therefore, its study is of utmost importance.

5.1 Hydrogen emission from metal during vacuum annealing

A continuously cast $\varnothing 100$ -mm ingot of 99.996 % aluminium was made at the casting speed of 20 cm/min. From this ingot $\varnothing 90$ mm cylindrical rods, 250 mm high, were lathed and then pressed at temperature $T = 600$ °C into 12 mm bars.

The metallographic and X-ray microanalyses did not detect any discontinuity flaws in the metal. The content of gas in the metal bars was $0.10 \text{ cm}^3/100 \text{ g}$. Eight mm test specimens, twenty mm high, lathed from aluminium bars according to the procedure presented in work [58], were placed into the installation, where a high vacuum was provided (see Chapter 1). Then the specimen was pushed into the quartz vacuum degassing tube, where the gas released from the specimen was pumped out at a steady rate. Changes in the hydrogen partial pressure in the system were recorded by the sensor of the mass-spectrometric analyzer.

The dependence of the ionic current on the time of the analyses was outlined on the chart of the potentiometer recorder. Having in mind that ionic current is proportional to hydrogen partial pressure, we obtain the area under the 'signal-time' curve (on the chart of the potentiometer) proportional to the total amount of hydrogen in the specimen. Similarly the area under the 'signal-time' curve (from the time t until the end of the extraction S_t) is proportional to the amount of hydrogen remained in the specimen by the moment of time t .

We found that some time after the start of the analysis the dependence

$$\lg S_t = K \lg \frac{Q_t}{Q_0} \text{ on time became linear (Fig. 5.1).}$$

This proves the correctness of the assumptions for equation (2.1) and allows using equation (2.4) for the determination of hydrogen diffusion coefficients in aluminium (see Chapter 2).

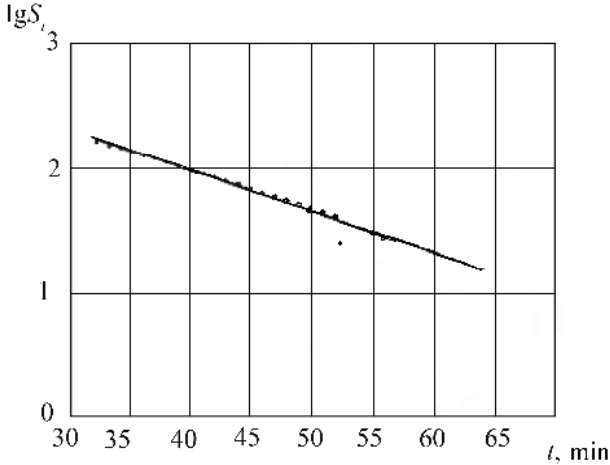


Fig. 5.1 The time dependence of the amount of hydrogen remained in the specimen

5.2 The results of hydrogen extraction during air and inert atmosphere annealing

The interaction of aluminium with air can lead to the formation of nitrides and oxides.



Reactions (1) and (3) are highly exothermic. According to reaction (3), the heat of aluminium oxide formation at 298 °C amounts to 1672 kJ/mol [91]. The heat of aluminium nitride formation makes 240 kJ/mol [92].

The equilibrium constant of reaction (1) for temperature 500 °C, according to [93], is

$$K_p = \frac{P_{\text{H}_2}^3}{P_{\text{H}_2\text{O}}^3} = 3.97 \cdot 10^{44}.$$

In other words, this means that the reaction is strongly shifted to the right.

In the common air atmosphere, the partial pressure of hydrogen makes around 10^{-5} mm Hg ($\sim 1.3 \cdot 10^{-3}$ Pa). The equilibrium solubility at temperature $T = 500$ °C corresponding to this pressure is as follows:

$$K_s = 5 \cdot 10^{-9} \text{ cm}^3/100 \text{ g}$$

The moisture partial pressure in the standard air atmosphere is about 5 mm Hg (666 Pa).

In literature there is no data concerning the equilibrium solubility of hydrogen in solid aluminium from the atmosphere of water steam. Assuming that the solubility of water steam hydrogen in solid aluminium is approximately the same as that of hydrogen from the pure hydrogen atmosphere we have that the equilibrium solubility of hydrogen at $T = 500$ °C and the partial pressure of water steam equal to 5 mm Hg comes up to

$$K_s = 2.7 \cdot 10^{-3} \text{ cm}^3/100 \text{ g}$$

In this way, the standard air atmosphere enables aluminium degassing during annealing when the hydrogen content in aluminium is around $0.1 - 0.3 \text{ cm}^3/100\text{g}$.

According to Fick's law, the rate of degassing is directly proportional to the difference of hydrogen concentrations in the metal and in the subsurface layer. If we assume that the subsurface layer of the metal is in equilibrium with air atmosphere, then the concentration of hydrogen in the subsurface layer makes around $2.7 \cdot 10^{-3} \text{ cm}^3/100 \text{ g}$, and therefore we can ignore this seemingly small value as compared to the concentration of hydrogen in the metal, making up to $0.1 - 0.3 \text{ cm}^3/100 \text{ g}$.

Thus, the rate of degassing will be proportional to hydrogen concentration in metal C , that is

$$\frac{\partial C}{\partial t} = -KC \tag{5.1}$$

The formation of nitrides proceeds at temperatures above 800 °C [94], therefore this reaction can be neglected in the process of aluminium annealing in air. The formation of the oxide layer begins right after aluminium contacting air due to its high affinity to oxygen.

The oxide layer on the metal forms even at room temperature and the thickness comes to 20 Å [95, 96]. The thickness of the aluminium oxide layer grows under heating and its structure changes.

A number of authors [95 – 103] focused their studies on the mechanism of aluminium oxidation. The oxidation of aluminium at room temperature and up to 300 – 350 °C follows the inverse logarithmic law [95, 96].

$$\frac{K_1}{\delta} = K_2 - \lg t, \quad (5.2)$$

where K_1 and K_2 – constants, δ – aluminium film thickness; t – time of oxidation.

The oxidation of aluminium follows to the parabolic law within the temperature range of 350 – 450 °C [97, 98]

$$\delta^2 = K_3 t. \quad (5.3)$$

The kinetics of aluminium oxidation is more complicated at temperatures above 450 °C [96, 101].

A thin homogeneous and amorphous oxide film up to 200 Å thick covers aluminium at temperatures up to 450 °C. The diffusion of metal cations to the oxide-gas interface limits the growth of the oxide film [103].

The long-term exposure of aluminium to an oxidizing atmosphere at 450 °C causes the formation of γ -Al₂O₃ nuclei [102] on the metal-oxide interface. The γ -Al₂O₃ crystals grow parallel to the surface of the metal up to the moment when the total metal-oxide interface is covered by a layer of crystalline γ -Al₂O₃. The transfer of oxygen from the gas phase to the metal-oxide interface limits the formation of crystalline aluminium oxide.

The oxidation of aluminium was studied in detail elsewhere [103] in the temperature range of 450 – 575 °C. It was shown that two independent processes determine the kinetics of aluminium oxidation.

The amorphous film of aluminium oxide grows due to the diffusion of metal cations to the oxide-gas interface. The kinetics of amorphous oxide film growth follows the parabolic law.

γ -Al₂O₃ crystals grow on the metal-oxide interface due to the diffusion of oxygen ions from the gas phase to this surface. The kinetics of this process also follows the parabolic law.

First, the amorphous oxide film covering the surface of aluminium grows. The intensive formation of crystalline γ -Al₂O₃ occurs significantly later than the oxidation starts, i.e. at 450 °C – after 140 hours, at 475 °C – after an hour, while at 500 °C it occurs after 12 hours.

Therefore, if the duration of annealing does not exceed the indicated time then the amorphous oxide film develops on the surface of aluminium and its kinetics follows the parabolic law

$$\delta = \delta_0 + \sqrt{K_0 t} \quad (5.4)$$

According to [103] $K_0, \text{g}^2/(\text{cm}^4 \cdot \text{sec})$,

$$K_0 = 1.25 \cdot 10^{-9} \exp\left(-\frac{225700}{RT}\right) \quad (5.5)$$

The coefficient of hydrogen diffusion in Al oxide is significantly lower than in aluminium as it is shown in Chapter 3. Thus, it is quite natural to assume that the transfer of hydrogen through the oxide film limits the degassing of metal during the annealing of aluminium in air and the degassing rate is in inverse proportion to the oxide film thickness δ , so taking into account equation (5.1) we get

$$\frac{dC}{dt} = -\frac{K_D C}{\delta} \quad (5.6)$$

or taking into account (5.4)

$$\frac{dC}{dt} = -\frac{K_D C}{\delta_0 + \sqrt{K_0 t}} \quad (5.7)$$

where C – the concentration of hydrogen in the specimen at moment t ;
 δ – the initial thickness of the oxide film; K_0 – the constant of the parabolic law of oxidation; K_D – the coefficient of hydrogen mass-transfer through the oxide film.

On integrating equation (5.7), we shall have the following expression

$$\ln \frac{C}{C_0} = -\frac{2K_D}{\sqrt{K_0}} \int_0^t \frac{dt}{\sqrt{t} + \frac{\delta_0}{\sqrt{K_0}}} = -\frac{2K_D}{\sqrt{K_0}} \left\{ \sqrt{t} - \frac{\delta_0}{\sqrt{K_0}} \ln \left(\frac{\sqrt{K_0 t}}{\delta_0} + 1 \right) \right\}. \quad (5.8)$$

Equation (5.8) describes the variation of the hydrogen content in the specimen during the annealing of aluminium in air.

It makes sense that at long-time annealing there should be a linear relationship between $\ln \frac{C}{C_0}$ and the square root of time.

In fact dividing both parts of equation (5.7) by \sqrt{t} we shall have

$$\frac{\ln \frac{C}{C_0}}{\sqrt{t}} = -\frac{2K_D}{\sqrt{K_0}} \left(1 - \frac{\ln \left(\frac{\sqrt{K_0 t}}{\delta_0} + 1 \right)}{\sqrt{\frac{K_0 t}{\delta_0}}} \right) \quad (5.9)$$

When $t \rightarrow \infty$

$$\lim_{t \rightarrow \infty} \frac{\ln \left(\frac{\sqrt{K_0 t}}{\delta_0} + 1 \right)}{\sqrt{\frac{K_0 t}{\delta_0}}} = 0 \quad (5.10)$$

and, respectively, at $t \rightarrow \infty$

$$\ln \frac{C}{C_0} = -\frac{2K_D}{\sqrt{K_0}} \sqrt{t} = -K_\Sigma \sqrt{t} \quad (5.11)$$

where

$$K_\Sigma = \frac{2K_D}{\sqrt{K_0}} \quad (5.12)$$

It is possible to determine the activation energy of hydrogen in the oxide film if the activation energy values of the total process of aluminium degassing and the activation energy of oxide film growth are known.

Taking the logarithm of (5.12), we shall have

$$\ln K_\Sigma = 2 \ln K_D - \frac{1}{2} \ln K_0 \quad (5.13)$$

Differentiating (5.13) on $\frac{1}{T}$ we shall have

$$\frac{d \ln K_{\Sigma}}{d\left(\frac{1}{T}\right)} = \frac{d \ln K_D}{d\left(\frac{1}{T}\right)} - \frac{d \ln K_0}{2d\left(\frac{1}{T}\right)} \quad (5.14)$$

The time-dependence of K_{Σ}, K_D, K_0 is given by

$$\begin{cases} K_{\Sigma} = K_{\Sigma}^0 \exp\left(-\frac{E_{\Sigma}}{RT}\right) \\ K_D = K_D^0 \exp\left(-\frac{E_D}{RT}\right) \\ K_0 = K_0^0 \exp\left(-\frac{E_0}{RT}\right) \end{cases} \quad (5.15)$$

where E_{Σ} – the activation energy of the aluminium degassing process;
 E_D – the activation energy of hydrogen diffusion through the oxide film;
 E_0 – the activation energy of the process of aluminium oxidation.

Substituting (5.14) in (5.11) and differentiating we shall have

$$\begin{aligned} E_{\Sigma} &= E_D - \frac{E_0}{2} \\ E_D &= E_{\Sigma} + \frac{E_0}{2} \end{aligned} \quad (5.16)$$

We studied the emission of hydrogen from aluminium during annealing in air at 400 – 550 °C to check up the assumptions mentioned above.

10 mm thick and 100 mm high aluminium specimens were turned from a hot-pressed 12 mm thick aluminium rod. The annealing of specimens was carried out in the resistance furnace. The maximum duration of the annealing was 48 hours. The determination of hydrogen content in the annealed specimens was provided according to the procedure described in Chapter 1.

The results of our research are summarized in Fig. 5.2.

It can be seen that the annealing of aluminium in the common air atmosphere leads to the degassing of the metal. The intensity of degassing grows with temperature.

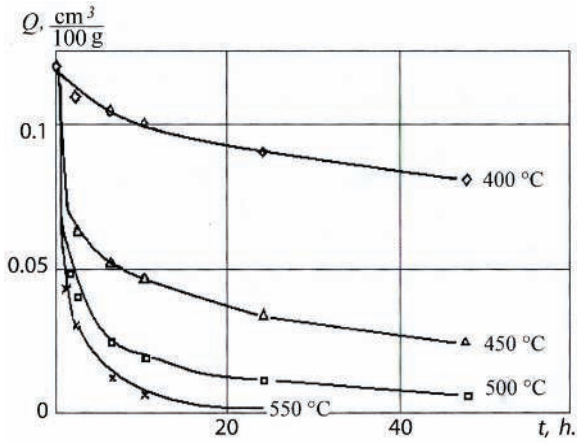


Fig. 5.2 The time and temperature dependences of hydrogen content in the aluminium specimen during annealing in air

The dependence of $\lg \frac{C}{C_0}$ on the root square of the annealing time is given in Fig. 5.3.

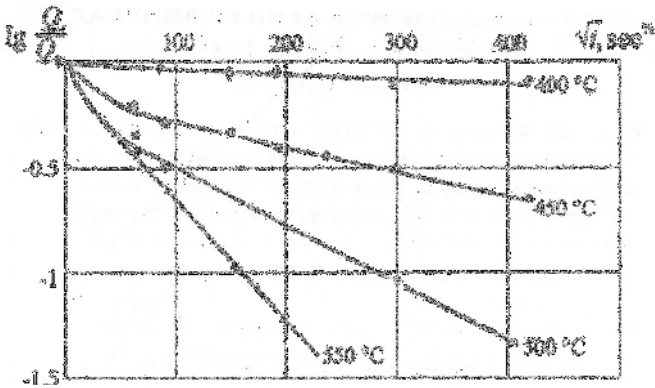


Fig. 5.3 The dependence of the hydrogen content ratio in aluminium at the moment t to the initial hydrogen content on the time of annealing

It appears that this dependence takes up a linear character for some time after the start of the annealing in conformity with the previous assumptions.

Therefore, it is possible to make a conclusion concerning the truthfulness of the fundamental assumptions for the mathematical equation of the kinetics of aluminium degassing during annealing in air. That is the assumption supposing that the rate of degassing is limited by the transfer of hydrogen through the aluminium oxide film and the reduction of the degassing rate is a function of the oxide film growth during annealing.

From the slope ratio of the linear part of the dependence of $\lg \frac{C_t}{C_0}$ on time, we found K_Σ .

Fig. 5.4 demonstrates the temperature dependence of K_Σ . The activation energy of the overall process of aluminium degassing during annealing in air is 158.8 kJ/mol.

The temperature dependence of $K_\Sigma, \text{sec.}^{-1}$ can be expressed in the following way

$$K_\Sigma = 6.6 \cdot 10^2 \exp\left(-\frac{79400}{RT}\right) \quad (5.17)$$

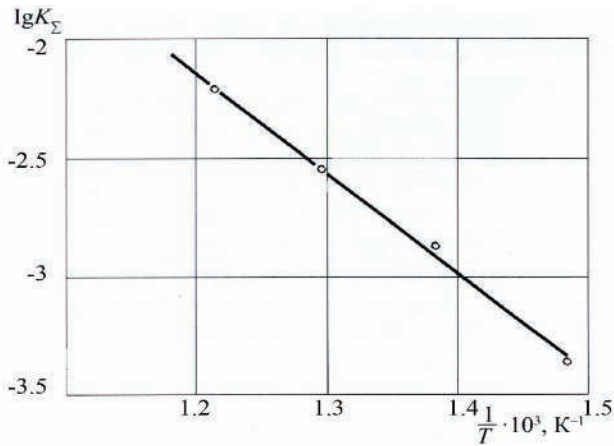


Fig. 5.4 The temperature dependence of the kinetic coefficient characterizing the rate of aluminium degassing during annealing in air

Taking into account equations (5.5) and (5.16) the activation energy of hydrogen diffusion in aluminium oxide would make 271.7 kJ/mol. This value seems to be no relevant to the diffusion by the interstitial diffusion mechanism.

Besides the emission of hydrogen during aluminium annealing in air we studied hydrogen release during the annealing of aluminium in nitrogen under high pressure too. We placed 10 mm thick and 100 mm high Al specimens, turned of hot-pressed aluminium rod into an airtight high-temperature bulb, and then heated them up to 500 °C under the gage pressure of 400 atm ($4 \cdot 10^7$ Pa) for 10 hours, not more.

It was shown that the rate of degassing in nitrogen under a high pressure is higher than during the annealing of aluminium in the standard air atmosphere.

CHAPTER 6. WORKING OUT A METHOD OF METAL AND ALLOY PROCESSING TO REMOVE GASES AND POROSITY (HOT ISOSTATIC PRESSING TECHNIQUE)

There is a well-known method of treating of metals and alloys through vacuum annealing to remove both gas and porosity.

A too long duration of the process resulting in the formation of gas porosity during the processing of massive work-pieces negatively affects the method efficiency. The pores herewith can get so large that no further annealing after the complete degassing of the metal can remove them.

The goal of this new method was to accelerate degassing treatment and porosity removal in aluminium alloys. This is achieved by annealing in pressurized media during the period of time sufficient for providing a required rate of degassing and eliminating porosity. The pressurized media absorb the gases escaping from the metal, to which purpose as substances for pressure transfer to the specimen there are used neutral gases or oils of silicon liquids (e.g. silanes) with suspensions capable of absorbing the gases released while not oxidizing the metal (e.g. a mixture of metal oxides).

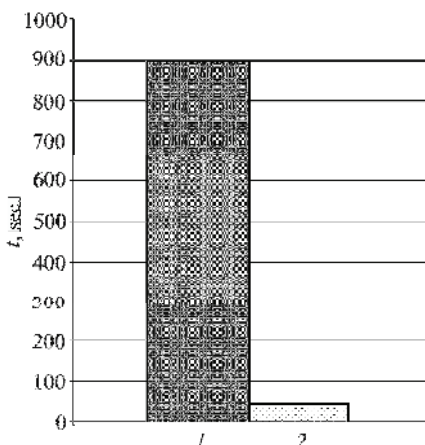


Fig. 6.1 The efficiency of the proposed method: 1 - annealing in dry air; 2 - annealing in dry air compressed up to 400 atm

The method was tested using 10 mm thick pure aluminium rods. The rods were annealed at 500 °C in dry air compressed under 400 atm. As compared to the annealing of rods in a dry atmosphere the time of complete hydrogen evacuation at the same temperature is reduced by 20 times.

As the gas pressure in the metal and the gas pressure in the pores get equal, the removal of gas from the metal leads to gas elimination from the pores and their closing.

The testing of this method was carried out at the State Insti-

tute of Nitrogen Products at the laboratory of Professor I. R. Krichevsky in 1969–1970.

The certificate of authorship protects the results of this work [104] (see Appendix).

The effectiveness of the technique for decreasing porosity in aluminium alloys have been illustrated in later research (e.g. I. F. Vorobieva, B. A. Kopeliovich et al. “Porosity and Hydrogen Content in Aluminium Castings Subjected to Hot Isostatic Pressure” in *Technology of Light Alloys*, 1987, No. 9, pp. 14 – 16).

A. G. Padalko in his book “Practice of Hot Isostatic Pressing for Non-Organic Materials” (2007) states that the technique ensures porosity elimination and higher mechanical properties in titanium alloy castings. By the end of 1990s and at the beginning of 2000s there were published many books on hot isostatic pressing, such as those by H. V. Atkinson, B. A. Rickinson //*Hot Isostatic Processing*// Springer (1999) or A. Bose, W. B. Eisen //*Hot Consolidation of Powders and Particulates*// MPIF (2003).

CHAPTER 7. OF THE THEORY OF GAS POROSITY EVOLUTION IN METALS

Today, as it was noted in Chapter 1, there is no unified theory of gas porosity evolution in metals. There are several hypotheses [105–114, 115–117] concerning probable mechanisms of gas porosity evolution.

In fact, the evolution of gas porosity is a complex process which depends on many factors such as the nature of metal-gas interaction, the technology of metal production, the initial gas content, the presence of non-metallic inclusions and structural imperfections, the conditions of metal deformation and heat treatment, the nature of metal interaction with the ambient atmosphere in the course of products and semi-products making, as well as the mechanical properties of metals, the external dimensions of semi-products or finished products etc. Therefore, in each specific case the formation of gas flaws in the metal has its own peculiar features.

At the same time, there are some common patterns of gas porosity evolution in metals. The theory of gas porosity evolution based on the methods of thermodynamic and kinetic description of some aspects of gas-metal interaction will be presented later.

Previous studies of hydrogen diffusion in aluminium (Chapter 2) facilitated significantly the development of this theory. The values of the hydrogen diffusion coefficients in aluminium found in Chapter 2 permit evaluating approximately the role of hydrogen diffusion to pores as a possible controlling mechanism of the formation of the pores.

Let us calculate the time needed for the formation of a 1 μm pore in aluminium at 400 $^{\circ}\text{C}$, assuming that hydrogen diffusion to pores limits the rate of their growth. The pressure of hydrogen in pores exceeding the yield point of aluminium should result in increasing pore size.

According to Fick's law the gas flow into the pore Q , cm^3/sec (NTP) is equal to

$$Q = DS \frac{\partial C}{\partial x} = \frac{D4\pi r^2 (C - C_0)}{\delta} \quad (7.1)$$

where D – the diffusion coefficient of hydrogen in aluminium. cm^2/sec .;
 r – a pore radius, cm ; C – the concentration of hydrogen in the metal;
 C_0 – hydrogen concentration near the surface of the pore, equal to hydrogen solubility at temperature of T , K and hydrogen pressure in the pore of P , atm ; δ – half a distance between pores, cm .

The gas volume in a pore V , cm³(NTP) is equal to

$$V = \frac{4}{3}\pi r^3 \frac{22.4 \cdot P}{RT} \quad (7.2)$$

The time required to create hydrogen pressure P inside the pore of radius r can be calculated as follows

$$t = \frac{V}{Q} \quad (7.3)$$

or, taking in consideration equations (7.1), (7.2) and (7.3) as

$$t = \frac{4\pi r^3 \cdot 22.4 \cdot P\delta}{3RTD4\pi r^2(C - C^0)} = \frac{7.47 \cdot P\delta \cdot r}{RTD(C - C^0)} \quad (7.4)$$

Let us specify the values of the parameters included into equation (7.4), assuming the hydrogen content in the metal C equal to 0.12 cm³/100 g or 3.2·10⁻³ cm³ (NTP)/cm³.

According to our data obtained during the study of hydrogen porosity in aluminium (Chapter 5) and the data elsewhere [118] we can assume to a first approximation the mean distance between pores as ~1.8·10⁻². We determined the yield point of aluminium in the temperature range of 400 – 550 °C. The results of this study are given in Table 7.1.

Table 7.1

Yield point of 99.96% aluminium

t , °C	Yield point, kg/cm ²
400	110
450	80
500	48
550	35

Let us assume the value of hydrogen pressure in a pore at the annealing temperature of 400 °C as equal to the yield point value at the same temperature (see table 7.1). The C_0 values are determined from Siverts's law $C^0 = K_S \sqrt{P} = 1.89 \cdot 10^{-4} \cdot \sqrt{110} = 1.98 \cdot 10^{-3}$ cm³(NTP)/cm³.

At 400 °C, $D = 8.3 \cdot 10^{-6}$ cm²/sec (Chapter 2), thus time t of a 1 μm pore formation is

$$t = \frac{7.47 \cdot 110 \cdot 0.9 \cdot 10^{-2} \cdot 10^{-4}}{0.083 \cdot 673 \cdot 8.3 \cdot 10^{-6} (3.2 \cdot 10^{-3} - 1.98 \cdot 10^{-3})} = 1.32 \cdot 10^3 \text{ sec} \approx 0.37 \text{ h.}$$

This value is near the real one observed in experiments, in other words it means that our conjecture concerning the limiting role of diffusion is valid.

Our concept supposes that at sufficiently high temperatures the tendency to adjusting the thermodynamic equilibrium between the gas dissolved in the lattice of the metal and the gas in the pores causes evolution of gas porosity in solid metals, while the gas diffusion to the surface of pores restricts their growth.

At each annealing temperature there is some critical gas pressure in pores caused by the resistance of the metal to deformation in a microvolume surrounding the pore. The excessive resistance of the metal to the deformation results in the growth of the pore volume. This growth can proceed according to any mechanism, which is not considered by this theory or not related to it.

Thus, the theory does not comprise the very mechanism of the process of metal deformation in the course of pores growth.

According to the present concept, the growth of porosity occurs only when the concentration of a gas dissolved in the metal surpasses the value of solubility corresponding to a given temperature and the critical gas pressure in pores. The growth of pore volume results in reduction of the gas pressure below the critical pressure, and the growth of pores stops. The gas pressure increases with the diffusion of its new portions into a pore and on reaching the critical pressure, the growth of the pores revives. The growth of the pores stops on reaching the thermodynamical equilibrium between the gases dissolved in the lattice of the metal and the gas in the pores.

Within the framework of these assumptions, we shall derive later equations describing the kinetics of gas porosity evolution in metals.

In Chapter 8 we shall compare the solution of these equations with the experimental data concerning the formation of gas porosity in aluminium.

If the size of pores is not too small ($\frac{2\sigma}{r} \ll P$) then we can ignore the value of metal surface tension and assume the pressure of the gas in pores as constant at a given temperature.

Now we shall discuss the situation when the total content of gas in metal does not change with annealing time and hence the growth of pore volume fully determines the decrease of the gas dissolved in the lattice of the metal, i.e.

$$\frac{dC}{dt} = -\frac{22.4N \cdot P}{RT} \cdot \frac{dV}{dt}, \quad (7.5)$$

where C – the concentration of gas dissolved in the metal lattice, %; N – number of pores, $1/\text{cm}^3$; V – pore volume, cm^3 ; P – gas pressure in the pore equal to the critical one, atm; t – annealing time; T – annealing temperature, K.

This statement is valid for substantially massive specimens coated with the surface oxide film impenetrable for hydrogen. As for thin-wall specimens (see Chapter 5) their vacuum degassing occurs during annealing. Since the diffusion of gas limits the growth of pores, the rate of pores growth will be proportional to the area of their surface as well as to the difference between the concentration of the gas dissolved in the metal and the concentration of the gas on the surface of pores. At the same time, the gas concentration on the pore surface corresponds to the solubility of the gas in the metal at a given pressure and temperature of this gas in pores, i.e.

$$\frac{dV}{dt} = \frac{RT}{22.4} \cdot \frac{K_1'(C - C_0)V^{2/3}}{\delta} \quad (7.6)$$

where C_0 – gas solubility in metal at temperature T and gas pressure P , %; K_1' – the constant proportional to the coefficient of gas diffusion in metal, cm^2/sec .; δ – the parameter of diffusion, cm.

It is possible to show that the diffusion parameter is proportional to the pore radius [119]. The diffusion equation in spherical coordinates is as follows,

$$\frac{D}{r^2} \frac{\partial}{\partial r} \left(r^2 \frac{\partial C}{\partial r} \right) = \frac{\partial C}{\partial t} \quad (7.7)$$

Under steady conditions

$$\frac{\partial C}{\partial t} = 0 \quad (7.8)$$

and

$$r^2 \frac{\partial C}{\partial r} = \text{const} = K_2. \quad (7.9)$$

Integrating (7.9) we shall have

$$C = -\frac{K_2}{r} + K_3, \quad (7.10)$$

where K_3 – constant

In the case of diffusion to a sphere

$$C_{|r \rightarrow \infty} = C_0 \text{ and } C_{|r \rightarrow r_0} = 0,$$

where r_0 is the sphere radius.

Therefore

$$C = C_0 \left(1 - \frac{r_0}{r} \right) \quad (7.11)$$

and

$$\left(\frac{\partial C}{\partial r} \right)_{r \rightarrow r_0} = \frac{C_0}{r_0} \quad (7.12)$$

The flow

$$Q = D \cdot 4\pi r_0^2 \left(\frac{\partial C}{\partial r} \right)_{r \rightarrow r_0} = 4\pi r_0 D C_0 \quad (7.13)$$

Thus in the case of diffusion to a sphere the diffusion parameter is proportional to the full-sphere radius.

With accounting for this, equation (7.6) takes the form

$$\frac{dV}{dt} = \frac{RT}{22.4P} K_1 (C - C^0) V^{1/3} \quad (7.14)$$

As the result, we can describe the growth of gas porosity using the system of two differential equations

$$\begin{cases} \frac{dC}{dt} = -\frac{22.4NP}{RT} \cdot \frac{dV}{dt} \\ \frac{dV}{dt} = \frac{RT}{22.4NP} K_1 (C - C^0)^{1/3} \end{cases} \quad (7.15)$$

with initial conditions

$$\begin{cases} C|_{t=0} = C_0 \\ V|_{t=0} = V_0 \end{cases} \quad (7.16)$$

where C_0 – initial gas concentration in the metal lattice; V_0 – initial porosity.

Integrating the first equation of the system (7.15) we have

$$C - C_0 = -\frac{22.4N \cdot P}{RT} (V - V_0) \quad (7.17)$$

$$C - C^0 = -\frac{22.4NP}{RT} (V - V_0) + C_0 - C^0 \quad (7.18)$$

Putting (7.18) into the second equation of system (7.15) we have

$$\frac{dV}{dt} = K_1 \left[C_0 - C^0 - \frac{22.4NP}{RT} (V - V_0) \right] V^{1/3} \frac{RT}{22.4P} \quad (7.19)$$

The total gas concentration in the metal

$$C_1 = C_0 + \frac{22.4N \cdot P \cdot V_0}{RT} \quad (7.20)$$

$$C_0 = C_1 - \frac{22.4N \cdot P \cdot V_0}{RT} \quad (7.21)$$

By putting (7.21) into (7.19) we have

$$\begin{aligned} \frac{dV}{dt} &= K_1 \left[C_1 - C^0 - \frac{22.4N \cdot P \cdot V}{RT} \right] V^{1/3} \frac{RT}{22.4P} = \\ &= K_1 \left[\frac{(C_1 - C^0)RT}{22.4N \cdot R} - V \right] NV^{1/3} \end{aligned} \quad (7.22)$$

Let us designate

$$\frac{(C_1 - C^0)RT}{22.4N \cdot P} = A^3; \quad (7.23)$$

and $V = Z^3, \quad dV = 3Z^2 dZ, \quad (7.24)$

then

$$\frac{dV}{dt} = K_1 N (A^3 - Z^3) Z. \quad (7.25)$$

Integrating equation (7.25) gives

$$\int_{z_0}^Z \frac{3Z^2 dZ}{(A^3 - Z^3)Z} = K_1 N t. \quad (7.26)$$

It is known that

$$\int \frac{ZdZ}{(A^3 - Z^3)} = \frac{1}{6A} \ln \frac{Z^2 + AZ + A^2}{(A - Z)^2} - \frac{1}{A\sqrt{3}} \operatorname{arctg} \frac{2Z + A}{A\sqrt{3}} \quad (7.27)$$

or
$$\int \frac{ZdZ}{(A^3 - Z^3)} = \frac{1}{6A} \left[\ln \frac{W^2 + W + 1}{(1 - W)^2} - 2\sqrt{3} \cdot \operatorname{arctg} \frac{2W + 1}{\sqrt{3}} \right], \quad (7.28)$$

where $W = \frac{Z}{A}. \quad (7.29)$

With provision for (7.26) and (7.28) we have

$$\begin{aligned} & \ln \frac{W^2 + W + 1}{(1 - W)^2} - 2\sqrt{3} \operatorname{arctg} \frac{2W + 1}{\sqrt{3}} - \\ & - \ln \frac{W_0^2 + W_0 + 1}{(1 - W_0)^2} + 2\sqrt{3} \operatorname{arctg} \frac{2W_0 + 1}{\sqrt{3}} = \tau, \end{aligned} \quad (7.30)$$

where

$$\left\{ \begin{array}{l} W = \frac{Z}{A} = V^{1/3} \left[\frac{(C_1 - C_0)RT}{22.4N \cdot P} \right]^{-1/3} \\ W_0 = \frac{Z_0}{A} = V_0^{1/3} \left[\frac{(C_1 - C_0)RT}{22.4N \cdot P} \right]^{-1/3} \\ \tau = 2AK_1N \cdot t = 2 \left[\frac{(C_1 - C_0)RT}{22.4N \cdot P} \right]^{1/3} K_1N \cdot t = 2K_1N \frac{V_0^{1/3}}{W_0} t = \frac{K_\tau (NV_0)^{1/3}}{W_0} t \\ K_\tau = 2K_1N^{2/3} \end{array} \right. \quad (7.31)$$

Equation (7.30) describes the kinetics of gas porosity growth in metals with regard for initial gas content in the metal, initial porosity, gas solubility in the metal, the coefficient of gas diffusion in the metal, rupture resistance in the microvolume around the pore, as well as conditions of heat treatment – its duration and temperature.

Equations (7.15) show, in particular, that the curve of porosity evolution should be S-shaped.

At the initial stage of annealing, the surface of pores is small, and the growth rate of pores is low too. The surface of the pores grows with their size and their growth rate increases.

Finally, the growth rate of pores will go down when a considerable portion of the gas will go from the metal into the pores, and the gradient of concentrations in the gas phase and close to the surface of pores in the metal will become lower. The growth of pores will stop when the concentration of the gas in the metal would be equal to the concentration on the surface of the pores.

The experimental dependence of pore volume on annealing time

$$V^{1/3} = f(t) \quad (7.32)$$

and the theoretical dimensionless curve

$$W = \varphi(t) \quad (7.33)$$

in double logarithmic coordinates should differ only in scale.

In fact

$$\ln W = \frac{1}{3} \ln V + A; \quad (7.34)$$

$$\ln \tau = \ln t + B, \quad (7.35)$$

where A and B are constants.

Hence, the experimental and the theoretical dependences of pore volume on annealing time must coincide in double logarithmic coordinates under the parallel shifting of coordinate axes of the theoretical curve relatively to the experimental one.

It is possible to determine values W_0 and hence the critical pressure of gas in pores as well as coefficient K_1 specifying the rate of the gas delivery via the metal to the surface of pores using the value of the shift of coordinate axes.

To this purpose, we can specify arbitrary values for W_0 and K_τ and calculate the theoretical dependence of pore volume on annealing time for each pair of these parameters

$$V_{\text{theoretical}} = f(t) \quad (7.36)$$

The coincidence of theoretical and experimental dependences of pore volume on annealing time provides the values of W_0 and K_τ .

It is possible to accelerate the procedure of fitting by means of exclusion of one parameter. Allowing for the fact that from equation (7.31) it follows that

$$W = W_0 \left(\frac{V}{V_0} \right)^{1/3} \quad (7.37)$$

we can present the equations for two values of $V = f(t)$

$$\ln \frac{W_0^2 \left(\frac{V_1}{V_0} \right)^{2/3} + W_0 \left(\frac{V_1}{V_0} \right)^{1/3} + 1}{\left[1 - W_0 \left(\frac{V_1}{V_0} \right)^{1/3} \right]^2} - 2\sqrt{3} \operatorname{arctg} \frac{2W_0 \left(\frac{V_1}{V_0} \right)^{1/3} + 1}{\sqrt{3}} - \ln \frac{W_0^2 + W_0 + 1}{(1 - W_0)^2} + 2\sqrt{3} \operatorname{arctg} \frac{2W_0 + 1}{\sqrt{3}} = \frac{K_\tau (NV_0)^{1/3}}{W_0} t_1; \quad (7.38)$$

$$\ln \frac{W_0^2 \left(\frac{V_2}{V_0} \right)^{2/3} + W_0 \left(\frac{V_2}{V_0} \right)^{1/3} + 1}{\left[1 - W_0 \left(\frac{V_2}{V_0} \right)^{1/3} \right]^2} - 2\sqrt{3} \operatorname{arctg} \frac{2W_0 \left(\frac{V_2}{V_0} \right)^{1/3} + 1}{\sqrt{3}} -$$

$$- \ln \frac{W_0^2 + W_0 + 1}{(1 - W_0)^2} + 2\sqrt{3} \operatorname{arctg} \frac{2W_0 + 1}{\sqrt{3}} = \frac{K_\tau (NV_0)^{1/3}}{W_0} t_2. \quad (7.39)$$

Let us divide (4.34) by (4.35) and we shall have

$$\ln \frac{W_0 \left(\frac{V_1}{V_0} \right)^{2/3} + W_0 \left(\frac{V_1}{V_0} \right)^{1/3} + 1}{\left[1 - W_0 \left(\frac{V_1}{V_0} \right)^{1/3} \right]^2} - 2\sqrt{3} \operatorname{arctg} \frac{2W_0 \left(\frac{V_1}{V_0} \right)^{1/3} + 1}{\sqrt{3}} - \ln \frac{W_0^2 + W_0 + 1}{(1 - W_0)^2} + 2\sqrt{3} \operatorname{arctg} \frac{2W_0 + 1}{\sqrt{3}} \quad (7.40)$$

$$\ln \frac{W_0 \left(\frac{V_2}{V_0} \right)^{2/3} + W_0 \left(\frac{V_2}{V_0} \right)^{1/3} + 1}{\left[1 - W_0 \left(\frac{V_2}{V_0} \right)^{1/3} \right]^2} - 2\sqrt{3} \operatorname{arctg} \frac{2W_0 \left(\frac{V_2}{V_0} \right)^{1/3} + 1}{\sqrt{3}} - \ln \frac{W_0^2 + W_0 + 1}{(1 - W_0)^2} + 2\sqrt{3} \operatorname{arctg} \frac{2W_0 + 1}{\sqrt{3}} = \frac{t_1}{t_2}$$

Thus, we have the equation with one unknown W_0 . This equation is easy to be solved for each pair of points on the experimental curve

$$V_{\text{experiment}} = f(t) \quad (7.41)$$

When values W_0 are determined for each pair of points $V_{\text{experiment}} = f(t)$ we have to determine the value of K_τ substituting the determined value W_0 into any of equations (7.38) or (7.39).

Thus, we have the values of W_0 and K_τ for each pair of points from the experimental curve. Then we determine the root mean square values of W_0 and K_τ for the whole curve and calculate the theoretical dependence of the volume of pores on the time of annealing.

$$V_{\text{theoretical}} = f(t) \quad (7.42)$$

If at that the theoretical and the experimental curves coincide it means that we have calculated the values of W_0 and K_τ correctly.

Having defined the value of W_0 and respectively the value of gas pressure in pores, it is possible to calculate the highest possible volume of pores for a given annealing temperature.

The volume of porosity reaches its possible maximum at thermodynamical equilibrium between the gas dissolved in the metal lattice and the gas in the pores and remains unchangeable later on.

With this the concentration of the gas dissolved in the metal will be equal to the value of gas solubility in the metal corresponding to the critical value of gas pressure in the pores at a given pressure, that is

$$C^0 = K_s \sqrt{P} \quad (7.43)$$

where K_s – the constant of gas solubility in the metal at temperature T and pressure P .

With accounting for (7.43) and (7.15) we shall obtain for the limiting volume of porosity

$$V_{\text{lim}} - V_0 = \frac{RT}{22.4N \cdot P} (C_0 - C^0) \quad (7.44)$$

Taking into account (7.20) we have

$$V_{\text{lim}} = \frac{RT}{22.4N \cdot P} (C_1 - K_s \sqrt{P}) \quad (7.45)$$

That is, at a given temperature and total gas content C_1 in metal, the maximum possible volume of porosity does not depend on the initial volume of porosity.

The initial volume of porosity affects the porosity growth kinetics (7.30) and (7.31). One can see from equation (7.45) that the highest possible volume of porosity is linearly dependent on the initial gas content in the metal. The maximum possible volume of porosity decreases with increasing gas solubility. When the quantity of pores as well as the breaking strength of the metal within a microvolume grow the highest possible volume of porosity decreases also. The influence of temperature on V_{lim} is ambiguous. With rising temperature the metal rupture strength gets reduced together with the pressure of the gas in pores while the value of V_{lim} grows. On the other hand, with increasing temperature the gas solubility in the metal grows, resulting in the reduction of V_{lim} according to the equation below

$$K_S = K_S^0 \exp\left(-\frac{E_S}{RT}\right), \quad (7.46)$$

The minimum critical gas content in the metal corresponds to the gas pressure value in pores causing the formation of porosity i.e.

$$C_{\text{critical}} = C^0 = K_S \sqrt{P}. \quad (7.47)$$

Indeed, if the gas concentration in the metal is lower than the gas solubility at a pressure P then the growth of pores is impossible.

Hence knowing the value of the gas pressure in pores it is possible to determine the critical concentration of the gas in the metal below which no porosity will form.

Equation (7.47) shows a linear relationship between the critical gas concentration in the metal and the gas solubility in the metal. The critical gas concentration in the metal is proportional to the root square of the yield point of the metal in the microvolume surrounding a pore, equal to the gas pressure in the pore.

Thus, the developed theory allows us to determine *a priori* the values of porosity volume for any heat treatment conditions, and besides to predict the highest possible volume of porosity for specified initial gas contents and annealing temperatures. At that we have to know the characteristics of the metal–gas interaction (i.e. the gas solubility in the metal and the gas diffusion coefficient in the metal) as well as the yield point of the metal in the microvolume and the value of initial porosity.

If the value of the rupture strength of the metal in the microvolume is not known then the theory makes it possible to determine this value experimentally from the porosity formation kinetics data or from the specified gas content, and then to predict the gas porosity kinetics in the metal at any gas content.

Besides, the theory allows predicting the gas content value for a given temperature when no gas porosity will form [120, 121] using the defined values of the gas pressure in pores.

CHAPTER 8. THE EXPERIMENTAL TESTING OF THE THEORY OF GAS POROSITY FORMATION IN METALS

We carried out the comparison of the theory of gas porosity formation in metals with the experimental data obtained on the 'aluminium-gas' system. We used 12 mm cylindrical specimens of 99.96 % aluminium, 100 mm high, lathed from a hot-pressed rod. The initial content of hydrogen in the specimens was $0.12 \text{ cm}^3/100 \text{ g}$.

The results of the research of gas porosity evolution during the annealing of aluminium at $400 - 500 \text{ }^\circ\text{C}$ will be presented below.

A special electroplating technique was used for coating the specimens with oxide. The specimens were placed into the electrolyte composed of 5 % CrO_3 , 0.5 % $\text{H}_2\text{C}_2\text{O}_4$ and 0.4 % H_3BO_4 , which was then heated up to $40 \text{ }^\circ\text{C}$. The current intensity of the circuit was kept within the range of $0.3 - 0.4 \text{ A}$, and the voltage at 60 V . The voltage was increased gradually to 60 V in 30 minutes.

The specimens after the electrolytic oxidation were subjected to heat treatment at $500 \text{ }^\circ\text{C}$ for 48 hours to check the protective properties of the anodic oxide film, coating the specimens. The content of hydrogen in the specimens after the annealing was $(0.13 \pm 0.01) \text{ cm}^3/100 \text{ g}$. It is obvious that the hydrogen content in the anodized aluminium specimens after the annealing at $500 \text{ }^\circ\text{C}$ during 48 hours corresponds to the initial content of hydrogen, in other words there was no degassing of the specimens during the annealing.

We determined the porosity evolution in the aluminium in the course of the annealing by measuring the aluminium density using the method of hydrostatic weighing. This method involves the determination of density by weighing specimens in two media of different density. For a more precise determination of density, specimens should have a simple shape and a perfectly processed surface. The lathed 40 mm high aluminium specimens had 40 mm in diameter. The technique of their surface finishing is of much importance.

It is recommended to rinse at first the specimens with hot water and then to clean them with alcohol. The layout of the installation for determining the porosity of aluminium is given in Fig. 8.1.

To increase the accuracy of the experiment we used the analytical balance BM-20M providing the accuracy of $1 \cdot 10^{-5} \text{ g}$ for specimens of up to 20 g .

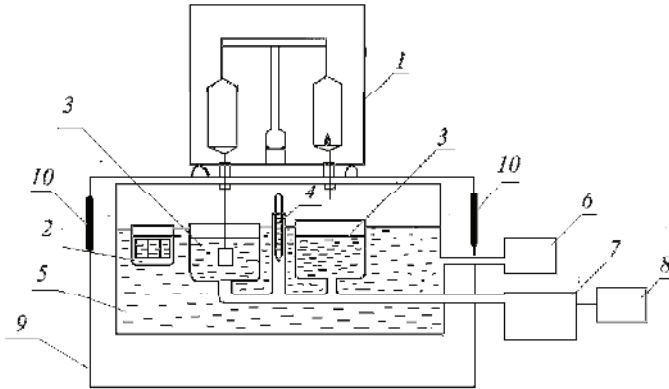


Fig. 8.1 The layout of the installation for determining the porosity of aluminium by its density:

- 1* – analytical balance BM-20M; 2 – specimens' separator; 3 – glass caps for diethyl phthalate; 4 – thermometer; 5 – glass reservoir;
- 6 – thermostat; 7 – pump; 8 – pump driver; 9 – organic glass guard;
- 10* – process slots in the guard

The specimens were weighed in air or in the process liquid. The ether of diethyl phthalic acid was used as a process liquid. The accuracy of the process liquid temperature stabilization was ± 0.1 °C, which was realized by submerging the process liquid reservoir into a water vessel, where the water temperature was controlled with a thermostat.

To increase the accuracy and the sensitivity of porosity determination by density we made few alterations to the method [51]. It was shown that the weight of porous and solid specimens had changed in a different way.

The weight of a porous specimen submerged in liquid grows with time, and 1.5 hour after submerging, it reaches the constant value (Fig. 8.2, curve 1). The weight of a solid specimen in liquid practically does not change with time (Fig. 8.2, curve 2).

This difference can be explained in the following way.

The pores on the surface of porous specimens get open during their lathing. During weighing in liquid, a long-time exposure of porous specimens is required for a complete air from these pits.

Therefore, before weighing the specimens in liquid we exposed them to the process liquid at least within 1.5 h. However, such a long exposure strongly reduced the efficiency of the method.

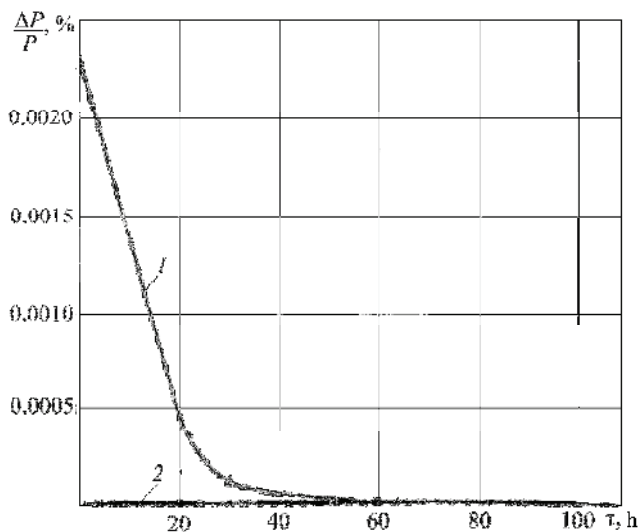


Fig. 8.2 The variation of a specimen weight increment depending on the time of exposure to diethyl phthalate for porous (1) and solid (2) specimens

To increase its efficiency we placed the perspex separator with 18 specimens at a time into the process liquid. At first, we successively weighed all specimens in air and then placed them into the separator. Then, after the exposure for an hour and a half in the process liquid the specimens were weighed successively in liquid with the time interval of 5 – 7 minutes. This allowed increasing the efficiency. When the weight of the specimen in liquid and in air is known it is possible to calculate the volume of the liquid displaced by the specimen, i.e. the volume of this specimen.

The equation for calculating the specimen density ρ , g/cm^3 is as follows

$$\rho = \frac{W^\sigma d - W^d \sigma}{W^\sigma - W^d}, \quad (8.1)$$

where W^σ – the weight of the specimen in air, g; W^d – the weight of the specimen in liquid, g; d – the density of process liquid, g/cm^3 (at 20 °C density of diethyl phthalate makes 1.11700 g/cm^3); σ – the density of air at the temperature of the experiment.

To find the density d of the process liquid the following technique was used. A specimen of aluminium was weighed many times in air and in

distilled water of a known density, thus determining the density of the specimen. Then the specimen was weighed in air and in diethyl phthalate to determine the density of diethyl phthalate.

The estimation of the accuracy and sensitivity of the method was provided by measuring the density of a series of specimens lathed from hot-pressed 12mm rods of 99.996% aluminium. Metallographic and radiographic studies showed no porosity in the specimens. The density of these specimens was assumed as the standard one. The density of hot-pressed aluminium specimens was $(2.70090 \pm 2.5 \cdot 10^{-5}) \text{ g/cm}^3$.

The porosity of specimens V , % abs. was determined from the equation

$$V = \frac{\rho_{\text{standard}} - \rho}{\rho_{\text{standard}}} \cdot 100, \quad (8.2)$$

where ρ – the density of the standard specimen of hot-pressed aluminium having no porosity ($\rho_{\text{standard}} = 2.70090 \text{ g/cm}^3$); ρ – the density of the specimen under study.

We used this technique for studying the formation of porosity in aluminium, The obtained results are presented in Fig. 8.3.

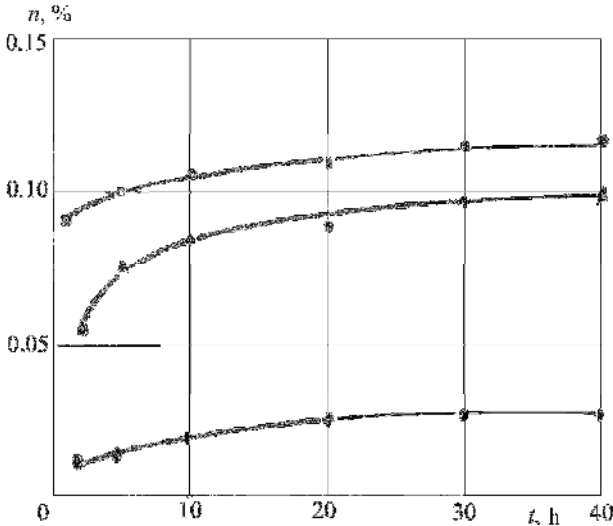


Fig. 8.3 Dependence of pore volume in aluminium on the temperature and the time of annealing: (o – $T = 500 \text{ }^\circ\text{C}$; Δ – $T = 450 \text{ }^\circ\text{C}$; \diamond – $T = 400 \text{ }^\circ\text{C}$) – the experimental data; solid lines – the calculated data, the concentration of hydrogen $C = 0.12 \text{ cm}^3/100 \text{ g}$

One can notice that the porosity of aluminium starts forming during annealing. The porosity of aluminium increases with increasing annealing temperature. After about 36 hours from the start of the annealing, the growth of porosity slows down.

We compared the theoretical data with the experimental results, obtained according to the procedure given in Chapter 7. Fig. 8.4. shows this comparison. One can see a good coincidence of theoretical and experimental results some time after the start of the annealing

Besides, we compared the theory of pore volume dependence on the time of annealing with experimental data obtained by D. Talbot and D.A. Granger [118] for aluminium with a hydrogen content of $0.4 \text{ cm}^3/100 \text{ g}$ (see Fig. 8.4).

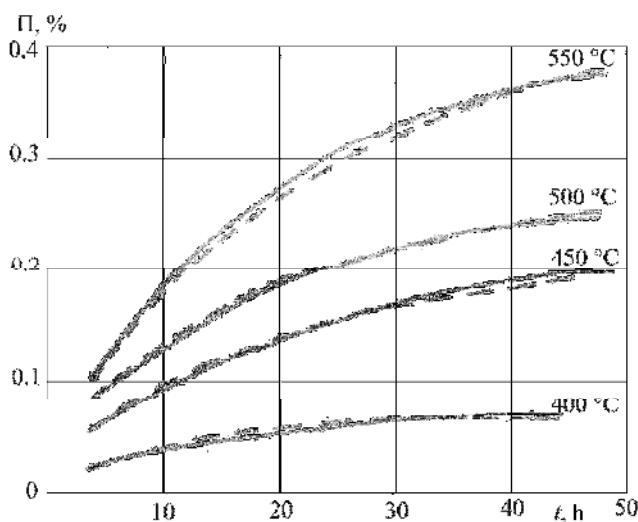


Fig. 8.4 The time and temperature dependence of pore volume in aluminium during annealing: from of literature data [118] (dashed lines) and theoretically calculated data (solid graphs). The concentration of hydrogen $C = 0.4 \text{ cm}^3/100 \text{ g}$

Here we have also got quite a satisfactory coincidence of theoretical and experimental data.

To describe the initial section of the experimental curve we have to bear in mind the contribution of the surface tension of the metal to the kinetics of pore growth, besides, we have to account for the possibility of widening of

the pores compressed during the pressing of cast aluminium. We determined the values of W_0 and K_τ by the coincidence of experimental and theoretical curves of time dependencies of pore growth during annealing.

Fig. 8.5 gives the dependence of K_τ on temperature. The activation energy of the pore growth rate calculated from these data makes 52.25 kJ/mol. This figure is in satisfactory agreement with the data of the activation energy of hydrogen diffusion in aluminium (~62 kJ/mol).¹

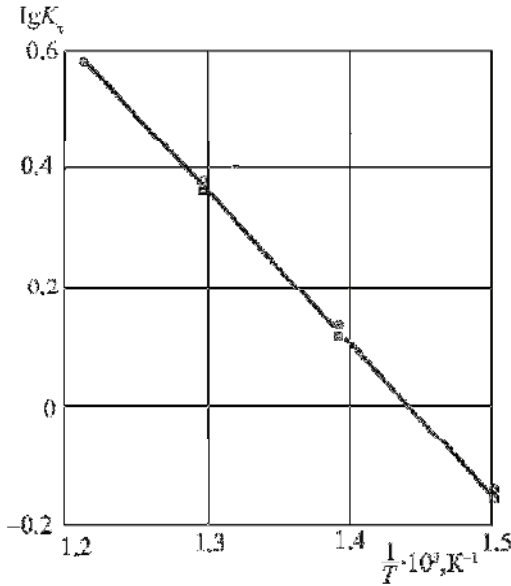


Fig. 8.5 Temperature dependence of the kinetic coefficient of aluminium vaporization
 ○ – literature data [118]; □ – the author's data

This confirms the correctness of our theoretical concept of pore growth suggesting the limiting role of gas diffusion in the metal to the surface of pores.

We were able to determine the value of hydrogen pressure in pores P, atm^{1/2} since we knew the values of W_0 . According to (7.31)

¹ To coefficient K_τ comprises N too (see equation 7.5). Within the limits of experimental error there was no any substantial disagreements observed at various temperatures for values of N from one specimen to another

$$\sqrt{P} = -\frac{K_S RTW_0^3}{22.4NV_0} + \sqrt{\left(\frac{K_S RTW_0^3}{22.4NV_0}\right)^2 + \frac{C_1 RTW_0^3}{22.4NV_0}}. \quad (8.3)$$

Fig. 8.6 shows the dependence of hydrogen pressure in pores and yield point on the temperature of annealing.

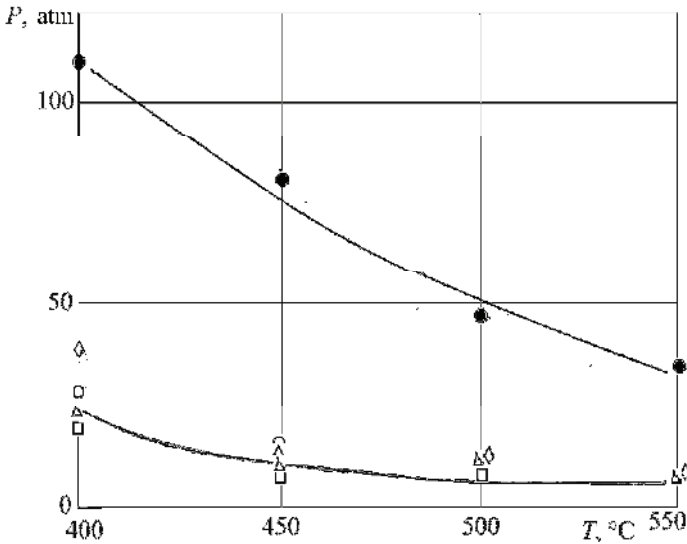


Fig. 8.6 Temperature dependence of hydrogen pressure in pores and yield point:

- – our direct measurement of yield point of aluminium;
- – the data obtained from the time dependence of pore volume;
- △ – the same from literature source [118];
- – own data obtained from the limit value of porosity;
- ◇ – the same from literature source [118]

We can see that hydrogen pressure in pores is noticeably lower than the yield point of aluminium. This could be explained by the difference between the yield point and the rupture strength of the metal in a microvolume and, besides, by porosity nucleation in the most defective zones of the metal.

While the temperature rises from 400 °C up to 450 °C, the pressure in pores drops from ~23 down to ~10 atm approximately and at 500 °C it reaches ~6.5 atm and remains stable up to the temperature of 550 °C.

Another method to define gas pressure in pores is based on measuring the highest volume of porosity achieved at the equilibrium between the gas dissolved in the metal and the gas in the pores.

According to (7.45)

$$\sqrt{P} = -\frac{K_S RT}{22.4NV_{\text{lim}}} + \sqrt{\left(\frac{K_S RT}{22.4NV_{\text{lim}}}\right)^2 + \frac{C_1 RT}{22.4NV_{\text{lim}}}} \quad (8.4)$$

Figures 8.3 and 8.4 show that the growth rate of pores slows down drastically after an annealing for 36 – 40 hours, whereas after a 48 hour annealing the value of porosity can be assumed to be in equilibrium for aluminium.

The results of measuring the hydrogen pressure in pores at the near-equilibrium porosity of aluminium are presented in Fig. 8.6. The results of the two different methods of measuring the hydrogen pressure in pores are in good agreement. The lowest hydrogen content in the metal, at which the porosity starts forming (i.e. is $C_{\text{critical}} = C^0$), corresponds to the gas pressure value in the pores. The dependence of the critical hydrogen concentration in aluminium, found from equation (7.47), on annealing temperature is given in Fig. 8.7. The K_S coefficient values were taken from work [90].

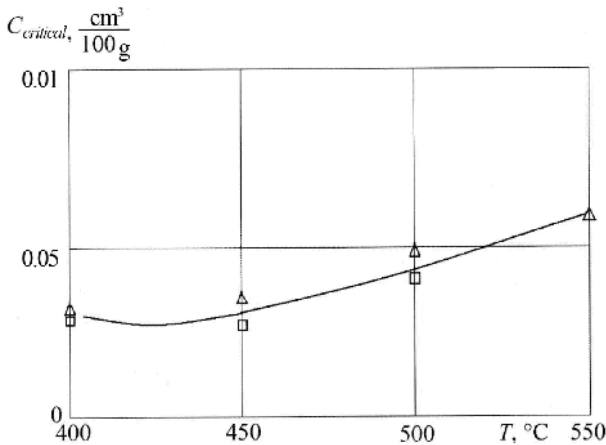


Fig. 8.7 Temperature dependence of critical concentration of hydrogen in aluminium: □ – based on our experimental data; Δ – based on data elsewhere [118]

The porosity will develop in aluminium specimens related to the area above the curve. In specimens below the curve no porosity will occur. The distribution of hydrogen between the solid solution and pores is presented in Fig. 8.8.

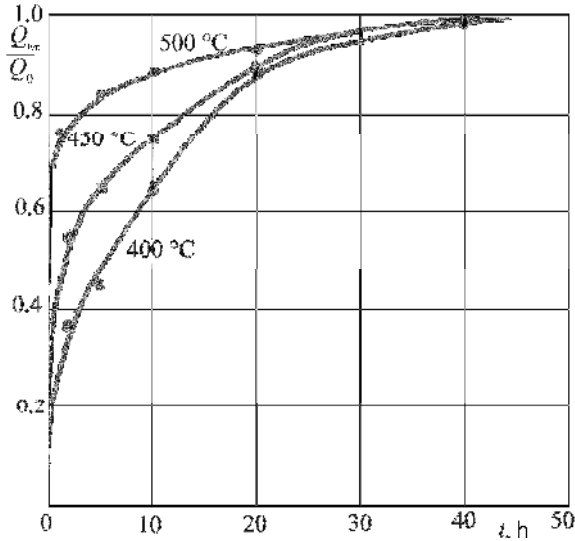


Fig. 8.8 The dependence of hydrogen fraction in pores of aluminium on the temperature and the time of annealing

It is worth noting that the curve of the critical concentration of hydrogen in aluminium reaches its minimum near 450 °C. This can be explained by the fact that while hydrogen solubility grows smoothly within the temperature range of 400 – 450 °C, the pressure in pores drops rapidly thus determining the overall decrease of the critical concentration of hydrogen with increasing temperature. The hydrogen pressure in pores remains almost constant with the further growth of temperature while hydrogen solubility in aluminium increases thus determining the overall growth of the critical concentration of hydrogen in the metal.

The critical concentration passes through the minimum (0.03 cm³/100 g) and then at the temperature of 550 °C it increases up to 0.06 cm³/100 g approximately.

With current manufacture technologies for aluminium products and semi-products it is not possible to obtain the metal with the hydrogen content lower than the critical one (see Fig. 8.7). Nevertheless, the kinetics of porosity growth as well as the highest possible value of porosity depends on the initial gas content in aluminium. The lower the initial gas content in aluminium is, the lower the highest possible volume of porosity is and the longer time to achieve this volume is needed.

We had carried also metallographic studies of porosity evolution in aluminium.

Metallographic specimens were prepared using a polishing paste. Then the samples were etched in hydrofluoric, nitric or hydrochloric acid to study the connection between porosity and grain boundaries. The results of the study are given in Fig. 8.9 – 8.11.

The pores were of similar size both in the body of grain and at the grain boundary for the same duration of annealing. At the same time, there occurred a redistribution of pores between the grain boundary and its body.

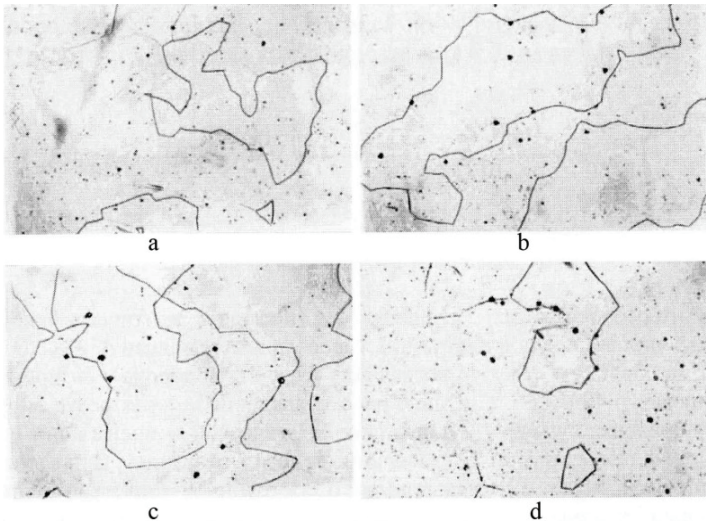


Fig. 8.9 The microstructure of aluminium after annealing at $T = 400\text{ }^{\circ}\text{C}$ during 1 hour (a); 2 hours (b); 10 hours (c); 42 hours (d) (magnification: $\times 200$)

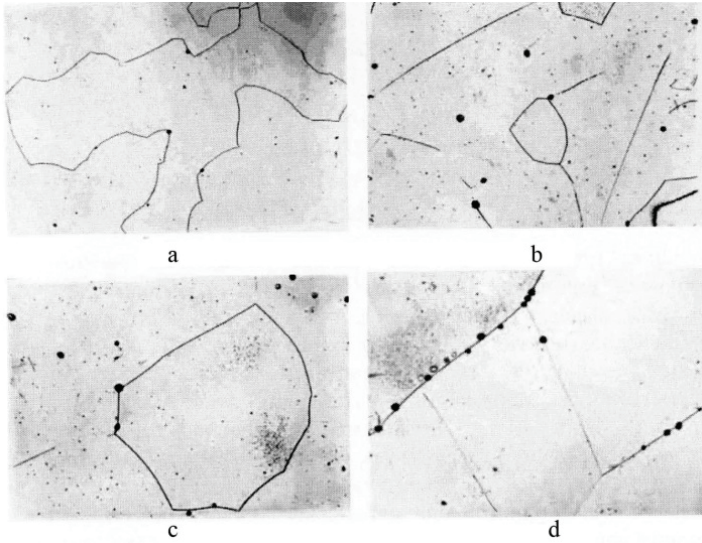


Fig. 8.10 The microstructure of aluminium after annealing at $T = 450\text{ }^{\circ}\text{C}$ during 1 hour (a); 2 hours (b); 10 hours (c); 42 hours (d) ($\times 200$)

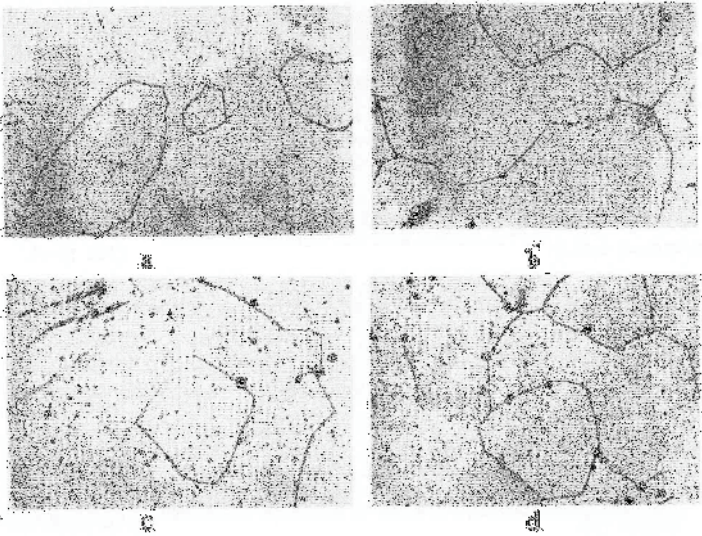


Fig. 8.11 The microstructure of aluminium after annealing at $T = 550\text{ }^{\circ}\text{C}$ during 1 hour (a); 2 hours (b); 10 hours (c); 42 hours (d) ($\times 200$)

The longer the time of annealing the more pores appear at the grain boundary while the number of pores in the grain body decreases, i.e. a preferential accumulation of pores at grain boundaries of aluminium takes place there. This probably occurs because of a higher energy state of the grain boundaries as compared to the grain body. Increasing annealing temperature results in pore size growth. In the course of annealing, the number of pores does not change both at the same temperature and at different temperatures.

The experimental trial of the proposed theory of gas porosity evolution in metals allows us to make a conclusion about the validity of the concepts laid in the basis of the theory.

Indeed, the tendency of the system to move towards the thermodynamical equilibrium between the gas dissolved in the lattice of the metal and the gas in the pores causes the evolution of gas porosity in solid metals. The gas diffusion through the metal to the pore surface is the limiting factor of porosity growth.

For each annealing temperature there is a critical gas pressure in pores related to the rupture strength of the metal in the microvolume around a pore. The surpassing of this critical gas pressure in pores results in porosity growth. Further growth of porosity stops immediately as soon as the thermodynamical equilibrium between the gas dissolved in the metal lattice and the gas in the pores is achieved. The surpassing of the critical concentration of the gas related to the gas solubility at a given temperature and the gas pressure in pores results in the evolution of porosity.

CHAPTER 9. THE APPLICATION OF THE RESULTS OBTAINED TO THE DEVELOPMENT OF THE PROCESS TECHNIQUE, PROVIDING THE MINIMIZATION OF ALUMINIUM ALLOY SHEETS REJECTS CAUSED BY HYDROGEN BLISTERS

The clarification of the mechanism of gas porosity formation in metals and the study of hydrogen diffusion processes in aluminium make it possible to propose a few recommendations concerning the removing of structural imperfections caused by the presence of gases in specific aluminium or aluminium alloy semi-products.

The problems of the reduction of the rejects of sheathing plates of aluminium and its alloys caused by near-surface cavities as well as the results of the commercial scale trials of offered recommendations are discussed in this chapter.

One of the main flaws of aluminium and aluminium alloy sheet is the formation of gas cavities. Until now there is no technique capable of determining the reason of the occurrence of this negative phenomenon. There is also no reliable method for the differentiation of cavities, caused by hydrogen contained in the metal, and blisters-rolling defects, formed due to poor penetration, improper reduction conditions etc.

As it was shown in Chapters 7 and 8, the defects caused by the gas contained in the metal develop during the heat treatment of the metal. Therefore, the identification of the process stage when cavities or blisters appear could be one of the methods for revealing the reasons of these phenomena.

If cavities are formed after rolling and further heat treatment then their formation is caused by the hydrogen contained in the metal. If blisters are formed straightforwardly during rolling then their formation is caused probably by the rolling defects. The development of blisters in thin plates seems to be a particular case of the formation of structural defects caused by the presence of a gas in the metal. Therefore, the formation of blisters in thin plates follows the laws given in Chapter 7.

Gas cavities in thin plates develop because of the system tendency to move towards thermodynamical equilibrium between the hydrogen dissolved in the lattice of the metal and the hydrogen in the gas phase (in a blister).

Therefore, according to the theory of the development of defects caused by the gas presenting in the metal, there exists a critical concentration of hydrogen below which gas cavities in the metal will not occur (see Chapter 8, Fig. 8.7). The decrease of hydrogen concentration in the metal below this limit could prevent the formation of gas cavities in the metal.

The up-to-date methods of liquid melt processing (refining and vacuum degassing) are not capable of lowering the concentration of hydrogen in aluminium below the critical level. It would seem that there is no way of avoiding the formation of gas pores in Al thin plates. However, the results of aluminium degassing in the course of annealing in air shown in Chapters 5 and 7 look very promising. Particularly the one and a half hour annealing of 12 mm aluminium rods at the temperature of 550 °C decreases the content of hydrogen in aluminium down to 0.01 cm³/100 g.

Thus, we can prevent the formation of defects in aluminium caused by the presence of a gas in the metal, through a preliminary degassing of the metal in the course of annealing in air.

This method could be effective for sufficiently thin-walled products and semi-products since the rate of degassing is inversely related to the square root of the metal thickness, such as thin-walled pipes, shaped rolled products, stamped parts and thin plate material. The accounting for gas defects formation during the degassing of metal is obligatory since the content of hydrogen in the metal at the initial stage of degassing surpasses the critical concentration of hydrogen below which structural defects do not form. During the further stages of degassing, the hydrogen will go out both from the metal and the gas defects as well. Therefore, an additional deformation of the metal would be required right after the degassing in air to remove the defects formed. This operation seems to be quite efficient as there will be no hydrogen remained in structural defects and cavities will be welded during the deformation.

As a result, it is possible to suggest the following process to remove gas cavities from thin plate materials.

At first, the billet is to be rolled down to a thickness surpassing the final thickness by several millimeters. Then the billet is to be annealed in air to remove hydrogen from the metal. Heat treatment conditions must be selected according to the data given in Chapters 5, 7 and 8. Then the billet is rolled down to a specified final thickness.

This production process was industrially tested for the removal of gas cavities from large size sheathing sheet metal of Al-plated alloy Д16.

The commercial process of sheathing sheet production comes down to the following. 8 mm thick hot rolled aluminium sheet is placed on the ingot of Д16 alloy. Then the alloy Д16 ingots together with the aluminium sheet are hot rolled down to the thickness of 6 – 8 mm. Then the hot rolled sheets are heat-treated – quenched at the temperature of 500 °C. The main type of defects in these semi-products is surface blisters occurring after the heat treatment.

From the above said, it may be deduced that the formation of blisters is caused by the hydrogen contained in the metal [122].

For this particular case, the following process technique may be quite efficient.

It is necessary to decrease the hydrogen content in the metal down to 0.04 cm³/100 g approximately. The initial content of hydrogen in the aluminium sheet determined according to the procedure described in Chapter 1, made around 0.2 cm³/100 g. The time required for decreasing the hydrogen percentage in aluminium sheet from 0.2 down to 0.04 cm³/100 g during annealing in air can be calculated from the data given in Chapters 5 and 7.

Let us assume the temperature of annealing equal to 540 °C. The process of degassing proceeds rather intensively at this temperature, but, at the same time, this temperature is not too high for aluminium.

The time of degassing can be calculated by equation (5.11)

$$\ln \frac{C}{C_0} = -K_{\Sigma} \sqrt{t}$$

or by

$$t = \frac{\left(\ln \frac{C}{C_0} \right)^2}{K_{\Sigma}^2}. \quad (9.1)$$

The value of K_{Σ} makes $5.47 \cdot 10^{-3} \text{sec}^{-1}$ for temperature of 540 °C.

Since the ratio

$$\frac{C}{C_0} = \frac{0.04}{0.2} = 0.2, \quad (9.2)$$

$$\text{we have } t = \frac{(\ln 0.2)^2}{(5.47 \cdot 10^{-3})^2} \approx 24 \text{ h}, \quad (9.3)$$

i.e. the annealing of aluminium billet in air at the temperature of 540 °C for about 24 hours would bring a decrease of hydrogen content from 0.2 cm³/100 g down to 0.04 cm³/100 g, the critical value of hydrogen concentration, that is the limit below which no porosity occurs. Therefore, porosity will not form with further heat treatment.

Finally, to remove gas cavities from the Al-plated Д16 alloy the following process was proposed:

- rolling of aluminium thin plate down to 12 mm;
- annealing in air at the temperature of 540 °C for about 24 hours;
- further rolling down to the final thickness of 8 mm.

Further operations of simultaneous rolling of Д16 ingots and the aluminium sheet as well as their heat treatment are carried out according to the standard practice. Fig. 9.1 presents the results of the process technique developed at one of the plants of the industrial sector. The comparative results were obtained for the total weight of processed aluminium ingots of around 300 t. It appears that advanced technologies of rolling and argon blowing of liquid metal do not help much in decreasing the rejects caused by blisters. Nevertheless, these measures make it possible to increase the yield thanks to the elimination of other defects.

Table 9.1

The effect of technology factors on the yield and the reject of Al-plated Д16 sheathing production

Period	Reject caused by blisters and cavities, % from total weight of ingots processed by rolling	Yield, % from total weight of ingots processed by rolling	Production process technique
I–VIII 1970	21.1	12	Standard production technique
VIII–X 1970	18.2	23.8	Advanced 1. The elimination of mechanical defects from the surface of thin plate 2. Rinsing in water 3. The change of the direction of rolling 4. Continuous refining of aluminium with argon
I–IX 1971	10.8	34.3	Advanced +: 1. The annealing of 12 mm thick aluminium rolled stock a $T = 540\text{ }^{\circ}\text{C}$, $t = 24\text{ h}$. 2. The rolling of billets down to a final thickness

The implementation of this technology has reduced the blister rejects by about two times and thus increased the prime output by 1.5 times.

The proposed process has been commercially tested and protected by the author's certificate [123].

CHAPTER 10. A NEW METHOD OF MEASURING THE SURFACE TENSION OF SOLID METALS

V.I.Rolugin in his book [124] highlights several well-known methods for measuring the surface tension of solid bodies.

1. *The method of `zero-creep`*. The specimen having the shape of a long string or foil is heated up to a sufficiently high temperature so that it gets shorter under the effect of surface tension. An external force is applied to this specimen in order to preserve the specimen shape. The surface tension is determined by this force value.

2. *The method of crystal fracture (cleavage)*. The cleavage of a layer from the crystal is carried out. The surface tension corresponds to the work spent for cleaving the crystal.

3. *The method of powder dissolution*. The temperature of dissolution of a massive crystal and a powder of the same weight, serves as the basis of this method. The area A_p of the powder is determined independently. The surface tension can be determined by the equation

$$\sigma^s = \frac{\Delta Q}{A_p} \quad (10.1)$$

where ΔQ – the difference of the heats of dissolution.

4. *The method of neutral drop*. The value of surface tension can be determined by the shape of an equilibrium drop of another substance placed on the surface of the tested solid body.

5. *The method of `scratch healing`*. The surface tension is determined by the time required for half-healing of a scratch of a given width on the surface of the crystal. It is necessary to know the value of the surface diffusion coefficient too. This coefficient also determines the rate of `healing`.

The experimental results concerning the surface tension of solid bodies including solid aluminium are also presented in [124]. The surface tension at 180 °C makes (1.14 ± 0.2) J/m².

The authors in [125] presented the method allowing to determine the surface tension of a solid body, applicable to metals, silicate and polymer materials in the whole temperature range for the solid state of materials. The method comprises annealing of a string-type sample subjected to

stretching strain within the limits of elastic deformation. After the annealing the temperature of the specimen is to be decreased down to the temperature of measurement, the stretching load shall be removed and the maximum deflection measured. The surface tension shall be determined by the equation

$$\sigma_T = \frac{8\pi^2 EJ_{\min}}{b\mu^2(8\ell^2 - \pi^2 f_{\max}^2)}, \quad (10.2)$$

where E – the modulus of elasticity of the specimen, N/m²; J_{\min} – minimum value of the main moment of inertia of the cross-section, m²; b – the perimeter of cross-section, m; π – the coefficient accounting the method of specimen ends fixation; ℓ – the specimen length, m; F_{\max} – the maximum transversal sag of the specimen, m.

The method of surface tension determination proposed in [126] is based on the equilibration of a mechanical lever by means of displacing the compensation load along the right arm of the lever. There is a small mirror fixed at the end of the lever being part of the optical system together with the scale and the lamp. The specimen in the form of an inverted Π is heated to a specified temperature by passing electric current through it.

The surface tension shall be determined by the equation

$$\sigma = \frac{1}{\pi d} \left(P + \frac{\Delta \ell}{L} P \right), \quad (10.3)$$

where d – the diameter of a specimen at working temperature; L – the arm of the lever from the pivot to the specimen; P – the compensation load weight; $\Delta \ell$ – the displacement of the compensation load.

One more known method for surface tension determination, the method of pore coalescence is based on the tendency of the system to minimize the surface energy of a porous body. This tendency results in coalescence of fine pores and formation of bigger ones. The rate of self-diffusion defines the rate of the process.

The disadvantage of the standard method is that we have to know the value of the diffusion coefficient to determine the surface tension, and the diffusion coefficient is structure-sensitive to high extent. A considerable error of experimental determination of the diffusion coefficient is one of

its demerits. Moreover, this method can be used at temperatures close to the melting point of the metal where the rate of self-diffusion is very high. The rate of self-diffusion dwindles exponentially with decreasing temperature, whereas the time of asymptotic distribution of pores by their sizes increases to such an extent that the determination of surface tension becomes almost impossible.

We have proposed a new method for the measurement of surface tension of solid metals to enhance the accuracy and the efficiency of analyses and to widen the temperature range of measurements.

The value of surface tension σ , $\text{H}\cdot\text{m}^{-1}$ is obtained from the equation

$$\sigma = 5 \cdot 10^2 \cdot \bar{R} \left[\left(\frac{RTK_S}{44.8 \cdot V} \right) \sqrt{\left(\frac{RTK_S}{44.8 \cdot V} \right) + \frac{RTC_0}{22.4 \cdot V}} \right]^2, \quad (10.4)$$

where \bar{R} – mean pore radius, cm; T – temperature, K; K – gas solubility in the metal, %; V – porosity volume, % abs.; $R = 0.082 \frac{\text{l} \cdot \text{atm}}{\text{mol} \cdot \text{K}}$;

C_0 – total gas content in the specimen, $\frac{\text{cm}^3(\text{NTP})}{\text{cm}^3 \cdot \text{Me}}$

The proposed method increases considerably the efficiency of the measurement because the time required to obtain the maximum porosity in the specimen is limited by the rate of the dissolved gas diffusion through the metal. This rate can be several orders higher than the rate of self-diffusion. This method is protected by the author's certificate [127].

Referenses

1. Бэррер Р. Диффузия в твердых телах. М.: ИЛ, 1948. (Barrer R. Solid phase diffusion. M.: IL, 1948.)
2. Дэшман С. Научные основы вакуумной техники. И.: Изд-во МИР, 1961. (Desman C. Scientific basis of vacuum engineering. I.: Publishing house MIR, 1961.)
3. Смителлс К. Газы и металлы. М.: Metallurgy, 1940. (Smithells K. Gases and metals. M.: Metallurgy, 1940.)
4. Галактионова Н.А. Водород в металлах. М.: Metallurgy, 1967. (Galaktionova N.A. Hydrogen in metals. M.: Metallurgy, 1967.)
5. Borrelius G., Lindblom S. // Ann. d. Physik. 1927. 32. 201.
6. Smithells C.J., Ransley C.E // Pros. Roy. Soc. A. 1935. 150. 172.
7. Stress T.M., Tomkins P.C. // J. Chem. Soc. 1956. 230.
8. Melville H., Rideal B. // Pros. Roy. Soc. A. 1936. 155. 89.
9. Smithells C.J., Ransley C.E. // Pros. Roy. Soc. A. 1936. 157. 292.
10. Wang J.S. // Pros. Comb. Phil. Soc. 1936. 32. 657.
11. Barrer R.M. //Trans. Far. Soc. 1940. 36. 1235.
12. Chang P.L., Bennett W.D.G. // J. Iron and Steel Inst. 1952. 170. 3. 205.
13. Зайдель А.Н. и др. Спектрально-изотопный метод определения водорода в металлах. Л.: Изд-во ЛГУ, 1957. (Seidel A.N. et al. Spectral-isotope technique of measurement of hydrogen content in metals. L.: Publishing house of LGU, 1957.)
14. Зайдель А.Н., Петров А.А. // ЖТФ. 1955. 25. 2571. (Seidel A.N. et al. Spectral-isotope technique of measurement of hydrogen content in metals. L.: Publishing house of LGU, 1957.)
15. Зайдель А.Н., Петров А.А. // Заводская лаборатория. 1956. 22. 923. (Seidel A.N. Petrov A.A. // Plant laboratory. 1956. 22. 923).
16. Langmuir J. // Ind. Eng. Chem. 1915. 7. 348.
17. Ransley C.E. // Analyst. 1947. 72. 504.
18. Sloman H.A. Hi. Inst. Metals. 1945. 71. 391.
19. Martin G.S. // Australas Engr. 1955. 46. 58.
20. Hatfield W.H., Newell W.G. // J. Iron and Steel Inst. 1919. 148. 35.
21. Smiley W.G. //Anal. Ghem. 1955. 27. 1098.
22. Steinhauser K. // Z. Metallkunde. 1934. 26. 6. 136.
23. Griffith C.B., Mallett H.W. // Anal. Chem. 1953. 25. 7. 1085.
24. Ronner P. // Schweis. Arch. 1957. 23. 8. 243.
25. Eborall R. // The determination of gases in metals, Special Report № 68. The Iron and Steel Inst. London, 1960. 192.
26. Данилкин В.А. Качественные и количественные методы определения водорода в жидких и твердых алюминиевых сплавах. М.: ВИЛС, 1968. (Da-

nilkin V.A. Qualitative and quantitative measurements of hydrogen in liquid and solid aluminium alloys. M.: VILS (All Union Institute Of light alloys), 1968.)

27. Данилкин В.А. // Методы определения и исследования состояния газов в металлах. М.: Наука, 1968. 24. (Danilkin V.A. // Methods for measurement and study of the state of gases in metals. M.: Nauka (Science), 1968. 24.)

28. Hipple J.A., Sommer H., Thomas H.A. // Phys. Rev. 1949. 76. 1877.

29. Alpert D., Buritz R.S. // J. Appl. Phys. 1954. 25. 202.

30. Klopfer A., Schmidt W. // Vacuum. 1960. 10. 363.

31. Улановский Я.Б., Данилкин В.А., Томлянович В.Д. // Технология легких сплавов. М.: ВИЛС, 1971. 4. 95. (Ulanovskiy I.B., Danilkin V.A., Tomlyanovich V.D. // M.: VILS (All union institute Of light alloys), 1971. 4. 95.)

32. Клячко Ю.А. // Заводская лаборатория. 1936. 5. 5. 572. (Klyachko U.A. // Plant laboratory. 1936. 5. 5. 572.)

33. Клячко Ю.А. // ЖПХ. 1937. 10. 1.329. (Klyachko U.A. // HPCh (Journal of applied chemistry). 1937. 10. 1.329.)

34. Клячко Ю.А. // ЖПХ. 1941. 14. 1.84. (Klyachko U.A. // JACH (Journal of applied chemistry). 1941. 14. 1.84.)

35. Клячко Ю.А. // ЖПХ. 1941. 14.3.342. (Klyachko U.A. // JACH (Journal of applied chemistry). 1941. 14.3.342.)

36. Авт. свидет. № 453623. Способ определения концентрации водорода в сплавах, содержащих компоненты с высокой упругостью пара / Я.Б. Улановский, Г.И. Егорова. Опубл. 15.12.1974. (Author's certificate № 453623. The method of hydrogen content determination in alloys containing components characterized by high vapour pressure / I.B. Ulanovskiy, G.I. Egorova. Published on 15.12.1974.)

37. Ransley C.E., Newfeld B. // J. Inst. Metals. 1948. 74. 12. 599.

38. Eichenauer W., Hattenbach C, Pebler A. PZ. Metallkunde. 1961. 52. 10. 682.

39. Eichenauer W. // Z. Metallkunde. 1968. 59. 8. 613.

40. Eborall R., Ransley C.E. // J. Inst. Metals. 1945. 71. 525.

41. Константы взаимодействия металлов с газами / Я.Д. Коган, Б.А.Колачев, Ю.В. Левинский и др. М.: Металлургия, 1987. (Constants of metals interaction with gases / J. D. Cogan, B. A. Kolachev, U.V. Levinsky et al.: Metallurgy, 1987.)

42. Андреев Л.А., Гельман Б.Г., Жуховицкий А.А., Полосина Е.Е. Наводороживание металлов при взаимодействии с водой // Изв. вузов. Черная металлургия. 1972. 1. (Andreev L. A., Gelman B. G., Zhukhovitsky A. A., Polosina E. E. Hydrogenation of metals during interaction with water. // Izv. Vouzov (News of Higher Educational Institutions). Ferrous metallurgy. 1972. 1.)

43. Пименов Ю.П. Об окиси алюминия и водорода в алюминии: Автореф. дис. ... канд. техн. наук. М., 1967. (Pimenov Yu. P. Behavior of Aluminium oxide and hydrogen in aluminium: The abstract of Ph.D. thesis in Engineering Science. M., 1967.)

44. Гельман Б.Г. Взаимодействие твердого алюминия с водородом и водой: Автореф. дис. ... канд. техн. наук. М.: 1972. (Gelman B. G. Interaction of solid aluminium with hydrogen and water: The abstract of Ph.D. thesis in Engineering Science. M. : 1972.)

45. Андреев Л.А., Левчук Б.В., Гельман Б.Г. и др. Растворимость водорода в сплавах алюминий-магний. Технология легких сплавов. М.: ВИЛС, 1972.4. (Andreev, L. A., Levchuk B. V., Gelman, B. G. et al. Hydrogen solubility in aluminium –magnesium alloys. Process of production of light alloys. M.: VILS (ALL UNION INSTITUTE OF LIGHT ALLOYS), 1972.4.)

46. Жуховицкий А.А., Гельман Б.Г., Андреев Л.А. Наводороживание твердого алюминия в парах воды. Доклады АН СССР. 1972. 6. (Zhukhovitsky A. A., Gelman B. G., Andreev L. A. Hydrogenation of solid aluminium in water steam. Reports of the Science Academy of the USSR, 1972. 6.)

47. Растворимость водорода в интерметаллических соединениях алюминия с магнием, медью, марганцем, титаном и цирконием / Р.М. Габидуллин, И.В. Швецов, Б.А. Колачев, Ю.И. Аргаков. В кн.: Строение, свойства и применение металлидов. М.: Наука, 1974. (Hydrogen solubility in intermetallic compounds of aluminium, copper, manganese, titanium, and zircon / P.M. Gabidullin, I.V. Shvetcov, B.A. Kolachev, Ju.I. Argakov. In the book: Structure, properties and application of intermetallic compounds. M.: Science, 1974.)

48. Bramley A., Jinkins A. // Carnegie School. Mem. Iron and Steel Inst. 1926. 15. 17.

49. Coehn A., Specht W. // Z. Physik. 1930. 62. 1.

50. Coehn A., Sperling K. // Z. Physik. 1933. 83. 291.

51. Ransley C.E., Talbot D.E.J. // Z. Metallkunde. 1955. 46. 5. 328.

52. Eichenauer W., Pebler A. // Z. Metallkunde. 1957. 48. 7. 373.

53. Johnson E.W., Hill W.L. // Trans. AIME. 1960-1961. 218. 1104.

54. Buringer G. // Z. Physik. 1935. 96. 37.

55. Hill M.L., Johnson E.W. // Acta Metallurgia. 1955. 3. 566.

56. Holst // Z. Physic. 1933. 86. 338.

57. Watson Hill // Bull. Amer. Phys. Soc. 1936. 11.2.

58. Данилкин В.А. Определение содержания водорода в деформируемых алюминиевых сплавах методом вакуум-нагрева: Дис. ... канд. техн. наук. М.: ВИЛС. 1969. (Danilkin V.A. Measurement of hydrogen content in wrought aluminium alloys through vacuum heating: Ph.D. thesis in Engineering Science. M.: VILS (All Union Institute Of Light Alloys). 1969.)

59. Исследование диффузии атомов водорода в кристаллах ГЦК-металлов методом молекулярной динамики / Н.А. Калабухова, Г.М. Полетаев, М.Д. Старостенков и др. // Изв. вузов. Физика. 2011. 12. 86-91. (The study of hydrogen diffusion in crystals of FCC metals through molecular dynamics method / N.A. Kalabukhova, G.M. Poletaev, M.D. Starostenkov and др. // News of Higher Educational Institutions. Physics. 2011. 12. 86-91.)

60. Спивак Л.В., Скрябина Н.Е., Кац М.Я. Водород и механическое последствие в металлах и сплавах. Пермь: Изд-во ПГУ, 1993. 344. (Spivak L.V., Skriabina N.E., Kats M. Ia. Hydrogen Водород mechanical aftereffect in metals and alloys. Perm: Publisher PGU (Perm State University), 1993. 344.)
61. Hashimoto H., Kino T. Hydrogen diffusion in aluminium at high temperatures // J.Phys. Metal. Phys. 1983. 13. 1157.
62. Ishikawa T., McLellan R.B. The diffusivity of hydrogen in aluminium. Acta metal. 1986. 34. 1091.
63. Кинетические закономерности взаимодействия водорода с твердым алюминием / Л.А. Андреев, А.Ф. Вяткин, Б.В. Левчук и др. // Изв. вузов. Цветная металлургия. 1975. 5. (Kinetics of hydrogen interaction with solid aluminium / L.A. Andreev, A.F. Viatkin, B.V. Levchuk et al // News of Higher Educational Institutions. Nonferrous industry. 1975. 5.)
64. Matsuo S., Hirata T. // J. Japan. Inst. Metals. 1967. 31. 590.
65. Rapp K, Kovacs E. Csetenyi // Scripta Metallurgica. 1977. 11. 92.
66. Rapp K., E. Kovacs. Csetenyi. Diffusion of Hydrogen in High Purity // Aluminium Scripta Metallurgica. 1981. 15. 161.
67. Outlaw R.A., Peterson D.T., Schmidt F.A. Diffusion of Hydrogen in Pure Large Grain // Aluminum Scripta Metallurgica. 1982. 16. 287.
68. Ichimura M., Imabayashi M., Hayakawa M. // J. Japan. Inst. Metals. 1979.43.876.
69. Saitoh H., Iijima Y., Tanaka H. Hydrogen diffusivity in aluminium measured by a glow discharge permeation method // Acta Metall. 1994. 42. 2. 493.
70. Добаткин В.И., Габидуллин Р.М., Колачев Б.А. Газы и окислы в алюминиевых деформируемых сплавах. М.: Металлургия, 1976. 264. (Dobatkina V.I., Gabidullin R.M., Kolachev B.A. Gases and oxides in aluminium wrought alloys. M.: Metallurgy, 1976. 264.)
71. Свойства элементов. Физические свойства: Справ./ Под ред. Г.В. Самсонова. М.: Металлургия, 1976. 600. (Properties of elements . Physical properties: Guidebook. / under the editorship of G.V. Samsonov. M.: Metallurgy, 1976. 600.)
72. Исследование водородопроницаемости алюминия методом концентрационных импульсов // Е.А. Денисов, Т.Н. Компанией, А.А. Курдюмов и др. М.: Материаловедение, 2006. 5. (The study hydrogen permeability of aluminium through the method of concentration pulses // E.A. Denisov, T.N. Kompaniei, A.A. Kurdiumov et al . M.: Material engineering, 2006. 5.)
73. Young G.A., Scully J.R. The diffusion and trapping of hydrogen in high purity aluminium // Acta Materialia. 1998. 46. 11. 6337.
74. Beck A.F. // Corrosion Science. 1967. 7. 1.
75. Клячко Ю.А. // Легкие металлы. 1934. 7. (Klyachko U.A. // Light metals. 1934. 7.)
76. Klaschko // Kolloid Zeit. 1935. 73. 226.

77. Альтман М.Б. // Неметаллические включения в алюминиевых сплавах. М.: Металлургия, 1965. (Altman M.B. // Nonmetallic inclusions in aluminium alloys. M.: Metallurgy, 1965.)
78. Иванов В.П., Спасский А.Г. // Литейное производство. 1963. 12. 18. (Ivanov V.P., Spassky A.G. // Foundry industry. 1963. 12. 18.)
79. Иванов В.П., Спасский А.Г. // Изв. вузов. Цветная металлургия. 1963. 1. 141. (Ivanov V.P., Spassky A.G. // News of Higher Educational Institutions. Nonferrous metallurgy. 1963. 1. 141.)
80. Ловцов Д.П. // Литейное производство. 1955. 12. 18. (Lovtsov D.P. // Foundry engineering. 1955. 12. 18.)
81. Авт. свидет. № 246060. Способ получения литых композиционных материалов. Промышленные образцы и товарные знаки / Г.Л. Эскин, П.Н. Швецов. Бюлл. изобретения. 1969. 20. 81. (Author's certificate № 246060. A method of cast composite material production / G.L. Eskin, P.N. Shvetsov. Bulletin of inventions. 1969. 20. 81.)
82. Matano C. // Japan. J. Phys. 1933. 8. 109.
83. Бао Сюэ Синь, Бокштейн Б.С., Жуховицкий А.А. // ФТТ. 1961.3.3.723. (Bao Siue Sin, Bokshtein B.S., Zhukhovitsky A. A. // Solid State Physics. 1961.3.3.723.)
84. Улановский Я.Б. // Технология легких сплавов. М.: ВИЛС, 1971. 5. 18. (Ulanovskiy I.B. // Operational procedure of light alloys production . M.: VILS (All Union Institute Of Light Alloys), 1971. 5. 18.)
85. Smithells C.J., Ransley C.E. // Pros. Roy. Soc. A. 1935. 152. 706. 86. Russell A.S. // Metal Progress. 1949. 55. 827.
87. Cochran C.N. // J. Electrochem. Soc. 1961. 108. 4. 317.
88. Вяткин А.Ф., Андреев Л.А., Данилкин В.А. Водородопроницаемость алюминия // Изв. вузов. Черная металлургия. 1975. 3. 23. (Viatkin A.F., Andreev L.A., Danilkin V.A. Hydrogen permeability of aluminium // News of Higher Educational Institutions. Ferrous Metallurgy. 1975. 3. 23.)
89. Данилкин В.А., Улановский Я.Б., Томлянович В.Д. // Технология легких сплавов. М.: ВИЛС, 1971. 5. 87. (Danilkin V.A., Ulanovskiy I.B., Tomlianovich V.D. // Process of production of light alloys. M.: VILS (All Union Institute Of Light Alloys), 1971. 5. 87.)
90. Андреев Л.А., Гельман Б.Г. // Заводская лаборатория. 1971. 10. 1205. (Andreev L.A., Gelman B.G. // Plant laboratory. 1971. 10. 1205.)
91. Герасимов В.И., Крестовников А.Н., Шахов А.С. Химическая термодинамика в цветной металлургии. М.: Металлургия, 1966. (Gerasimov V.I., Krestovnikov A.N., Shakhov A.S. Thermochemistry in nonferrous metallurgy. M.: Metallurgy, 1966.)
92. Neuman B., Kroger G., Hoebler H. // Z. Anorg.-Allg. Chem. 1932. 204. 31.
93. Kostron H. HZ. fur Meletallkunde. 1952. 43. 8. 269; 1952. 43. 11. 273.
94. Richter P., Sprengel A. // Z. Anorg. Allg. Chem. 1943. 82. 192.

95. Cabrera N., Mott N.F. // Rep. Prog. Phys. 1948. 12. 163.
96. Cabrera N., Hamon J. // Rep. Prog. Phys. 1947.
97. Smeltzer W.W. // J. Electrochem. Soc. 1956. 103. 209.
98. Gulbransen E., Wysong W.S. // J. Phys. Colloid Chem. 1947. 57. 1087.
99. Aytmore D.W., Greegy S.J., Jepson W.B. // J. Inst. Metals. 1950. 88. 205.
100. Hunter M.S., Fowle P. // J. Electrochem. Soc. 1956. 103. 482.
101. Cochran C.N., Sloppy W.S. // J. Electrochem. Soc. 1961. 108. 322.
102. Thomas K., Roberts M.W. // J. Appl. Physics. 1961. 32. 70.
103. Beck A.F., Heine M.A., Caule E.J., Pryor M.I. // Corrosion Science. 1967. 7. 1.
104. Авт. свидет. № 428008. Я.Б. Улановский, А.А. Жуховицкий, В.А. Данилкин. Оpubл. 15.05.1974. (Author's certificate № 42808. Ulanovskiy I.B., A.A. Zhukhovitsky, V.A. Danilkin. Published on 15.05.1974.)
105. Фридляндер И.Н. // Металлургические основы литья легких сплавов. М.: Оборонгиз, 1957. (Fridliander I.N. // Metallurgical basis of casting of light alloys. M.: Oborongiz (State Publisher), 1957.)
106. Фридляндер И.П. Сб. Гидродинамика расплавленных металлов. М.: Изд-во АН СССР, 1958. (Fridliander I.N. Collection of articles . Hydrodynamics of molten alloys. M.: Publishing house of the Academy of sciences of the USSR, 1958.)
107. Тулянкин Ф.В. и др. // Металлургические основы литья легких сплавов. М.: Оборонгиз, 1957. (Tuliankin F.V. et al. // Metallurgical basis of casting of light alloys. M.: Oborongiz (State Publisher), 1957.)
108. Тейтель И.Л. // Металлургические основы литья легких сплавов. М.: Оборонгиз, 1957. (Teitel I.L. // Metallurgical basis of casting of light alloys. M.: OBORONGIZ (State Publisher), 1957.)
109. Захаров В.З. Некоторые вопросы технологии производства полуфабрикатов из алюминиевых сплавов: Дис. ... канд. техн. наук. М.: ВИЛС, 1967. (Zakharov V.Z. Problems of production of semi products from aluminium alloys: Ph.D. thesis in Engineering Science. M.: VILS (All Union Institute Of Light Alloys), 1967.)
110. Комков П.Ф. // Технология изготовления полуфабрикатов из алюминиевых сплавов. М.: ВИНТИ. 1964. (Komkov P.F. // Operational procedure of semi products production from aluminium alloys. M.: VINITI (All Union Institute of Scientific And Technical Information). 1964.)
111. Мурзов А.И. и др. // Алюминиевые и специальные сплавы. М.: ВИАМ, 1966. (Murzov A.I. et al // Aluminium and special alloys M.: VIAM (All Union Institute of Aviation Materials), 1966.)
112. Михнев Е.С. и др. // Технология легких сплавов. М.: ВИЛС, 1965. 3. (Mikhnev E.S. et al // Process of production of light alloys . M.: VILS (All Union Institute Of Light Alloys), 1965. 3.)

113. Курицына Г.И. // Технология изготовления полуфабрикатов из алюминиевых сплавов. М.: ВИНТИ, 1964. (Kuritsyna G.I.// Process of aluminium semi products production. M.: VINITI (All Union Institute of Scientific And Technical Information), 1964.)

114. Андреев А.Д., Соловьева В.В. // Технология легких сплавов. М.: ВИЛС, 1967.2. 106. (Andreev A.D., Soloveva V.V. // Process of production of light alloys . M.: VILS (All Union Institute Of Light Alloys), 1967.2. 106.)

115. Рапа М. Микропористость. Федеральный Политехнический институт в Лозанне, 1996. (M. Microporosity. The Federal Ecole Politechnique in Lausanne, 1996.)

116. Bruna M., Sladek A., Kurcharcik L. Formation of Porosity in Al-Si Alloys // Archives of Foundry Engineering. 2011. 12. 5.

117. Pequet Ch., Gremaud M., Pappaz M. Modelling of Microporosity, Macroporosity, and Pipe-Shrinkade Formation during the Solidification of Alloys Using a Mushy-Zone Refinement Method // Applications to Aluminum Alloys Metallurgical and Materials Transactions A. 2002. 33A. 7. 2095.

118. Talbot D.E.J., Granger D.A. // J. Inst. Metals. 1963. 92. 290.

119. Жуховицкий А.А., Шварцман Л.А. Физическая химия. М.: Металлургия, 1968. (Zhukhovitsky A. A., Shvartzman L.A. Physical Chemistry. M.: Metallurgy, 1968.)

120. Улановский Я.Б. // Технология легких сплавов. М.: ВИЛС, 1972.1.42. (Ulanovskiy I.B. // Process of production of light alloys . M.: VILS (All Union Institute Of Light Alloys), 1972.1.42.)

121. Улановский Я.Б., Жуховицкий А.А. // Известия АН СССР. Металлы, 1972.3. (Ulanovskiy I.B., Zhukhovitsky A. A. // Proceedings of the USSR Academy of Sciences. Metals, 1972.3.)

122. Добаткин В.И. Слитки алюминиевых сплавов. М.: Металлургиздат, 1960; // Технология легких сплавов. М.: ВИЛС, 1969. 2. 21; 1970. 3. 40; 1972. 1.90. (Dobatkin V.U. Ingots of aluminium alloys. M.: Metallurgizdat, 1960; // Process of Production of light alloys. M.: VILS, 1969. 2. 21; 1970. 3. 40; 1972. 1.90.)

123. Авт. свидет. № 423599. Способ изготовления плакированных листов из алюминиевых сплавов / Я.Б. Улановский, В.А. Данилкин, А.А. Жуховицкий. Опубл. 15.04.1974. (Author's certificate № 423599. A method of clad plate production from aluminium alloys / I.B. Ulanovskiy, V.A. Danilkin, A.A. Zhukhovitsky . Published on 15.04.1974.)

124. Ролдугин В.И. Физикохимия поверхности. Долгопрудный: Изд. дом «Интеллект», 2008. (Roldugin V.I. Physical chemistry of surface. Dolgoprudny: Publishing house «Intellect», 2008.)

125. Авт. свидет. SU 911228. Способ определения поверхностного натяжения твердых тел / В.Т. Федоров, Х.Б. Хоконов, Б. Карамурзов. Опубл. 07.03.1982. (Author's certificate SU 911228. A method for determination of sur-

face tension of solid bodies / V.T. Fedodorov, H.B. Hokonov, B. Karamourzov. Published on 07.03.1982.)

126. Патент на изобретение. G01N №2314515. Способ измерения поверхностного натяжения металлов в твердой фазе / М.В. Гедагова, В.К. Кумыков, В.А. Созаев и др. Оpubл. 10.01.2008. (Patent for an invention. G01N №2314515. A method for measuring the tension of metals in solid phase / M.V. Gedagova, V.K. Koumykov, V.A. Sozayev, et al. / . Published on 10.01.2008.)

127. Авт. свидет. № 462114. Способ определения поверхностного натяжения металлов / Я.Б. Улановский, Ф.С. Шубик. Оpubл. 28. 02. 1975. (Author's certificate № 462114. A method for measuring the surface tension of metals / Ulanovskiy I.B., F.S. Shoubik. Published on 28. 02. 1975.)

Appendices
(author's certificates)



Fig. A-1 Author's certificate No 423599:
'The method of clad aluminium alloy thin plate production'



Исходный номер
патента СССР
и дата публикации
в печати

О П И С А Н И Е ИЗОБРЕТЕНИЯ

(11) 423599

Д. ВЕТЕРИНАРНО-САНИТАРНО-СТРОИТ.

(31) Заявитель от имени изобретателя

(21) Заявлено (в 2-х экз.) (11) 174203/25-31

(31) М. Кл. В 22/05 4308

с приоритетом заявки №

(32) Приоритет

Службковско-18.04.74, Вспомог. № 14

(53) УДК 621.771.5:608.0

Дата опубликования списка № 14.10.74

(72) Авторы
Изобретения: В. А. Малавский, А. В. Демьяков, А. А. Жуковичев, М. М. Исаев
и Г. А. Волосинин, Л. М. Коржавин и Т. Д. Губкина

(74) Заявитель

(54) СПОСОБ ИЗГОТОВЛЕНИЯ ЛАКЕРОВАННЫХ ЛИСТОВ ИЗ АЛЮМИНОВЫХ СПЛАВОВ

Изобретение относится к области производства лакокрасочных металлов.

Известен способ получения лакерованных листов из алюминиевых сплавов, при котором из сплава алюминия получают листы, подвергают анодированию при 400—500°C в течение 6—24 час и шлифуют на глубину 8—12 мкм на сторону.

Затем на сплиты сплава с обеих сторон наносят краску и в собранном виде прокатывают до требуемой толщины.

Недостатком известного способа является наличие газовых дефектов (пузырей) на поверхности лакированной стороны листов, содержащих в металле растворенный водород, переходящий в оксиды при шлифовании.

С целью улучшения качества лакированных листов из алюминия сплавов и алюминиевых сплавов, содержащих водород, известной технологии, предложено подвергать анодированию оксиды при 500—650°C в течение 24ч и шлифовать листы алюминия со стороны, содержащей оксиды, перед лакированием в собранном виде.

Способ осуществляется следующим образом.

Листы алюминия прокатывают до толщины, превышающей заданную толщину оксидной пленки на 5—10 мкм, затем полученную заготовку подвергают дополнительному оксиду при 500—650°C в течение 24—40 час, удаляя из нее при этом до 90% водорода, и прокатывают до заданной толщины.

Листы алюминиевого сплава нагревают до 250—350°C в течение 2—4 час и шлифуют на глубину 8—12 мкм на сторону, удаляя включения водорода и оксиды с поверхности. После шлифования оксиды сплава подвергают анодированию.

При этом происходит удаление водорода из пористости оксидной пленки на глубину 8—12 мкм. Полученные оксиды сплава шлифуют на глубину 1—3 мкм на сторону с противоположной стороне оксидной пленки, формируя в сплаве равномерную оксидную пленку.

Полученные оксиды сплава шлифуют для удаления включений водорода и оксидов с поверхности оксидной пленки. Затем оксиды сплава шлифуют с обеих сторон шлифовальными дисками, содержащими абразивную смесь, содержащую оксиды алюминия и оксиды железа, удаляя оксиды с поверхности оксидной пленки.

Предмет изобретения

Способ изготовления лакерованных листов из алюминиевых сплавов, заключающийся в

катку ситка планшетного алюминия, там же
процесса прокатки ситка планшетного алю-

миния там же, ситка планшетного алю-
миния там же, ситка планшетного алю-

Составитель С. Милдант
Рецензент А. Шварцман
Индекс № 1548
СЭТИИИ Государственного комитета Совета Министров СССР
по делам изобретений и открытий
Москва, М-25, Бумажный пер. д. 4/6
Телефонный код 509114

<p align="center">The Union Of Soviet Socialist Republics</p>	<p align="center">THE SPECIFICATION OF AUTHOR'S CERTIFICATE</p>	<p align="center">(11) 423599</p>
	<p>(61) Dependent on the author's certificates – (22) The date of inventorship declaration 02. 15.72 (21) 1746693/25-27 with the application of the declaration No ----- (32) The priority --- Published 04.15.71 The bulletin No 14 The date of specification of author's certificate publishing 10.14.74</p>	<p>(51) M. Cl. B 23p 3/06 (53) UDC (Universal decimal classification) 621.771.8(088.8)</p>
<p align="center">THE STATE COMMITTEE FOR INVENTIONS AND DISCOVERIES</p>	<p>(72) The authors of invention: I.B.Ulanovskiy, V.A. Danilkin, A.A. Zhukhovitsky, V.I.Yakovlev, G.A. Balahontzev, L.M.Koganov, T.D.Geyhman (71) The claimer ----</p>	

(54) The Method Of Clad Aluminium Alloy Thin Plate Production

This invention relates to the area of production of clad alloys.

There is known the method of production of clad aluminium alloys plates comprising the rolling of aluminium thin plates-flatbeds and the homogenizing of the aluminium alloy ingot at a temperature of 400 – 500 °C within 6 – 24 hour duration, and its further peeling with the milling machine up to the depth of 8 – 12 mm from every side.

Then conditioned aluminium alloy ingot is covered from both sides with the flatbeds and the obtained sandwich is rolled down to a specified thickness.

The formation of gas defects (blisters and cavities) on the surface of plates after their heat treatment is considered to be as a disadvantage of this well-known method. These defects appear under the effect of redistributing hydrogen, which spreads along the structure of metal during heating.

The proposed method provides the additional annealing of the billet at 500 – 550 °C during 24 – 40 hours before the final homogenizing annealing to remove gas defects and to enhance the degree of degassing of clad thin plates during the rolling of an ingot of pure aluminium for flatbeds manufacturing.

The way of the proposed method implementation is as follows.

The ingot of aluminium is subjected to piercing up depth by 5 – 10 mm exceeding the thickness of the flatbed. Then the obtained billet is additionally annealed at 500 – 550 °C during 24 – 40 hours what provides the removing of up to 90 % of hydrogen, and then the purified billed is rolled down to a specified thickness.

The aluminium alloy ingot is heated up to 300 – 350 °C during 2 – 4 hours and then milled up to depth of 8 – 12 mm from every side. What makes it possible to remove the segregation beadings and roughness of surfaces. After milling, the ingot is subjected to homogenizing annealing.

Meanwhile the removal of hydrogen from near to surface layers occurred up to depth of 8 – 12 mm. The homogenized ingot is subjected to milling again up to depth of 1 –

3 mm to remove the oxide film formed in the course of homogenization on the surface of ingot. The most of degassed layer remain unchanged during the secondary milling.

To obtain the clad thin plate the aluminium flatbeds are placed on the ingot of alloy from both its sides and then the simultaneous rolling of the ingot together with the flatbeds placed there is carried out.

The nature of the invention

The method of clad aluminium alloys' thin plate comprising the rolling of aluminium ingot destined for production of flatbeds, the homogenizing annealing and the milling of aluminium alloy ingot with further simultaneous rolling of the aluminium alloy ingot and aluminium flatbeds superimposed on both its opposite sides. The proposed method differs from the other ones by the additional annealing of the billet at 500 – 550 °C during 24 – 40 hours right before the its final deformation to increase a degree of degassing and to remove structural defects caused by gases contained in clad thin plates in the course of rolling of aluminium billets for destined for production of aluminium flatbeds.



Московская печатная фабрика Гознак. 1974. Лист 1809.

Fig. A-2 Author's certificate No 462114
'The method of surface tension determination'



Соборный Ученый Совет
Высшей Школы Академии Наук
СССР
от имени Академии
научных исследований
и изобретений

О П И С А Н И Е ИЗОБРЕТЕНИЯ

№ 462114

К АВТОРСКОМУ СВИДЕТЕЛЬСТВУ

(51) Изобретения относится к области —

(21) Заявлено 18.07.75 (21) 184594/46-03

(52) М.Кл. G 01n 13/02

Учреждение науки №

(32) Адресат

Сибирский филиал ЦСНТИ, Новосибирск 36-8

(33) УДК 621.028.05
(685.8)

Дата опубликования изобретения 02.09.75

(73) Автор
изобретения

И. Е. Удальцовский и Ф. С. Шубин

(71) Заявитель

(54) СПОСОБ ОПРЕДЕЛЕНИЯ ПОВЕРХНОСТНОГО НАТЯЖЕНИЯ МЕТАЛЛОВ

Изобретение относится к области физико-материаловедения металлов и сплавов.

Известный способ определения поверхностного натяжения металлов — способ измерения угла смачивания на твердой поверхности с использованием жидкостной пленки в капиллярной трубке. Процесс измерения заключается в образовании более крупной капиллярной трубки, чем диаметр капиллярной трубки, в которой производится измерение.

Результаты измерения, однако, являются таковыми, что для определения поверхностного натяжения Удальцовский и Шубин предложили способ измерения угла смачивания и измерения смачиваемости жидкостной пленки в капиллярной трубке. Этот способ заключается в том, что капиллярную трубку, в которой производится измерение, погружают в жидкую среду, температура которой выше температуры кипения металла, тогда скорость диффузии металла с изменением температуры скорость диффузии значительно убывает, при этом время установления равновесия существенно увеличивается и увеличивается время измерения. Этот способ измерения поверхностного натяжения металлов является новым и позволяет измерять поверхностное натяжение металлов.

С целью повышения точности и надежности измерения предложено измерять поверхностное натяжение металлов

поверхностного натяжения в капиллярной трубке, измерять общее содержание газа в образце, общую пористость и формулу газовой фазы. При этом в капиллярную трубку вводят газ, который в момент достижения жидкостной пленки вытесняется.

Величину поверхностного натяжения определяют по формуле:

$$\sigma = \frac{1}{2} \left(\frac{1}{\cos \theta} - \frac{1}{\cos \theta_0} \right) \frac{r_0}{r} \frac{\rho_0}{\rho} \frac{g}{2} \quad (1)$$

- 1 — радиус капиллярной трубки;
- 2 — радиус пленки;
- 3 — радиус капиллярной трубки;
- 4 — радиус пленки;
- 5 — радиус капиллярной трубки;
- 6 — радиус пленки;
- 7 — радиус капиллярной трубки;
- 8 — радиус пленки;
- 9 — радиус капиллярной трубки;
- 10 — радиус пленки;

11 — общее содержание газа в образце;

12 — радиус капиллярной трубки;

Предлагаемый способ является новым и позволяет измерять поверхностное натяжение металлов в капиллярной трубке, измерять общее содержание газа в образце, общую пористость и формулу газовой фазы. При этом в капиллярную трубку вводят газ, который в момент достижения жидкостной пленки вытесняется.

Предмет изобретения

Способ определения поверхностного натяжения металлов в твердом состоянии, заключающийся в том, что с целью повышения точности измерения осуществляют измерение общего содержания газа в образце, объема воздуха в среднем пузырьке пар в поперечном сечении и максимальной высоты, а по формуле

$$\sigma = \frac{V_{\text{газ}} \cdot P_{\text{газ}}}{S_{\text{пузырька}} \cdot H_{\text{пузырька}}}$$

где σ — поверхностное натяжение, $P_{\text{газ}}$ — среднее давление паров, T — температура, $V_{\text{газ}}$ — объем газа в образце, $S_{\text{пузырька}}$ — площадь поперечного сечения пузырька, $H_{\text{пузырька}}$ — максимальная высота пузырька.

Составитель С. Белодченко

Издатель Л. Цесляра Черный М. Семин Черный М. Ровбинин

Выпуск 3957 Изд. № 1246 Выпуск 310 Подписной

по делам изобретений и открытий
Москва, М. 19, Ленинский вост. пр. 1/1

Сек. вып. Государственного изобретения коллектива ИЗОБРАТЕННИКОВ и ИЗОБРАТЕННИЦ

<p align="center">The Union Of Soviet Socialist Republics</p>	<p align="center">THE SPECIFICATION OF AUTHOR'S CERTIFICATE</p>	<p align="center">(11) 462114</p>
	<p>(61) Dependent on the author's certificates – (22) The date of inventorship declaration 07. 16.73 (21) 1945904/26-25 with the application of the declaration No ----- (32) The priority --- Published 02.28.75 The bulletin No 8 The date of specification of author's certificate publishing 09.03.75</p>	<p>(51) M. Cl. G 01n 13/02 (53) UDC (Universal decimal classification) 621.386.08(088.8)</p>
<p align="center">THE STATE COMMITTEE FOR INVENTIONS AND DISCOVERIES</p>		
<p>(72) The authors of invention: I.B.Ulanovskiy and F.S. Shubik (71) The claimer ----</p>		

(54) The Method Of Determination Of Surface Tension Of Metals

The invention relates to the sphere of physicochemical study of metals and alloys.

The standard method of surface tension determination, known as the method of pore coalescence bases on the tendency of reduction of the surface energy what brings to coalescence of small pores and formation of the bigger ones in porous bodies. The self-diffusion rate determines the process rate.

The disadvantage of the standard method is that we have to know the value of the diffusion coefficient to determine the surface tension, and the diffusion coefficient is structure-sensitive to high extent. A considerable error of experimental determination of the diffusion coefficient is one of its demerits. Moreover, this method can be used at temperatures nearby the melting point of metal where the rate of self-diffusion is consistently high. The rate of self-diffusion exponentially decreases with the lowering of temperature, and in parallel, the time of asymptotic distribution of pores by their sizes increases to such an extent that the determination of surface tension becomes almost impossible.

We proposed the new method for the measurement of surface tension of solid metals to enhance the accuracy and the efficiency of analyses and to widen the temperature rage of measurements.

The value of surface tension σ , $\text{H}\cdot\text{m}^{-1}$ is obtained from the equation

$$\sigma = 5 \cdot 10^2 \cdot \bar{R} \left[\left(\frac{RTK_s}{44.8 \cdot V} \right) \sqrt{\left(\frac{RTK_s}{44.8 \cdot V} \right) + \frac{RTC_0}{22.4 \cdot V}} \right]^2 \frac{\text{dyne}}{\text{cm}},$$

where \bar{R} – mean pore radius, cm; T – temperature, K; K – gas solubility in metal, %;

V – porosity volume, % abs.; $R = 0.082 \frac{\text{l} \cdot \text{atm}}{\text{mol} \cdot \text{K}}$; C_0 – total gas content in the speci-

men, $\frac{\text{cm}^3(\text{NTP})}{\text{cm}^3 \cdot \text{Me}}$

The proposed method enhances considerably the efficiency of the measurement because the time required to obtain the maximum porosity in the specimen is limited by the rate of the dissolved gas diffusion through the metal. This rate can be several orders higher than the rate of self-diffusion.

The nature of the invention

The method of definition of the surface tension of metals, comprising the degassing of metal, is distinctive in that to enhance the accuracy and the efficiency of the measurements of the total gas content in the specimen; the measurements of porosity volume and mean pore size at the moment of maximum porosity are carried out there, and the sought quantity is determined by the equation

$$\sigma = 5 \cdot 10^2 \cdot \bar{R} \left[-\frac{RTK_s}{44.8 \cdot V} \sqrt{\left(\frac{RTK_s}{44.8 \cdot V} \right)^2 + \frac{RTC_0}{22.4 \cdot V}} \right]^2 \frac{\text{dyne}}{\text{cm}},$$

where \bar{R} – mean pore radius, cm; T – temperature, K; K – gas solubility in metal, %;
 V – porosity volume, % abs.; $R = 0.082 \frac{\text{l} \cdot \text{atm}}{\text{mol} \cdot \text{K}}$; C_0 – total gas content in the specimen, $\frac{\text{cm}^3(\text{NTP})}{\text{cm}^3 \cdot \text{Me}}$

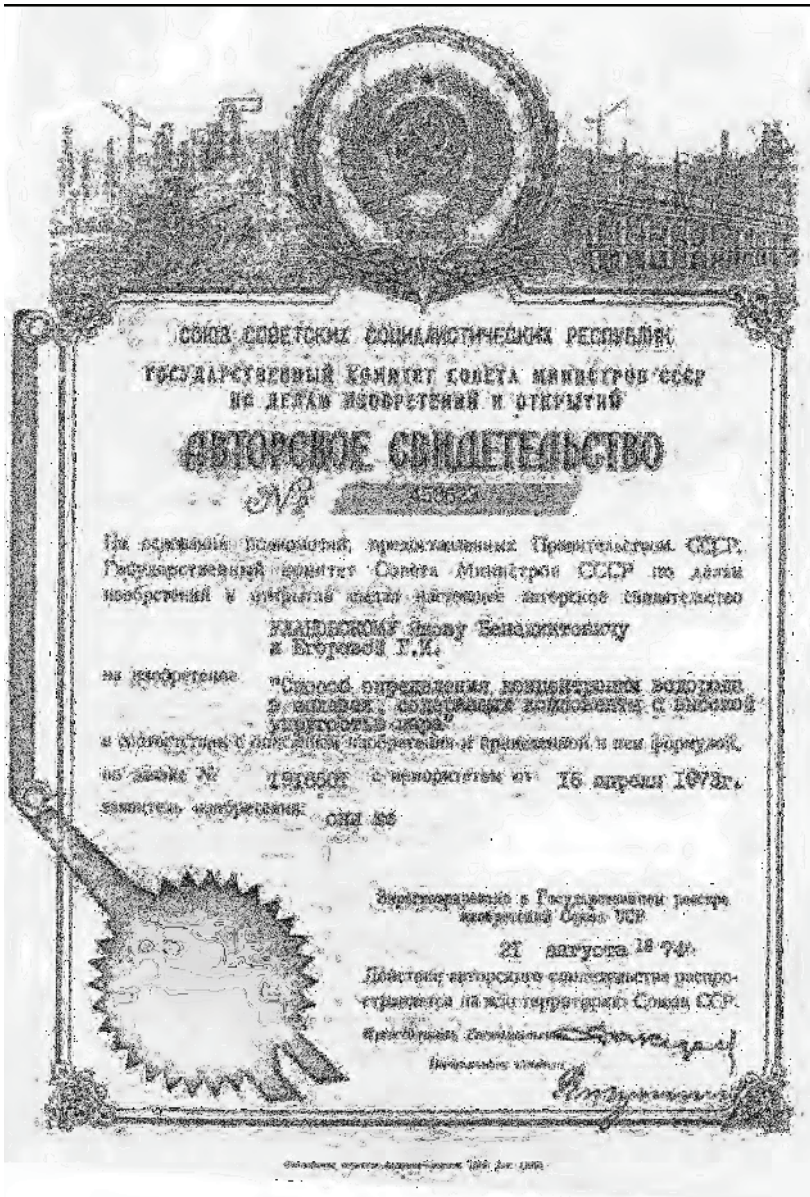


Fig. A-3 Author's certificate No 453623:
 'The method of hydrogen content determination in alloys containing the components characterized by high vapour pressure'

Союз Советских
Социалистических
Республик



Государственный комитет
Знаний Академии СССР
по делам изобретений
и открытий

О П И С А Н И Е ИЗОБРЕТЕНИЯ

М. А. БЕЛОРУССКОМУ СОЗДАТЕЛЮ

(11) 453623

(51) Зависимо от п.п. свидетельства. —

(52) Заявлено 16.04.73 (21) 18.6501.36.23

(51) М. Кл. G 01n 24/30

С присоединением заявки № 44

(53) Приоритет (—)

Обуздано 15.12.74. Водитель № 46

(53) УДК 548.27(084.6)

Дата опубликования описания 22.01.75

(72) Авторы

Изобретатели

Я. Е. Колосовский и Е. М. Спиркин

(71) Заявитель

(54) СПОСОБ ОПРЕДЕЛЕНИЯ КОНЦЕНТРАЦИИ ВОДОРОДА В СПЛАВАХ ОБЪЕДИНЕНИЯ КОМПОНЕНТОВ С ВЫСОКОЙ ТЕМПЕРАТУРОЙ ПЛАВА

Изобретение относится к области металлургии, в частности, к анализам слитков и металлов. Известны способы определения содержания водорода в сплавах объединенных компонентов с помощью индукционной печи на основе индукции электромагнитного поля при сжатии в вакууме. Существенным недостатком является

Данное изобретение относится к области металлургии, в частности, к анализам слитков и металлов. Известны способы определения содержания водорода в сплавах объединенных компонентов с помощью индукционной печи на основе индукции электромагнитного поля при сжатии в вакууме. Существенным недостатком является

Способ заключается в том, что перед анализом слитка в вакуумной камере, в которой находится индукционная печь, слиток нагревают в вакуумной аппаратуре, нагревают в вакуумной камере

мас-спектрометром количество водорода, выделяющегося из образца.

Предлагаемый предлагаемый способ состоит в том, что анализируемый образец обрабатывают индукционным и производят реакцию окислительных компонентов, в результате которой выделяется

Способ заключается в том, что перед анализом слитка в вакуумной камере, в которой находится индукционная печь, слиток нагревают в вакуумной аппаратуре, нагревают в вакуумной камере

Способ определения концентрации водорода в сплавах объединенных компонентов с высокой температурой плавления заключается в том, что перед анализом слитка в вакуумной камере, в которой находится индукционная печь, слиток нагревают в вакуумной аппаратуре, нагревают в вакуумной камере

<p align="center">The Union Of Soviet Socialist Republics</p>	<p align="center">THE SPECIFICATION OF AUTHOR'S CERTIFICATE</p>	<p align="center">(11) 453623</p>
	<p>(61) Dependent on the author's certificates – (22) The date of inventorship declaration 04. 16.73 (21) 1916501; 26 – 25 with the application of the declaration No ----- (32) The priority --- Published 12.15.74 The bulletin No 46 The date of specification of author's certificate publishing 22. 01.75</p>	<p>(51) M. Cl. G 01n 25.38 (53) UDC (Universal decimal classification) 543.27 (088.8)</p>
<p align="center">THE STATE COMMITTEE FOR INVENTIONS AND DISCOVERIES</p>	<p>(72) The authors of invention: I.B.Ulanovskiy and G.I. Yegorova (71) The claimer ----</p>	

(54) The Method Of Hydrogen Content Determination In Alloys Containing The Components Characterized By High Vapour Pressure

This invention relates to the field of metallurgy, to the analyzing the gas metals, in particular.

The standard methods of determination of hydrogen content in metals characterized by high vapour pressure of components are low productive and do not provide the complete extraction of hydrogen from specimens.

The method considers placing thin film pure aluminium on the specimen's surface right before it is placing into the vacuum apparatus to increase the efficiency of extraction and the efficiency of the process as well.

The realization of the proposed method might be as follows.

The specimens of pure aluminum are coated with a film of pure aluminium by means of short time dipping into pure molten aluminium.

Then the specimens are placed into the vacuum apparatus, subjected vacuum heating and thereby the volume of hydrogen eliminated from a specimen is measured by the mass-spectrometer.

The advantage of the proposed method is that the layer of pure aluminium covering the surface of a specimen sheds the fumes of easily volatile components but conducts the hydrogen.

The nature of the invention

The method of determination of hydrogen content in alloys, characterized by high vapour pressure of components, comprising the vacuum heating of a specimen and measuring the volume of eliminating hydrogen, is distinctive in that the surface of a sample right before its placing into the vacuum apparatus is covered with the layer of pure aluminium to enhance the completeness of extraction and the process efficiency, as well.



Медицинская литература фирмасы Москва, 1974, № 1, 1488.

Fig. A-4 The method of metals and alloys processing for elimination of gases



Государственный комитет
Совета Министров СССР
по делам изобретения
и открытий

О П И С А Н И Е ИЗОБРЕТЕНИЯ

К АВТОРСКОМУ СВИДЕТЕЛЬСТВУ

(11) 428008

(61) Заявлено от авт. свидетельства —
(22) Заявлено 05.08.70 (21) 1456937;22-1
с присоединением заявки № —
(32) Приоритет —
Опубликовано 15.05.74 Бюллетень № 18
Дата опубликования описания 30.01.75

(51) М.Кл. С 21d 1/74
С 21d 3/00
(53) УДК 621.78.062.
.26(088.8)

(73) Авторы
изобретения Я. Б. Уаановский, А. А. Жуховицкий и В. А. Данилкин
(71) Заявитель —

(54) СПОСОБ ОБРАБОТКИ МЕТАЛЛОВ И СПЛАВОВ ДЛЯ УДАЛЕНИЯ ИЗ НИХ ГАЗОВ

Изобретение относится к области термической обработки, в частности к обезгаживающему отжигу.

Известен способ обработки металлов и сплавов для удаления из них газов и устранения пористости путем вакуумного отжига.

Недостатком известного способа является длительность процесса, которая приводит к развитию газовой пористости при обработке массивных изделий. При этом поры могут достигнуть такого размера, что даже после полного обезгаживания металла последующим отжигом их нельзя устранить.

Цель изобретения — ускорение процесса обезгаживания и устранение пористости. Это достигается тем, что отжиг проводят в среде, находящейся под давлением и течение времени, достаточного для получения заданной степени обезгаживания и устранения пористости. Указанная среда поглощает выделяющиеся из металла газы, для чего в качестве вещества, передающего давление на образец, используют какой-либо инертный газ или смесь кремнеорганических жидкостей (силана и др.) с суспензией, способной поглощать выделяемые

газы и не окислять металл (например смесь оксидов металлов).

Способ был опробован на прутках чистого алюминия диаметром 10 мм. Прутки отжигают в сухом воздухе, сжатом под давлением 400 атм. при температуре 500°C. По сравнению с отжигом этих прутков в сухом воздухе при той же температуре время полного удаления водорода уменьшаются в 20 раз.

Между газом, растворенным в металле, и газом в порах устанавливается равновесие, и поэтому удаление газа из металла приводит к удалению газа из пор к закрытию последних.

Предмет изобретения

Способ обработки металлов и сплавов для удаления из них газов путем отжига, отличающийся тем, что, с целью ускорения процесса обезгаживания и устранения пористости, отжиг ведут в среде, находящейся под давлением и поглощающей выделяемые из металла газы.

<p>The Union Of Soviet Socialist Republics</p>	<p>THE SPECIFICATION OF AUTHOR'S CERTIFICATE</p>	<p>(11) 428008</p>
	<p>(61) Dependent on the author's certificates – (22) The date of inventor-statement declaration 06. 08.70 (21) 1456937/22-1 with the application of the declaration No ----- (32) The priority --- Published 15.05.74 The bulletin No 18 The date of specification of author's certificate publishing 30. 01.75</p>	<p>(51) M. Cl. C 21d 1/74 C 21d 3/00 (53) UDC (Universal decimal classification) 621.78.062.26 (088.8)</p>
<p>THE STATE COMMITTEE FOR INVENTIONS AND DISCOVERIES</p>	<p>(72) The authors of invention: I.B.Ulanovskiy, A.A. Zhukhovitsky and V.A. Danilkin (71) The claimer ----</p>	

(54) The method of metals and alloys processing for elimination of gases

This invention relates to heat treatment of metals, to metal degassing through annealing in particular.

Vacuum annealing is the most frequently used method for elimination of porosity and gases from metals.

Too long duration of the standard vacuum degassing process is its most obvious disadvantage resulting in gas porosity developing in the course of massive work pieces processing. The pores therewith can reach the sizes not allowing them to be eliminated even by further annealing after full degassing.

The aim of invention is the acceleration of degassing and pore removing process. This effect is achieved by means of annealing of specimens in the medium under pressure within a time sufficient for obtaining a specified degree of degassing and porosity removing.

The said medium venting the pressing should absorb gasses liberating from the metal. With this purpose, chemically inactive gases or oils of silicon-organic liquids (silicon hydrides, etc) together with a suspension (e.g. a mixture of metal oxides) capable to absorb the metal without its oxidation are used.

The method was tested with 10 mm thick rods of pure aluminium. The rods are annealed in dry air compressed under the pressure of 400 at at the temperature of 500 °C. As compared to annealing in dry air at the same temperature and atmospheric pressure the time of complete hydrogen elimination reduces by 20 times.

Equilibrium between the gas dissolved in the metal and the gas in pores results in gas removing from pores and their closure.

The nature of the invention

The method of metals and alloys processing aimed at accelerating the degassing process and porosity removing by means of annealing is being different from others by conducting the annealing under the pressure in the medium absorbing gasses liberating from the metal.

BIOGRAPHY

Iakov Benediktovich Ulanovskiy – Doctor of Engineering Sciences, Professor at the Physical Chemistry Department of the National Technological University ‘MISiS’.

The graduate of the Physical Chemistry Department of the Moscow Institute of Steel and Alloys, headed at that time by Professor Alexander Abramovich Zhukhovitsky – the outstanding physical chemist, Professor, Doctor of Engineering Sciences and Honored Worker of Science and Technology.

For many years he had worked at the All-Union Institute of Light Alloys (VILS), one of the major aviation research and technology centers in the USSR.

The area of expertise – material engineering, physical chemistry.

Today he is the Head of the R&D and manufacturing group of companies ‘Scienmet’, working on development and implementation of innovation technologies in ecology, power engineering and medicine.

Professor Ulanovskiy has been awarded with the honorary title ‘Engineer of Russia in 2005’ and awarded with the Grand Prix of the ‘EUREKA-2005’ Innovation Exhibition in Brussels. In 2015 he was elected a member of the European Academy of Natural Sciences.

He is the author of more than 100 scientific research papers and inventions.

Ulanovskiy Iakov B.

HYDROGEN DIFFUSION AND POROSITY FORMATION IN ALUMINIUM

Computer design by *L.Yu. Demina*

Подписано в печать 14.05.15	Бумага офсетная	
Формат 60 × 90 ¹ / ₁₆	Печать офсетная	Уч.-изд. л. 7,75
Рег. № 031-М	Тираж 500 экз.	Заказ 4590

National University Of Science And Technology ‘MISIS’,
4, Leninsky Prospect, Moscow, Russia, 119049

Izdatelskiy Dom ‘MISIS’,
4, Leninsky Prospect, Moscow, Russia, 119049
Tel. +7 (495) 638-45-22

Отпечатано в типографии Издательского Дома МИСиС
119049, Москва, Ленинский пр-т, 4
Тел. (499) 236-76-17, тел./факс (499) 236-76-35